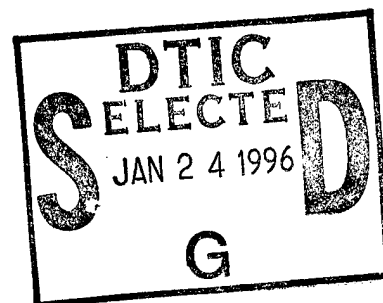


NAVAL POSTGRADUATE SCHOOL

Monterey, California



THESIS



RANDOM VIBRATION ANALYSIS OF THE TOPAZ II NUCLEAR REACTOR POWER SYSTEM

by

Sheryl Elaine Campbell

June 1995

Thesis Advisor:

Sandra L. Scrivener

Approved for public release; distribution is unlimited

19960122 076

DTIC QUALITY INSPECTED-1

REPORT DOCUMENTATION PAGE			Form Approved OMB No. 0704	
Public reporting burden for this collection of information is estimated to average 1 hour per response, including the time for reviewing instruction, searching existing data sources, gathering and maintaining the data needed, and completing and reviewing the collection of information. Send comments regarding this burden estimate or any other aspect of this collection of information, including suggestions for reducing this burden, to Washington headquarters Services, Directorate for Information Operations and Reports, 1215 Jefferson Davis Highway, Suite 1204, Arlington, VA 22202-4302, and to the Office of Management and Budget, Paperwork Reduction Project (0704-0188) Washington DC 20503.				
1. AGENCY USE ONLY (Leave Blank)		2. REPORT DATE June 1995	3. REPORT TYPE AND DATES COVERED Master's Thesis	
4. TITLE AND SUBTITLE Random Vibration Analysis of the TOPAZ-II Nuclear Reactor Power System			5. FUNDING NUMBERS	
6. AUTHOR Sheryl Elaine Campbell				
7. PERFORMING ORGANIZATION NAME(S) AND ADDRESS(ES) Naval Postgraduate School Monterey CA 93943-5000			8. PERFORMING ORGANIZATION REPORT NUMBER	
9. SPONSORING/MONITORING AGENCY NAME(S) AND ADDRESS(ES)			10. SPONSORING/MONITORING AGENCY REPORT NUMBER	
11. SUPPLEMENTARY NOTES The views expressed in this thesis are those of the author and do not reflect the official policy or position of the Department of Defense or the U.S. Government.				
12a. DISTRIBUTION/AVAILABILITY STATEMENT Approved for public release; distribution is unlimited			12b. DISTRIBUTION CODE	
ABSTRACT The TOPAZ-II Ya-21U is one of six Russian made space nuclear power systems which is based on thermionic power conversion. The U.S. is presently analyzing TOPAZ-II to determine the reliability and feasibility of using this system. A structural analysis test was conducted on the TOPAZ unit in May 1993 to provide data from which modal parameters could be identified. This test showed the fundamental frequency to be 10.5 Hz, yet the test results that the Russians conducted identified a fundamental frequency of 5 Hz. Another finite element model was created incorporating new developments in TOPAZ-II and modifications to the finite element model to better simulate the mass properties of the TOPAZ-II. A second structural analysis test was conducted on the TOPAZ unit 06-09 September, 1994. This thesis focuses on the random vibration analysis of the TOPAZ-II Ya-21U utilizing the most recent test results and the Master Series (updated version) I-DEAS software. The modal response of the model and simulated random vibration tests were within 8.33%. This model is a feasible tool which can be used to analyze the TOPAZ unit without testing the unit to fatigue.				
14. SUBJECT TERMS			15. NUMBER OF PAGES 115	
			16. PRICE CODE	
17. SECURITY CLASSIFICATION OF REPORT Unclassified	18. SECURITY CLASSIFICATION OF THIS PAGE Unclassified	19. SECURITY CLASSIFICATION OF ABSTRACT Unclassified	20. LIMITATION OF ABSTRACT UL	

NSN 7540-01-280-5500

Standard Form 298 (Rev. 2-89)
Prescribed by ANSI Std. Z39-18

Approved for public release; distribution is unlimited

**RANDOM VIBRATION ANALYSIS OF THE
TOPAZ II NUCLEAR REACTOR POWER
SYSTEM**

Sheryl Elaine Campbell
Lieutenant, United States Navy
B.S., Prairie View A&M University, 1985

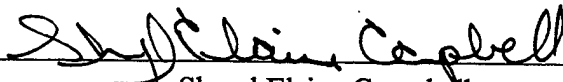
Submitted in partial fulfillment
of the requirements for the degree of

MASTER OF SCIENCE IN ASTRONAUTICAL ENGINEERING

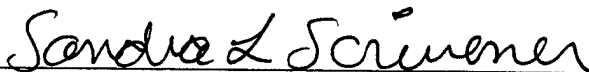
from the


**NAVAL POSTGRADUATE SCHOOL
June, 1995**

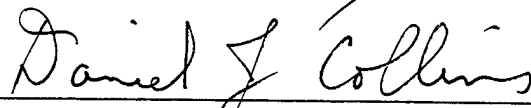
Author:


Sheryl Elaine Campbell

Approved by:


Sandra L. Scrivener, Thesis Advisor


Oscar Biblarz, Second Reader


Daniel J. Collins, Chairman
Department of Aeronautics and Astronautics

ABSTRACT

The TOPAZ-II Ya-21U is one of six Russian made space nuclear power systems which is based on thermionic power conversion. The U.S. is presently analyzing TOPAZ-II to determine the reliability and feasibility of using this system. A structural analysis test was conducted on the TOPAZ unit in May 1993 to provide data from which modal parameters could be identified. This test showed the fundamental frequency to be 10.5 Hz, yet the test results that the Russians conducted identified a fundamental frequency of 5 Hz. Another finite element model was created incorporating new developements in TOPAZ-II and modifications to the finite element model to better simulate the mass properties of the TOPAZ-II. A second structural analysis test was conducted on the TOPAZ unit 06-09 September 1994. This thesis focuses on the random vibration analysis of the TOPAZ-II Ya-21U utilizing the most recent test results and the Master Series (updated version) I-DEAS software. The modal response of the model and simulated random vibration tests were within 8.33%. This model is a feasible tool which can be used to analyze the TOPAZ unit without testing the unit to fatigue.

Accession For	
NTIS CRA&I	<input checked="" type="checkbox"/>
DTIC TAB	<input type="checkbox"/>
Unannounced	<input type="checkbox"/>
Justification _____	
By _____	
Distribution / _____	
Availability Codes	
Dist	Avail and/or Special
A-1	

TABLE OF CONTENTS

I.	INTRODUCTION	1
A.	BACKGROUND OF THE TOPAZ II REACTOR POWER SYSTEM	1
B.	OVERVIEW OF THE TOPAZ II STRUCTURAL ELEMENTS .	5
C.	BRIEF HISTORY OF STRUCTURAL TESTING	5
II.	TOPAZ II FINITE ELEMENT MODEL	9
A.	FINITE ELEMENT ANALYSIS	9
B.	I-DEAS DESIGN SOFTWARE	10
C.	TOPAZ FINITE ELEMENT MODEL	11
III.	THEORETICAL ASPECTS	15
A.	NORMAL MODE DYNAMICS	15
B.	DYNAMICS SIMULATION	16
C.	BUCKLING ANALYSIS	24
D.	FORCED RESPONSE	24
E.	RANDOM EXCITATION RESPONSE	24
	1. Mean-Squared Value	26
	2. Probability Density Function	27
	3. Auto-correlation Function	28
	4. Power Spectral Density	28
F.	RANDOM EXCITATION SIMULATION	28
IV.	VIBRATION TESTING OF THE YA-21U	33
A.	TEST PREPARATION/SETUP	33
B.	RANDOM VIBRATION TEST	36
V.	ANALYSIS/COMPARISONS	37

VI. CONCLUSIONS AND RECOMMENDATIONS	45
A. CONCLUSIONS	45
B. RECOMMENDATIONS	46
C. RESEARCH OPPORTUNITIES	46
APPENDIX A. THEORETICAL RANDOM VIBRATION PSD RESPONSE .	47
APPENDIX B. EXPERIMENTAL RANDOM VIBRATION PSD RESPONSE .	59
APPENDIX C. EXPERIMENTAL RANDOM VIBRATION PSD RESPONSE .	83
APPENDIX D. CORRELATION OF COORDINATE SYSTEMS	92
APPENDIX E. CORRELATION AND COMPARISON OF THEORETICAL AND EXPERIMENTAL RESULTS	94
LIST OF REFERENCES	103
INITIAL DISTRIBUTION LIST	105

I. INTRODUCTION

The TOPAZ-II Ya-21U is one of six Russian made space nuclear power systems which is based on thermionic power conversion. The U.S. is presently analyzing the TOPAZ system to determine the reliability and feasibility of using this system. To date, two series of structural analysis tests were conducted on the TOPAZ II Ya-21U unit. The first test indicated a fundamental frequency of approximately 10.5 Hz, yet the test results that the Russians conducted identified a fundamental frequency of 5 Hz. This thesis focuses on the correlation and comparison between random vibration analysis of the TOPAZ-II Ya-21U utilizing the most recent test results from the New Mexico Engineering Research Institute (NMERI) and a finite element model of TOPAZ-II.

LT Elisa Raney, on a companion thesis, concentrates on the correlation and comparison of the sine sweep vibration analysis tests of the Ya-21U and the finite element model of TOPAZ-II. LT Raney's thesis will be available after June 1995.

A. BACKGROUND OF THE TOPAZ II REACTOR POWER SYSTEM

The TOPAZ II power system generates electricity from nuclear heat. The nuclear heat is utilized by the in-core thermionic conversion units. The U.S Flight Safety Team (November 1992) indicates that when the Russians began to design the TOPAZ II power system, they had a number of requirements driving the design:

- A. The mass of the power system must not exceed 1061 kilograms.

- B. The system must provide 6 kilowatts (electric) from the thermionic fuel element (TFE) terminal at 27 volts.
- C. Design for a lifetime of 3 years, and a shelf life of at least 10 years.
- D. The reactor must not operate prior to achieving orbit.
- E. The coolant must not freeze prior to operation.

The TOPAZ II power system consists of 8 main subsystems: (1) the reactor subsystem, (2) the radiation shield, (3) the primary coolant pump, (4) the cesium supply system, (5) the gas systems, (6) the thermal cover, (7) the instrumentation and control system, and (8) the primary power system structure.

The reactor subsystem has 37 single-cell thermionic fuel elements (TFE). Thirty-four of the TFEs are used to control operate the reactor and the payload, and three are used to drive the electromagnetic pump. The core of the reactor is surrounded by reflectors. The radial reflectors contain 12 drums, each containing a section of boron carbon neutron poison used to control the nuclear reaction by rotating the drums. The nuclear fuel heats the TFE emitters, and the waste heat is removed by the coolant system.

The coolant system uses a sodium-potassium eutectic (NaK) as a coolant with stainless steel piping and a heat rejection radiator. The radiation shield is attached to the lower end of the reactor. Its main purpose is to reduce the accumulated radiation dose after three years of operation.

The cesium supply system provides cesium to the TFE interelectrode gap to suppress the charge near the emitters of the thermionic converters. The efficiency of the converter is increased by suppressing this charge.

The instrumentation and control system is an interface used to monitor and control the power system conditions.

This work concentrates on the primary power system structure. An illustration of the TOPAZ II power system is shown as Figure 1.1. Some TOPAZ II specifications are given in Table 1.1.

Other NPS theses which analyze the TOPAZ II system include those by Benke and Venable (1995) who report on the operational testing and thermal modeling of a TOPAZ-II single-cell thermionic fuel element test stand.

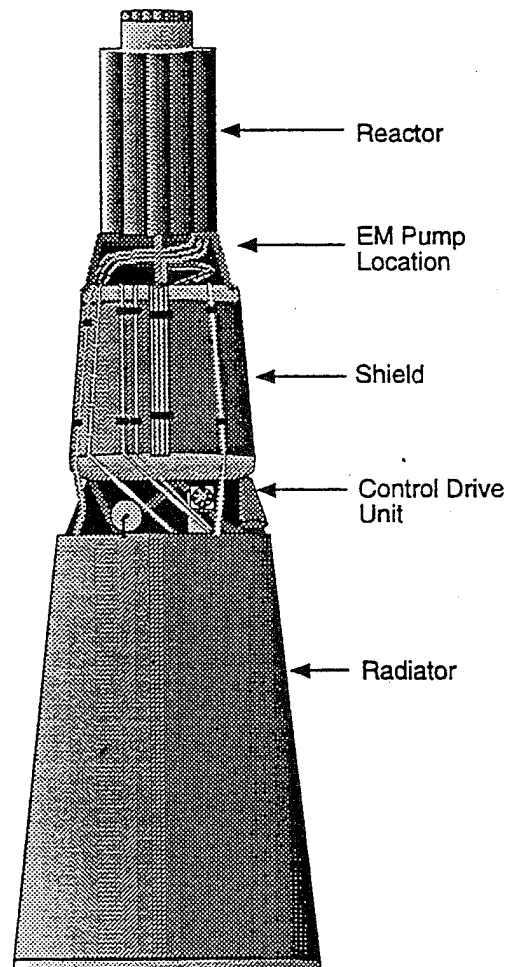


Figure 1.1. Illustration of TOPAZ-II Power System (U.S. TOPAZ-II Flight Safety Team, November 1992).

Lifetime	3 Years
Electric Power from the Reactor Terminal	6 +/- 0.7 (kWe)
Electric Power to the Spacecraft Bus	~5.5 (kWe)
Thermal Power BOL/EOL	115/135 (kWth)
Voltage	27 +/- 0.8 (volts)
Reactor System Mass (Excluding the ACS)	1061 (kg)
System Length	3.9 meters
Number of TFE Elements in the Core	37:34 for Primary Power and 3 to Power the Pump
Reactor Coolant	NaK: 78 w/o K and 22 w/o Na
Reactor Coolant Inlet Temperature BOL/EOL	470/500 (oC)
Reactor Coolant Outlet Temperature BOL/EOL	570/600 (oC)
Coolant Mass Flow Rate BOL	1.3 (kg/sec)
Pump Description	Electromagnetic Pump
Primary System Material	Stainless Steel
Reactor Neutron Spectrum	Epithermal
Reactor Fuel	UO2
Fuel Enrichment	0.96
Fuel Form	Pellets
Core Height	375 (mm)
Core Diameter	260 (mm)
Fuel Loading	27 (kg)
Reactor Height	920 (mm)
Reactor Diameter w/Radial Reflectors	408 (mm)
Moderator	ZrH1.85
TFE Emitter Material	Monocrystal Mo with ~3% Nb
TFE Emitter Surface Coating	W184
TFE Collector Material	Monocrystal Mo
TFE Insulator Material	Al2O3
Reactor Control Drums	9 Be Drums with 120 degree segments of B4C Canned in Stainless Steel
Reactor Safety Drums	3 Safety Drums
Excess Reactivity BOL Cold	0.53 - 0.65
Power Monitors	2 Fission Chambers
Shield Half Cone Angle	8 degrees and 16 seconds
Neutron Shield Material	LiH
Gamma Shield Material	Stainless Steel
Radiation Dose Limits (4 m plane 18.5 m from reactor centerline)	1.0 x 10 ¹¹ neutrons/cm ² (En>0.1 MeV) and 5.0 x 10 ⁴ roentgen
Total Cesium Supply	1 (kg)
Average Cesium Consumption per Day	0.5 (g/day)
Effective Radiator Surface	7.2 (m ²)
Number of Radiator Elements	78
Radiator Fin Material	Copper

Table 1.1. Specifications of the TOPAZ-II reactor power system as indicated by the U.S. TOPAZ-II Flight Safety Team (November 1992).

B. OVERVIEW OF THE TOPAZ-II STRUCTURAL ELEMENTS

There are three main structural members of the TOPAZ II reactor power system: (1) the reactor, (2) the shield, and (3) the frame.

The frame is bolted to the shield at six attachment points and supports the radiator, the volume accumulator, the gas bottles, and the coolant piping. The frame is also used for attachment of the spacecraft boom, at the bottom of the frame, at three attachment points. It is made of tubular stainless steel. It is approximately 2138 mm tall, and has a mass of approximately 45 kg. Figure 1.2 is a photo of the physical frame and its attachment to the radiator, the shield and the reactor.

The main form of support for the TOPAZ II reactor power system is a tubular stainless steel frame. The frame has the shape of a truncated three-sided pyramid. The circular diameters of the top and bottom of the frame are 680 and 1220 mm respectively. Some of the properties for stainless steel are contained in Table 1.2.

Mass Density	$7.86 \times 10^3 \text{ kg/m}^3$
Tensile Ultimate Strength	$860 \times 10^6 \text{ N/m}^2$
Tensile Yield Strength	$690 \times 10^6 \text{ N/m}^2$
Young's Modulus	$196 \times 10^9 \text{ N/m}^2$
Elongation	16%
Coefficient of Thermal Expansion	$11.2 \times 10^{-6}/^\circ\text{C}$

Table 1.2. Properties of 17-4PH H1150z Bar Steel.

C. BRIEF HISTORY OF STRUCTURAL TESTING

To date, there have been two series of structural testing conducted on the TOPAZ-II space nuclear power system by the

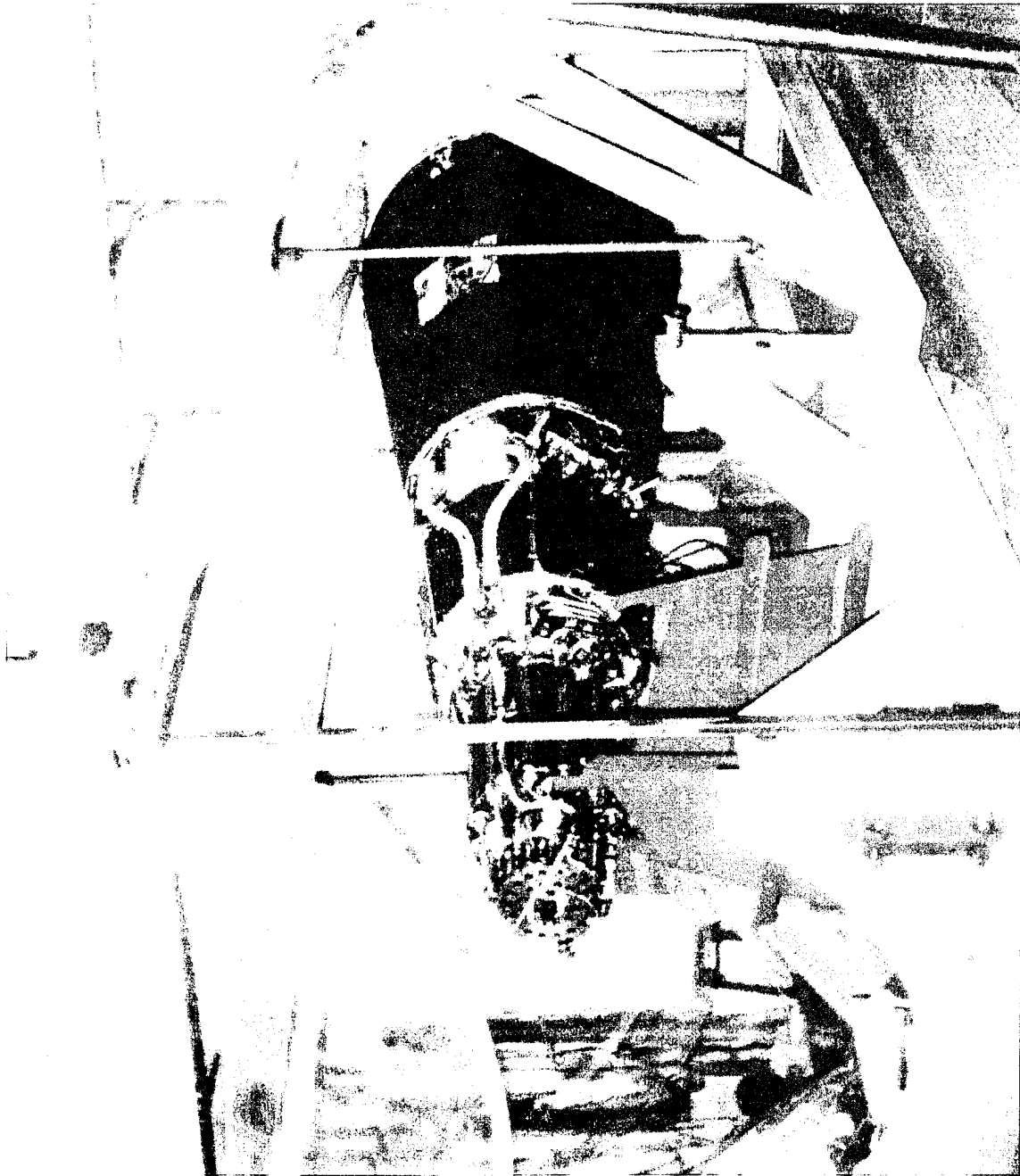


Figure 1.2. Photograph of TOPAZ-II unit taken at the New Mexico Engineering Research Institute in Albuquerque, NM.

United States. The first was a seismic mass testing series which used three shakers. Two of the shakers were configured to excite the bending modes and the third to excite the torsion and axial modes. The purpose of this test was to provide data from which the modal parameters could be extracted for use in correlation to a finite element model of TOPAZ-II. Mayes (1993) of Sandia National Laboratories concluded, from this test, that by shaking the TOPAZ-II unit at low levels, results obtained from the linear extraction algorithms fit those from analysis very well.

The second series of structural tests was conducted at Sandia Laboratories in early September, 1994. This work reports on the results from a portion of this series of tests, and the comparison to theoretical results.

II. TOPAZ II FINITE ELEMENT MODEL

A. FINITE ELEMENT ANALYSIS

A finite element model is a mathematical representation of a structure. In a spacecraft structure, there are usually many different structural elements or assemblies connected together by various attachments (discrete and continuous). Analyzing a structure becomes difficult when these elements are connected by a continuous attachment; the elements are connected at an infinite number of nodes. This creates a problem with the numerical solution but can be overcome by the use of the finite element method of analysis.

The finite element method for analyzing a structure predicts deflections and other effects of stress on a structure. It divides the existing infinite number of nodes into a finite number of nodes with a force representative of distributed stresses acting at the boundaries. Analysis of a spacecraft structure by the finite element method allows the accurate prediction of the mode shapes and frequencies of the structure.

The stiffness matrix, a component of the finite element method, can be obtained by first expressing the displacements at any point within the structure in terms of nodal displacements. If $\{u\}$ is a displacement vector at any point, and $\{\delta\}$ is a displacement vector at the nodes, then

$$\{u\} = [N] \{\delta\}$$

where $[N]$ is a transformation matrix. The strain vector $\{\epsilon\}$ can be represented by

$$\{\epsilon\} = [C] \{u\}$$

Let $[B] = [C][N]$. By using substitution,

$$\{\varepsilon\} = [B]\{\delta\}$$

The stress vector $\{\sigma\}$ can then be represented in terms of strain by

$$\{\sigma\} = [D]\{\varepsilon\}$$

The displacements, strains and stresses within the element can be obtained by considering a virtual displacement. The internal work done by internal forces and the external work done by nodal forces can then be found. Subsequently, the nodal forces can be obtained by multiplying the virtual displacement by $\{F\}$ where

$$\{F\} = \int [B]^T [D] [B] d(vol)$$

the stiffness matrix is calculated by

$$[K] = \int [B]^T [D] [B] d(vol)$$

Finally, the stress at any point can be found after the nodal displacements are determined as

$$\{\sigma\} = [D] [B] \{\delta\}$$

B. I-DEAS DESIGN SOFTWARE

The Integrated Design Engineering Analysis Software (I-DEAS) Master Series version 1.3C (Lawry, 1993), is a mechanical, computer aided, engineering design tool. Intricate three dimensional solid (or line drawing) models may be designed using this software. It is an outstanding tool

for mass properties calculations, interference studies, stress analysis, and manufacturing planning.

I-DEAS is one of several software tools used to design and analyze finite element models. The finite element modeling task in I-DEAS divides the structure into a grid of simple elements, forming a model of the actual structure. The finite element program in I-DEAS assembles the stiffness matrices for the combined elements and then forms a global stiffness matrix for the entire model.

C. TOPAZ FINITE ELEMENT MODEL

A finite element model of the TOPAZ II space nuclear power system was originally created, using the I-DEAS software by Schaefer (September 1993) of the Applied Physics Laboratories at John Hopkins University. A second finite element model was created and modified by Lacy (September 1993) at the Idaho National Laboratories. This model takes into consideration all of the data which have become available since Schaefer's model and since the first series of structural tests. Lacy made small changes to the geometry and to the system mass. Point masses are replaced by solid elements to better simulate the distributed mass properties. In addition, the rigidizing effect of the joints and the linear spring effect of the foot have been included.

Lacy's finite element model (the model used in this thesis) has four major sections: (1) the reactor, (2) the shield, (3) the frame, and (4) the test stand. Figure 2.1 shows a solid design of the TOPAZ II model. The reactor was designed using a modulus of elasticity of $2.068\text{E}+8$ mN/mm² and a mass density of $1.0634\text{E}-5$ kg/mm³. It has 21 nodes and 6 elements. The shield is attached to the reactor by 12 elements and 12 nodes and has a modulus of elasticity of

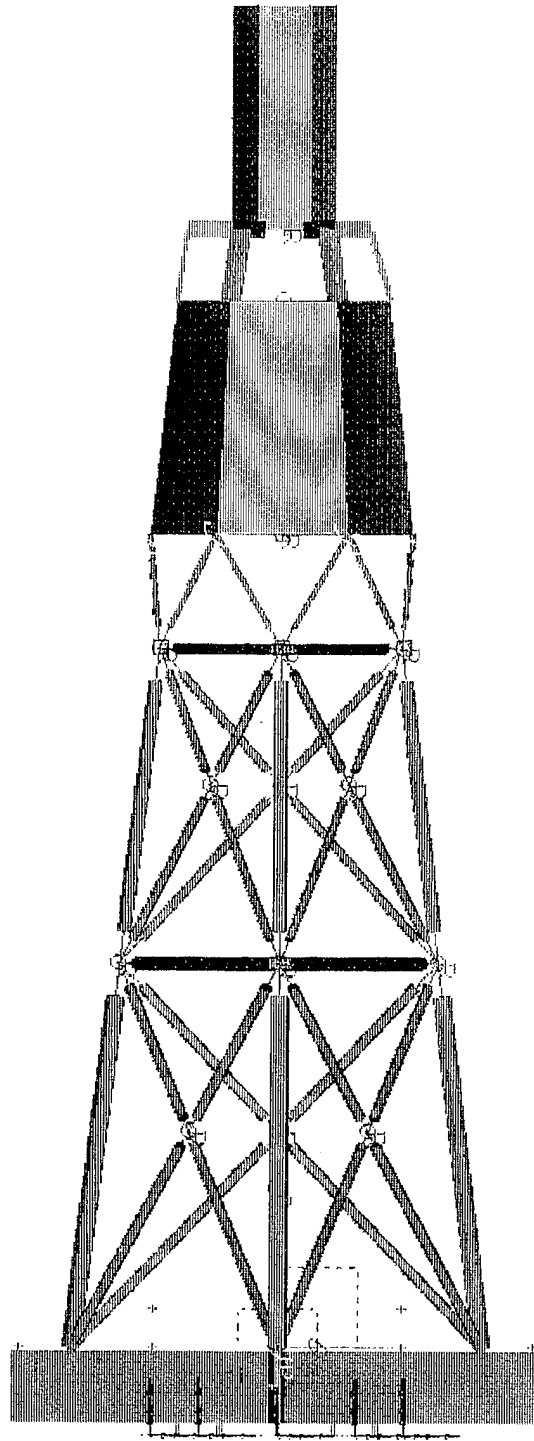


Figure 2.1. Solid Design of the TOPAZ-II as modeled using the I-DEAS software.

2.068E+8 mN/mm² and a mass density of 2.39E-6 kg/mm³. The shield has 14 nodes and 6 elements. The frame was modeled as tubular rods with properties of steel. The test stand is attached to the frame at three points. Notice that the design does not look exactly like the TOPAZ unit. The goal of a finite element model is to create a model which behaves structurally like the actual TOPAZ unit and not to make the model look like the actual structure.

Some detailed components, including the TFE's, the cesium block, the start-up unit, and the radiator, which are shown in Figures 1.1 and 1.2, are not included on this model.

III. THEORETICAL ASPECTS

Several analysis runs were conducted on the TOPAZ model to simulate the actual vibration tests on the Ya-21U unit. Simulation of the vibration tests include normal mode dynamics analysis, model response functions, and buckling analysis using the I-DEAS software. Results from this analysis are compared with the test results.

A. NORMAL MODE DYNAMICS

The equations of motion for dynamic system, such as the TOPAZ II system, can be shown in matrix form as

$$[M] \{\ddot{x}\} + [C] \{\dot{x}\} + [K] \{x\} = \{F(t)\}$$

where $[M]$ = mass matrix

$[C]$ = viscous damping matrix

$[K]$ = stiffness matrix

$\{x\}$ = coordinate vector (displacement, velocity, acceleration)

$\{F(t)\}$ = forcing function

In this case, the forcing function is the random frequency vibration. Let

$$\{x\} = [M]^{-\frac{1}{2}} \{X\}$$

This will give the eigenvalue solution of a symmetric matrix. Using substitution,

$$[I] \{\ddot{X}\} + [\bar{C}] \{\dot{X}\} + [\bar{K}] \{X\} = [M]^{-\frac{1}{2}} \{F(t)\}$$

where $[I]$ is the identity matrix,

$$[\bar{C}] = [M]^{-\frac{1}{2}} [C] [M]^{-\frac{1}{2}}$$

is the symmetric matrix, and

$$[\bar{K}] = [M]^{-\frac{1}{2}} [K] [M]^{-\frac{1}{2}}$$

is the positive definite matrix. The solution to these equations can be written as

$$\{X\} = \{\phi\} e^{i\omega t}$$

By substitution, the eigenvalue equation is

$$[\bar{K}] \{\phi\} = \omega^2 \{\phi\}$$

where ω^2 is the eigenvalue and $\{\phi\}$ is the eigenvector. By using this equation, the eigenvalues, ω_r^2 , and eigenvectors, $\{\phi_r\}$, can be obtained, where ω_r is the r^{th} natural frequency, and $\{\phi_r\}$ is the r^{th} mode vector.

B. DYNAMICS SIMULATION

Using the finite element model, a normal mode dynamics analysis incorporating simultaneous vector iteration was conducted. This analysis solves the model for natural frequencies and mode shapes using kinematic degrees of freedom in the case set. The TOPAZ model was first clamped at the bottom of the test stand. This boundary condition simulates the actual vibration test. No load was placed on the model for this analysis because the natural frequencies, when the structure is vibrating freely, are desired.

The first 40 modes were analyzed using the I-DEAS software. These 40 modes provide natural frequencies up to and including 200 Hz, simulating the frequency range of the experimental data. Solving the model for higher modes would give the higher natural frequencies associated with them, but would serve no purpose when comparing these higher frequencies to the Ya-21U experimental data.

The resulting natural frequencies, given by I-DEAS, and a description of the mode are given in Table 3.1. Included in this table are the relative maximum stresses for each mode. The first mode (first lateral bending) has a frequency of 9.29 Hz as seen in Figure 3.1. The first several modes are lateral bending, axial compression, and axial torsion as shown in Figures 3.2 and 3.3. The later modes display more radical shapes as shown in Figures 3.4 and 3.5.

Mode	Freq ~ Hz	Max Stress ~ mN/mm ²	Mode Description
1	9.29E+00	2.01E+06	1st bending in the +/- Y
2	9.43E+00	1.16E+06	1st bending in the +/- Z
3	2.76E+01	8.03E+05	1st axial torsion
4	4.06E+01	2.35E+06	2nd bending in the +/- Y
5	4.09E+01	1.28E+06	2nd bending in the +/- Z
6	5.10E+01	1.06E+07	1st axial compresssion
7	5.84E+01	1.97E+05	3rd bending in the +/- Y
8	5.84E+01	1.46E+05	3rd bending in the +/- Z
9	6.27E+01	8.37E+03	2nd axial compression
10	8.11E+01	2.11E+05	4th bending in the +/- Y
11	8.12E+01	1.48E+05	4th bending in the +/-Z
12	9.80E+01	5.15E+04	3rd axial compression
13	1.08E+02	9.06E+05	5th bending in the +/- Y
14	1.08E+02	7.24E+05	5th bending in the +/- Z
15	1.08E+02	1.46E+06	2nd axial torsion
16	1.21E+02	1.04E+05	4th axial compression (Frame)
17	1.21E+02	5.79E+05	6th multiple bending in the +/- Y
18	1.22E+02	2.90E+05	6th multiple bending in the +/- Z
19	1.24E+02	2.44E+05	7th multiple bending in the +/- Y
20	1.22E+02	6.92E+05	7th multiple bending in the +/- Z
21	1.25E+02	2.21E+05	3rd axial torsion
22	1.42E+02	6.25E+05	8th radical bending in the +/- Z
23	1.44E+02	4.37E+05	8th multiple bending in the +/- Y
24	1.45E+02	3.12E+05	9th multiple bending in the +/- Z
25	1.49E+02	1.98E+06	9th radical bending in the +/- Y
26	1.63E+02	2.75E+05	4th axial torsion
27	1.65E+02	4.53E+05	10th multiple bending in the +/- Y
28	1.65E+02	4.56E+05	10th bending in the +/- Z
29	1.72E+02	6.95E+05	11th multiple bending in the +/- Y
30	1.73E+02	5.39E+05	5th axial torsion
31	1.74E+02	1.41E+05	11th bending in the +/- Z (slight)
32	1.76E+02	3.05E+05	12th multiple bending in the +/- Y
33	1.76E+02	2.28E+05	12th bending in the +/- Z
34	1.82E+02	1.14E+06	13th multiple bending in the +/- Y
35	1.86E+02	8.06E+04	5th axial compression
36	1.86E+02	1.00E+05	14th multiple bending in the +/- Y
37	1.91E+02	1.00E+05	6th axial compression (Frame)
38	1.92E+02	1.03E+02	13th multiple bending in the +/- Z
39	1.93E+02	2.48E+06	7th axial compression (Reactor)
40	2.01E+02	1.33E+05	8th axial compression

Table 3.1. Theoretical normal mode dynamics analysis for the TOPAZ model with no acceration applied.

```

/tmp_mnt/d5/94-7/secampbe/topaz_3.mf1.2
RESULTS: 1- B.C. 6, MODE 1, DISPLACEMENT_1
MODE: 1      FREQ: 9.294983
DISPLACEMENT - MAG MIN: 0.00E+00 MAX: 1.00E+03
DEFORMATION: 1- B.C. 6, MODE 1, DISPLACEMENT_1
MODE: 1      FREQ: 9.294983
DISPLACEMENT - MAG MIN: 0.00E+00 MAX: 1.00E+03
FRAME OF REF: PART

```

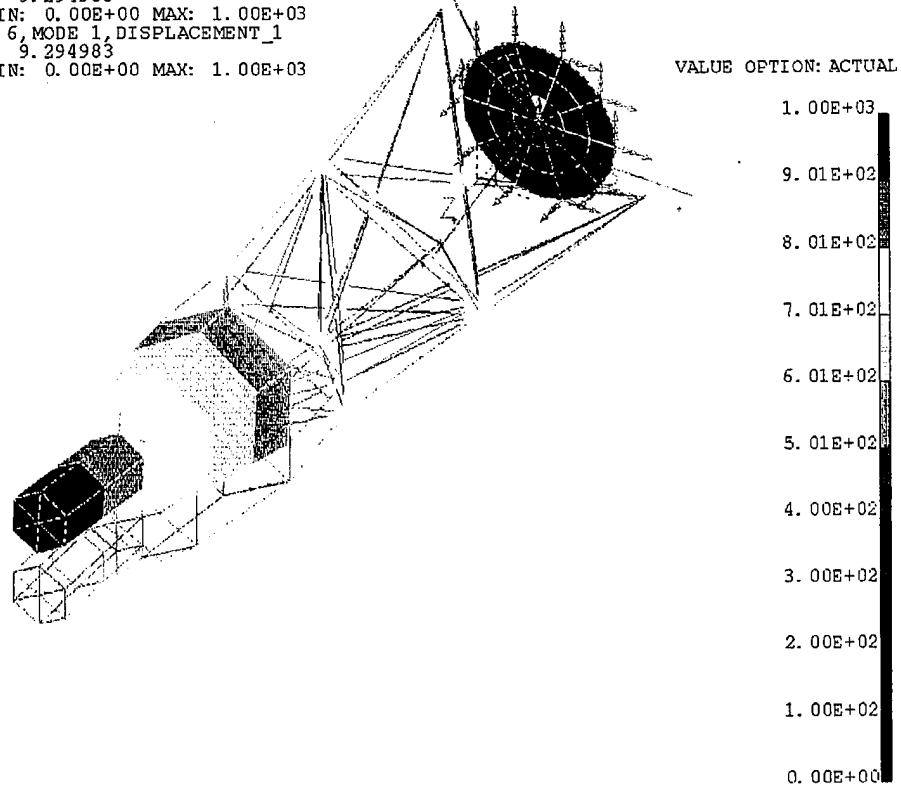


Figure 3.1. Illustration of mode 1 of the theoretical normal mode dynamics simulation. This illustration shows lateral bending in the +/- Y direction.

RESULTS: 3- B.C. 6, MODE 3, DISPLACEMENT_3 /tmp_mnt/d5/94-7/secampbe/topaz_3.mf1.2
 MODE: 3 FREQ: 27.61518
 DISPLACEMENT - MAG MIN: 0.00E+00 MAX: 3.38E+02
 DEFORMATION: 3- B.C. 6, MODE 3, DISPLACEMENT_3
 MODE: 3 FREQ: 27.61518
 DISPLACEMENT - MAG MIN: 0.00E+00 MAX: 3.38E+02
 FRAME OF REF: PART

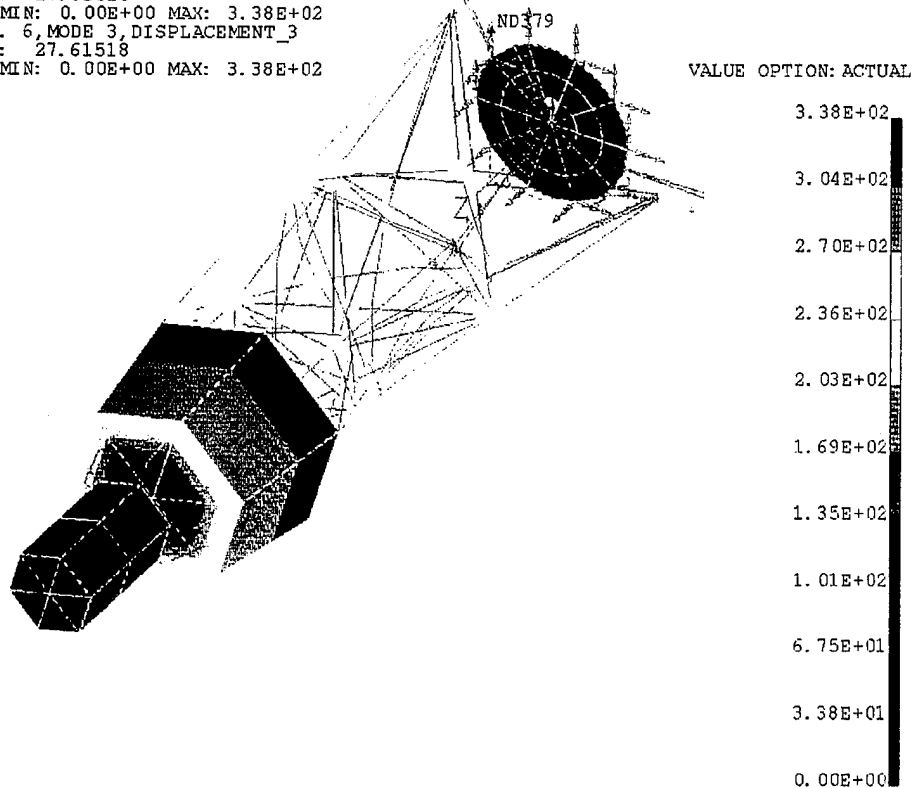


Figure 3.2. Illustration of mode 3 of the theoretical normal mode dynamics simulation for displacement. This illustration shows axial torsion in the +/- X direction.

/tmp_mnt/d5/94-7/secampbe/topaz_3.mf1.2
 RESULTS: 6- B.C. 6, MODE 6, DISPLACEMENT_6
 MODE: 6 FREQ: 51.03082
 DISPLACEMENT - MAG MIN: 0.00E+00 MAX: 1.00E+03
 DEFORMATION: 6- B.C. 6, MODE 6, DISPLACEMENT_6
 MODE: 6 FREQ: 51.03082
 DISPLACEMENT - MAG MIN: 0.00E+00 MAX: 1.00E+03
 FRAME OF REF: PART

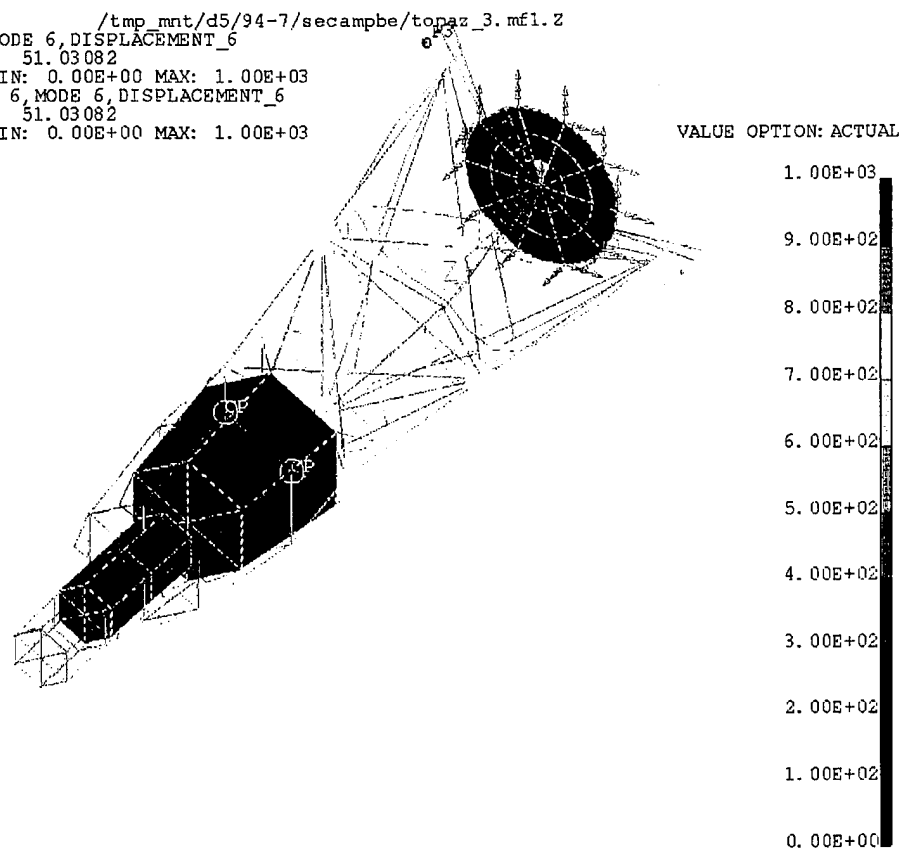


Figure 3.3. Illustration of mode 6 of the theoretical normal mode dynamics simulation for displacement. This illustration shows axial compression in the +/- X direction.

```

RESULTS: 38- B.C. 6, MODE 38, DISPLACEMENT_38
MODE: 38      FREQ: 191.9077
DISPLACEMENT - MAG MIN: 0.00E+00 MAX: 1.03E+02
DEFORMATION: 38- B.C. 6, MODE 38, DISPLACEMENT_38
MODE: 38      FREQ: 191.9077
DISPLACEMENT - MAG MIN: 0.00E+00 MAX: 1.03E+02
FRAME OF REF: PART

```

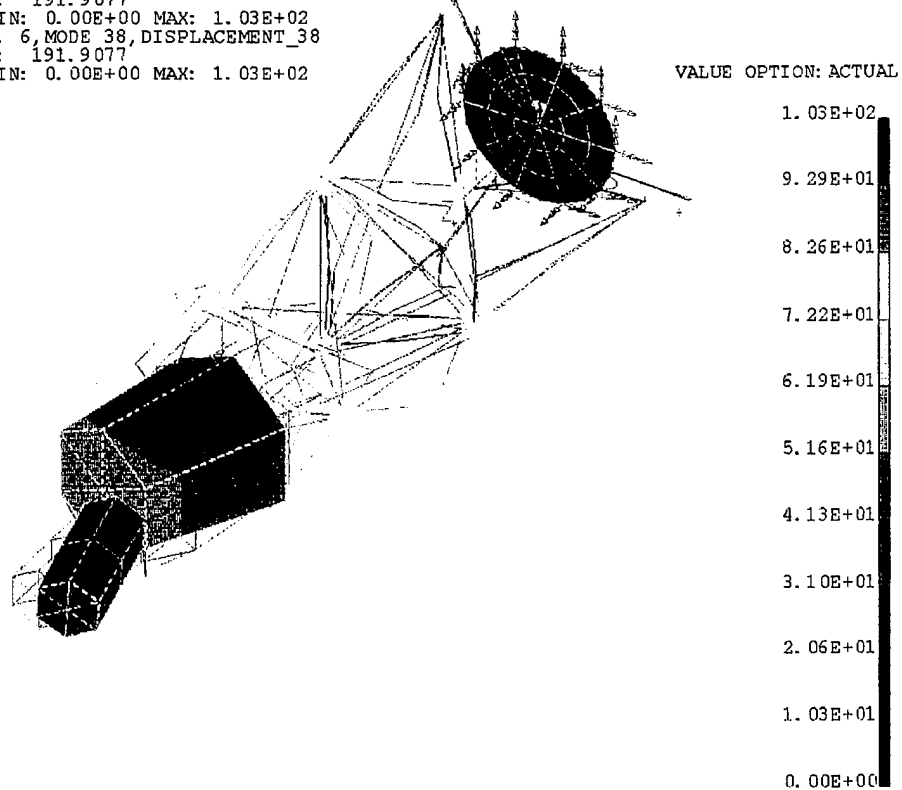


Figure 3.4. Illustration of mode 38 of the theoretical normal mode dynamics simulation for displacement. This illustration shows radical lateral bending in the +/- Z direction.

RESULTS: 82- B.C. 6, MODE 39, STRESS_82
 MODE: 39 FREQ: 193.368
 STRESS - VON MISES MIN: 1.41E+03 MAX: 2.48E+06
 DEFORMATION: 39- B.C. 6, MODE 39, DISPLACEMENT_39
 MODE: 39 FREQ: 193.368
 DISPLACEMENT - MAG MIN: 0.00E+00 MAX: 1.82E+02
 FRAME OF REF: PART

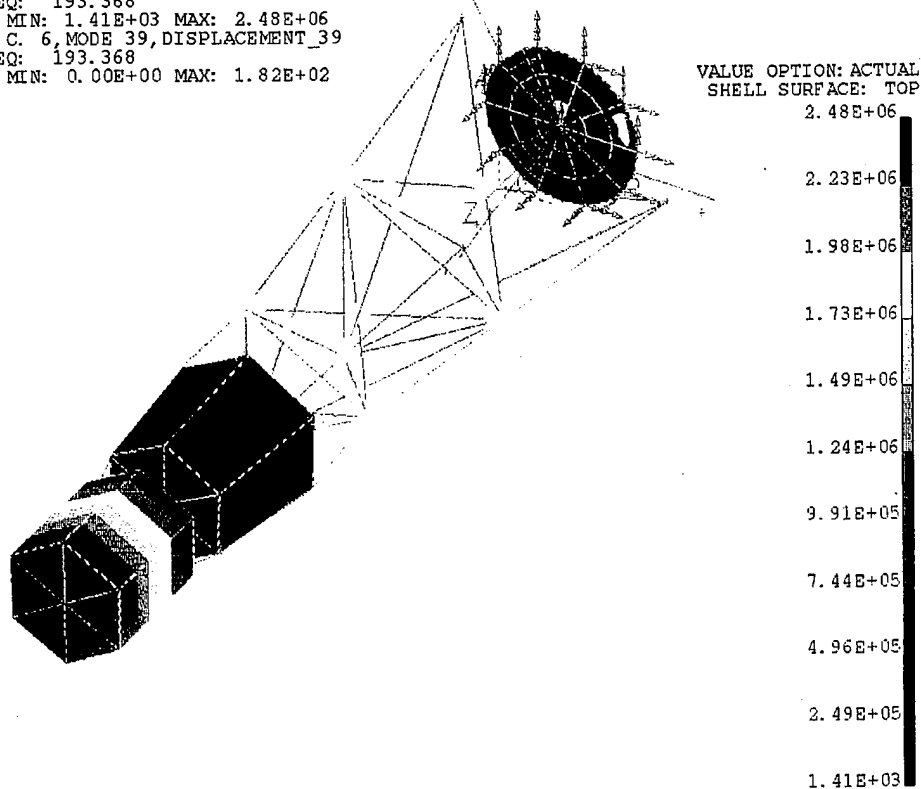


Figure 3.5. Illustration of mode 39 of the theoretical normal mode dynamics simulation for stress. This illustration shows radical axial compression in the +/- X direction.

C. BUCKLING ANALYSIS

The buckling analysis task in I-DEAS computes a requested number of buckling mode shapes. With this analysis one determines how close the given load is to the critical buckling load. In this case, the requested number of mode shapes is forty. An acceleration of 12g's ($12 \times 9.81 \text{ m/s}^2$) was applied to the structure. Complete results of the buckling analysis are given in Table 3.2. The buckling factor for the first mode is 14.2. This means that it would take an acceleration which is greater than 170 g's to cause the structure to buckle.

D. FORCED RESPONSE

If a multi-degree-of-freedom system is subjected to a base excitation, the equations of motion are

$$[M]\{\ddot{y}\} + [C]\{\dot{y}\} + [K]\{y\} = -[M]\begin{Bmatrix} 1 \\ 1 \\ 1 \\ \vdots \\ 1 \end{Bmatrix} \ddot{u}$$

where $\{u\}$ = base motion, and

$\{y\}$ = response vector relative to the base.

I-DEAS uses this equation to solve the forced response.

E. RANDOM EXCITATION RESPONSE

There are many physical phenomena which cause an excitation but cannot be described at some specific time in the future. These excitations are random, and are characterized as undeterministic. The response to this random excitation is also a random phenomenon. Most random phenomena

Mode	Max Disp	Max Stress ~ mN/mm ²	Buckling Factor
1	5.33E+02	2.26E+04	14.19923
2	5.01E+02	2.60E+04	14.22563
3	4.71E+02	1.08E+04	15.07019
4	1.95E+02	7.54E+04	19.29928
5	1.60E+02	7.31E+04	19.30463
6	7.45E+01	4.20E+04	22.01404
7	1.58E+02	1.92E+04	24.07015
8	2.07E+02	8.83E+03	25.9158
9	2.47E+02	1.09E+04	25.92
10	1.69E+02	2.70E+04	27.5443
11	1.59E+02	2.55E+04	27.5446
12	3.57E+02	2.58E+03	31.08792
13	2.69E+02	4.17E+05	34.6699
14	1.02E+02	1.02E+04	36.06585
15	1.02E+02	1.02E+04	36.07465
16	6.11E+01	5.50E+04	37.98394
17	4.48E+01	6.49E+03	45.2604
18	3.93E+01	4.35E+03	45.27362
19	4.50E+01	4.35E+03	45.28993
20	1.37E+02	1.87E+05	51.09995
21	1.54E+02	1.34E+05	51.40519
22	1.61E+02	1.67E+05	51.40895
23	1.54E+02	1.60E+05	54.57196
24	1.41E+02	1.57E+05	54.59474
25	1.12E+02	7.30E+04	61.70712
26	8.53E+02	1.38E+06	65.61707
27	4.85E+02	4.60E+05	66.50982
28	1.54E+02	9.31E+04	66.62384
29	1.15E+02	1.71E+05	67.98686
30	1.11E+02	1.23E+05	68.18298
31	1.26E+02	4.88E+04	75.00062
32	1.32E+02	7.79E+04	75.06561
33	1.07E+02	1.05E+05	75.13165
34	9.97E+01	7.42E+04	75.51292
35	1.18E+02	5.70E+04	80.30183
36	1.11E+02	4.03E+04	80.36268
37	1.00E+02	6.86E+04	109.26
38	9.75E+01	6.77E+04	109.283
39	1.21E+02	3.56E+04	116.9878
40	9.48E+01	4.70E+04	120.6542

Table 3.2. Theoretical buckling analysis for the TOPAZ model with an acceleration of 12g's lateral applied.

affecting a space power system, such as the launch vehicle and engine noise, exhibit a certain pattern. The characteristics of these random phenomena can be described in terms of statistical averages. The expected value ($E(X)$) or mean value (μ_x) of a random response at some time (t) in the future can be found by taking the instantaneous value of response at some time, (t), for each excitation, and dividing by the number of excitations. This mean value can be represented by

$$E(X) = \mu_x(t) = \lim_{n \rightarrow \infty} \frac{1}{n} \sum_{k=1}^n x_k(t)$$

where, n is the number of excitations. This random vibration is called stationary if the mean is constant for all time t . If the random vibration is stationary, all properties can be determined by finding the properties for a single sample excitation. The mean value for sample k is

$$\mu_x(k) = \lim_{T \rightarrow \infty} \frac{1}{T} \int_0^T x_k(t) dt$$

There are four basic properties for random data: (1) mean-square values, (2) probability density functions, (3) auto-correlation functions, and (4) power spectral density functions. These are described below.

1. Mean-Squared Value

The mean-squared value (ψ_x^2) of $x(t)$ is

$$\psi_x^2 = \lim_{T \rightarrow \infty} \frac{1}{T} \int_0^T x^2(t) dt$$

The variance (σ_x^2) is found by

$$\sigma_x^2 = \lim_{T \rightarrow \infty} \frac{1}{T} [x(t) - \mu_x]^2 dt,$$

$$\sigma_x^2 = E(X^2) - [E(X)]^2, \text{ or}$$

$$\sigma_x^2 = \psi_x^2 - \mu_x^2$$

where σ_x is the standard deviation.

2. Probability Density Function

The probability density function (pdf) is the probability that X takes on a value over the interval $[x, x + \Delta x]$. It can be defined as

$$p(x) = \lim_{\Delta x \rightarrow 0} \frac{\text{Prob}[x < x(t) < x + \Delta x]}{\Delta x}$$

The probability that $x(t)$ lies between x and $x + \Delta x$ is

$$P = \int_x^{x+\Delta x} p(x) dx$$

The expected value for this continuous random variable, X , with a pdf $p(x)$ is

$$E(X) = \mu_x = \int_{-\infty}^{\infty} xp(x) dx$$

and the mean-squared value is

$$\psi_x^2 = \int_{-\infty}^{\infty} x^2 p(x) dx$$

3. Auto-correlation Function

The auto-correlation function ($R_x(\tau)$) describes the dependence of the values at one time on the values at another time. This function can be described as

$$R_x(\tau) = \lim_{T \rightarrow \infty} \frac{1}{T} \int_0^T x(t) x(t+\tau) dt$$

and the mean-squared value at time displacement is

$$\psi_x^2 = R(0)$$

4. Power Spectral Density

The power spectral density function describes the spectral density of its mean-squared value. The power spectral density is defined as

$$S_x(f) = \lim_{\Delta f \rightarrow 0} \frac{\psi_x[f, f+\Delta f]}{\Delta f}$$

The mean-squared value can be shown to be

$$\psi_x^2 = \int_0^\infty S_x(f) df$$

F. RANDOM EXCITATION SIMULATION

I-DEAS uses the modes of vibration characterized by natural frequencies and mode shapes to calculate the dynamic responses. The random force in frequency excitation set, simulating the random vibration test for the TOPAZ II, is shown in Table 3.3.

The base excitation on the TOPAZ model was applied to the center of the test stand, for both the axial and lateral excitation, at node 339. A graph of this excitation is shown in Figure 3.6. Since the data furnished by the New Mexico Engineering Research Institute (NMERI) gave values for

Frequency ~ Hz	Power Spectral Density ~ (mm/s ²) ² /Hz
20 - 70	1,924,722
70 - 100	linear increase
100 - 800	5,774,166
800 - 2000	linear decrease
2000	1,251,069.3

Table 3.3. Random vibration frequency excitation.

the power spectral density (PSD) and accelerometers were used as a means of measuring data, the analysis was conducted using the PSD function in I-DEAS for acceleration. Figure 3.7 shows the PSD function at one of the reactor leg brackets, node 75, for an axial excitation in the X direction. The power spectral density functions for all analyzed nodes as specified in Table 4.1, for both axial and lateral excitations, are summarized in Appendix A.

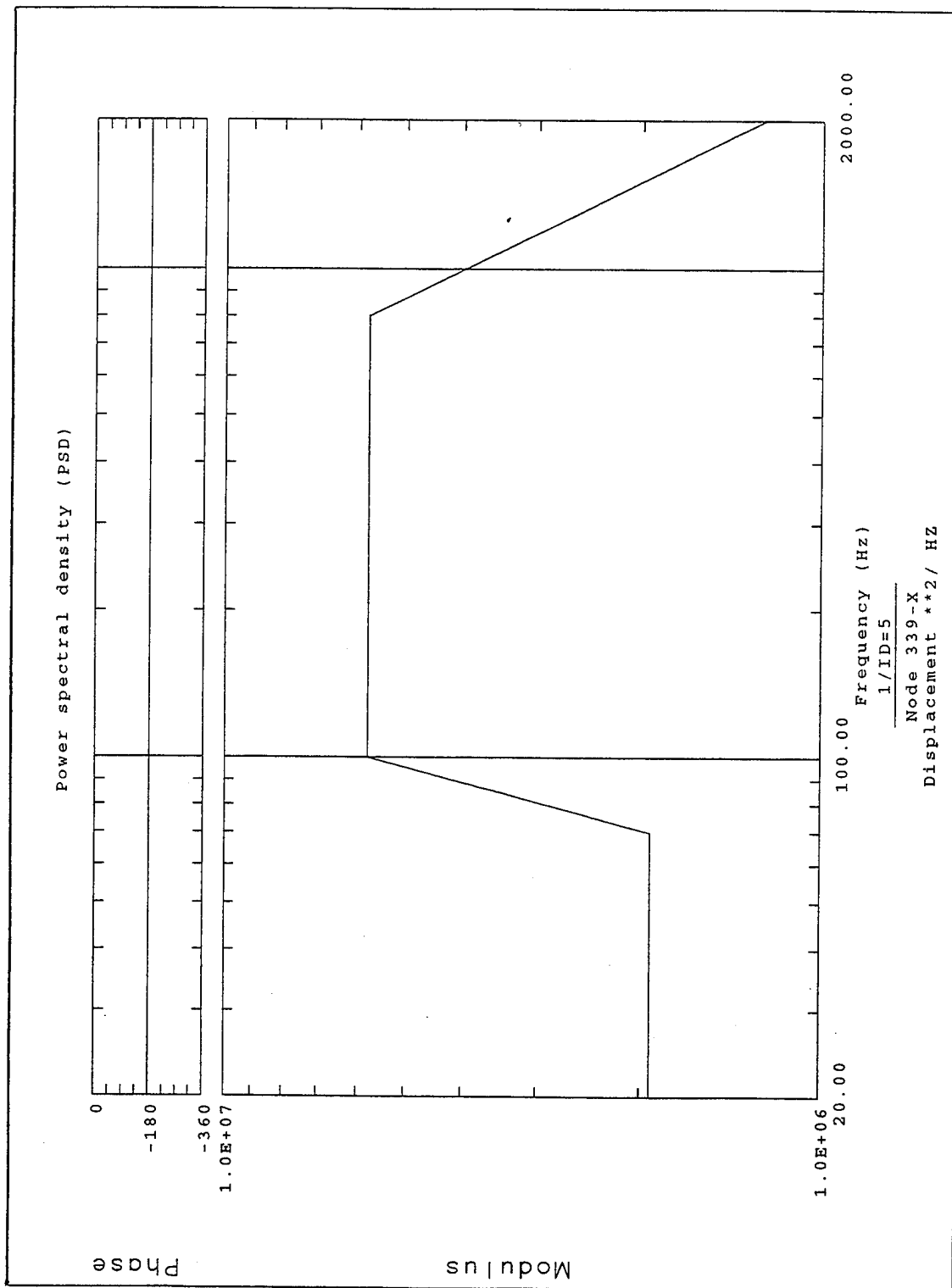


Figure 3.6. The base excitation on the TOPAZ model was applied to the center of the test stand, for both the axial and lateral excitation, at node 339.

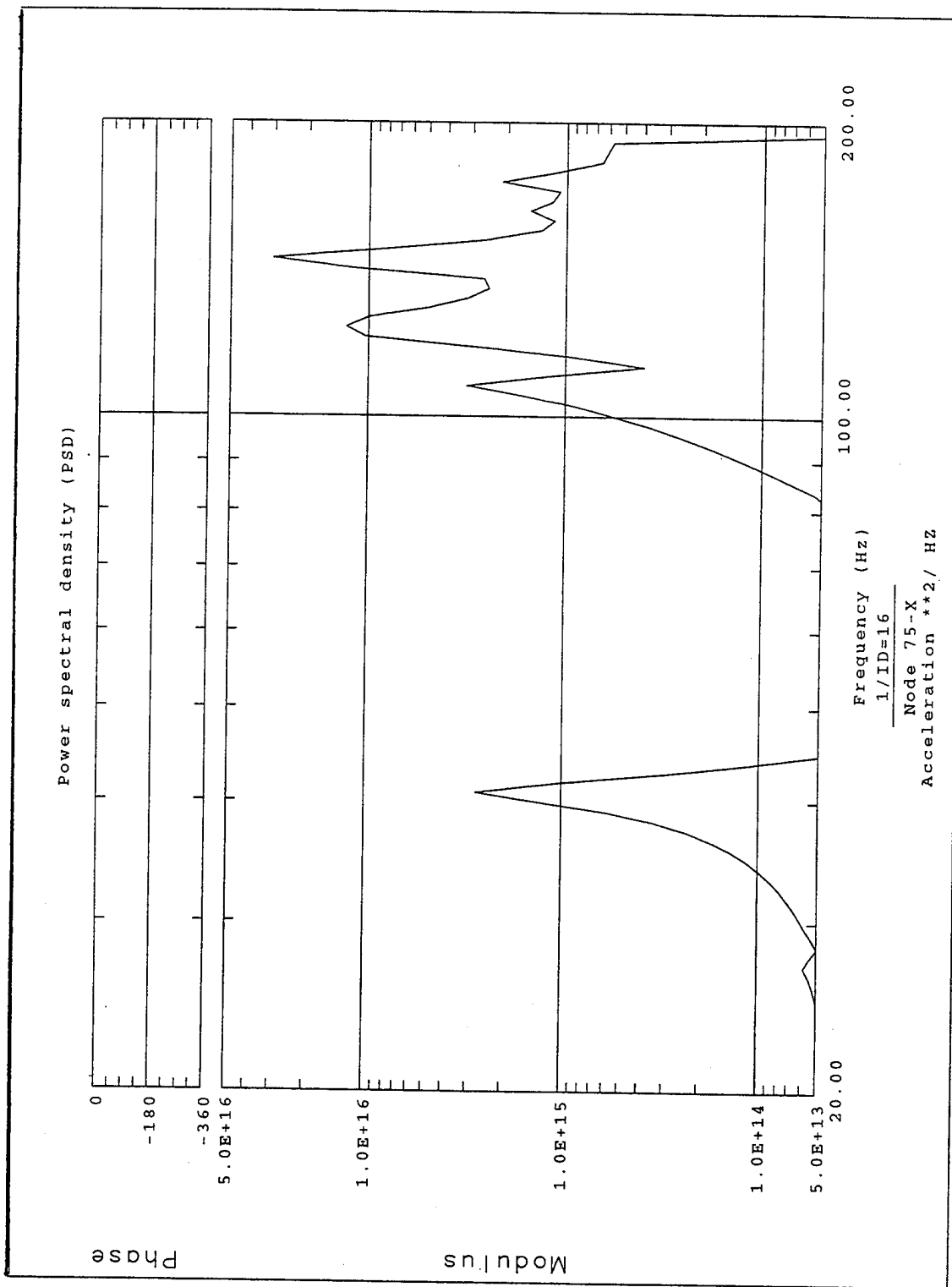


Figure 3.7. The PSD function at one of the reactor leg brackets, node 75, for an axial excitation in the X (axial) direction.

IV. VIBRATION TESTING OF THE YA-21U

The most recent series of structural tests conducted on the TOPAZ II space nuclear reactor system by American scientists were the vibration tests. This test was conducted 06 through 09 September, 1994 on the TOPAZ II Ya-21U unit. The purpose of these tests was to verify the test results which were documented previously by Russian scientists. In addition, the tests would demonstrate the power system's reliability and space capability when subjected to realistic conditions of space preparation and operation. These tests consisted of shock tests, random vibration tests, and sine sweep vibration tests.

A. TEST PREPARATION/SETUP

All TOPAZ II units, including the Ya-21U, are located at the New Mexico Engineering Research Institute in Albuquerque, New Mexico, however, there are no facilities for structural testing at this site. The shock and vibration tests were therefore conducted at the Sandia National Laboratories Vibration Test Facility, which is also located in Albuquerque, New Mexico. Prior to being transported to the testing site, accelerometer transducers were cemented to the Ya-21U unit. These instruments enabled measurements to be taken in three orthogonal directions.

Although several vibrations tests were desired for accurate analysis, time and equipment constraints limited the number of instruments to 12. The number of tests were limited to five: (1) shock test, (2) axial sine sweep, (3) lateral sine sweep, (4) axial random vibration, and (5) lateral random vibration tests. There were 24 channels available for monitoring performance. Of the 24 channels, two were used

for monitoring the table leaving 22 channels for the 12 instruments, three directions each. Naval Postgraduate School personnel assisted in the determination of the more critical instruments, and instrument directions, to monitor. Table 4.1 provides a list of the recommended instrument locations along with the respective node on the TOPAZ model. Figure 4.1 illustrates the accelerometer locations.

Instrument #	Node	Instrument Location
1	5	-Z Leg of frame at base
2	12	Leg between +Y and +Z of frame at base
3	**	Bottom collector of radiator on -Z axis
4	**	Bottom collector of radiator on +Y axis
5	29	Joint of frame
6	55	Leg between +Y and +Z of frame at top of radiator
7	79	Reactor leg bracket most closely aligned with -Z axis
8	75	Reactor leg bracket most closely aligned with +Y axis
9	97	Reactor top plenum on -Z axis
10	92	Reactor top plenum on +Y axis
11	**	Hard point on cesium unit
12	**	Start-up unit simulator

** No specific node identified on the TOPAZ model.

Table 4.1. Recommended Accelerometer Instrument Locations.

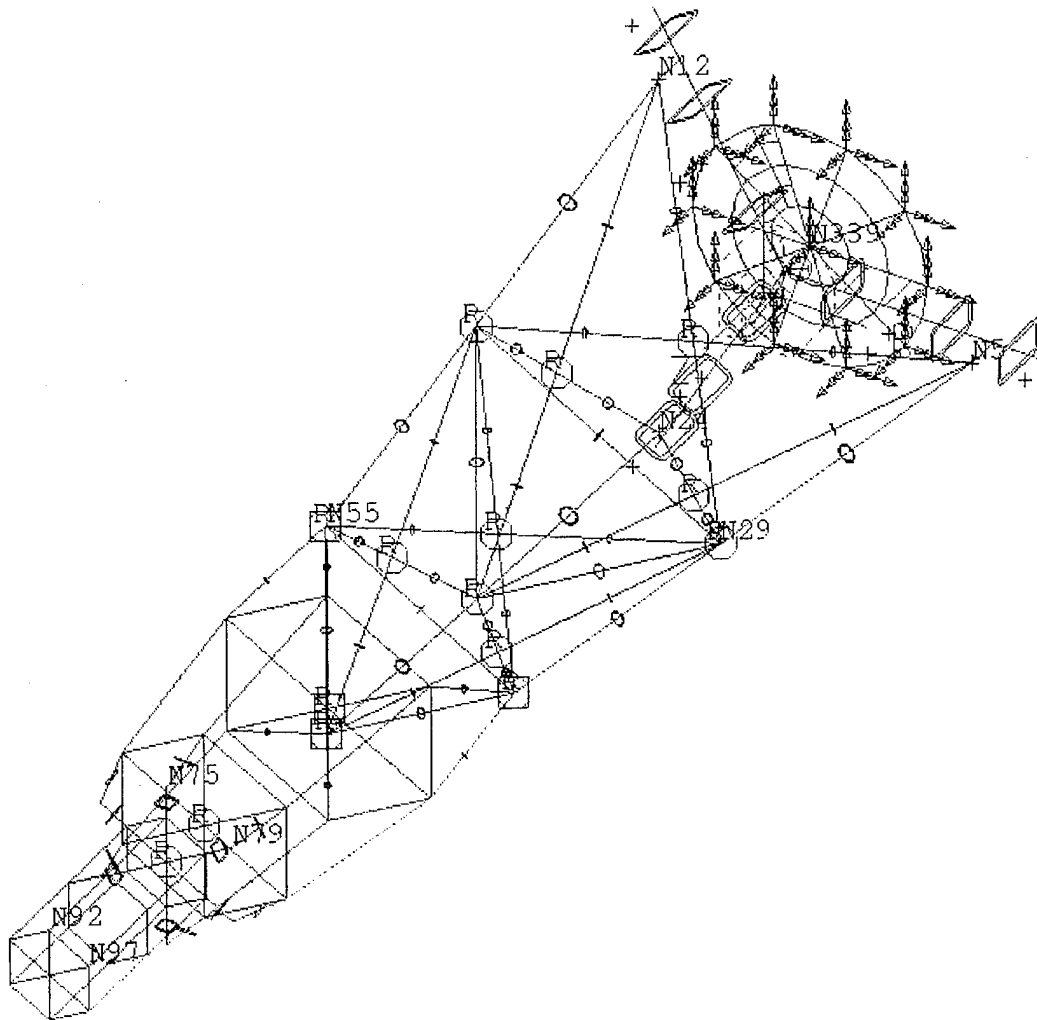


Figure 4.1. Illustration of the nodes corresponding to the accelerometer instrument locations.

B. RANDOM VIBRATION TEST

This section focuses on the random vibration tests only. Prior to testing, each instrument was checked and calibrated. The random vibration tests started at 20 Hz, ensuring that the first mode of the Ya-21U unit (8.8 Hz) would not affect on the response of the unit. The first frequency of the unit past 20 Hz, was noted to have shifted from the predicted value of 38 to 42 Hz, probably due to the test stand. When the TOPAZ unit is bolted to the test stand, it causes the TOPAZ unit to be more stiff, and therefore increases the frequencies of the system. The response was limited to 12 dB. The Ya-21U was excited for the random vibration tests as shown in Table 4.2. The input to this excitation is the same as that shown in Figure 3.6.

Frequency ~ Hz	Power Spectral Density ~ g^2/Hz
20 - 70	.02
70 - 100	linear increase
100 - 800	.06
800 - 2000	linear decrease
2000	.013

Table 4.2. Random vibration test frequency levels. The graph of this excitation was shown in Figure 3.6.

Each random vibration test, both axial and lateral, was one minute in duration. A MATLAB program was written to plot and analyze the test data files received from NMERI. These data files contain information on the test duration, number of data points, frequency and power spectral density (PSD) amplitude. The plotted results of the axial and lateral random vibration data are shown in Appendix B. A summary of this is given in Appendix C.

V. ANALYSIS/COMPARISONS

Since the actual test on the TOPAZ II Ya-21u was conducted for frequencies up to 200 HZ, no theoretical analysis was conducted on modes greater than 200 HZ. The theoretical analysis of the TOPAZ unit yields a fundamental frequency of 9.29 Hz while experimental data indicate a fundamental frequency of 8.8 Hz.

Before the theoretical results can be compared to the experimental data, the differences in coordinate systems between the Ya-21U unit, the TOPAZ model, and the accelerometers need to be identified. A chart identifying the relationship between the three is given as Appendix D.

The radiator, the cesium unit, and the start-up unit were not modeled on the TOPAZ finite element model; therefore, a comparison can not be made with the information given on these items.

Since there were limitations put on the amount of channels to measure accelerometer response, all possible responses were not recorded. The nodes and the direction in which the accelerometer was measured with respect to the Ya-21U are shown in Tables 5.1 and 5.2. All coordinate axes (directions) are given with respect to the Ya-21U unit.

Experimental results for the given nodes/directions were analyzed for peaks indicating responses at specific natural frequencies. This information was compared with the analyzed theoretical data at the corresponding nodes on the TOPAZ finite element model.

Example:

For the axial excitation, instrument number eight was placed at the reactor leg bracket closest to the +Y (lateral)

Node	Accelerometer	Direction measured
5	1	X, Y, Z
12	2	X, Y
29	5	X
55	6	X, Z
75	7	X
79	8	X
92	9	X, Z
97	10	X, Z

Table 5.1. Measured nodes and the TOPAZ based direction in which they were measured for axial vibration.

Node	Accelerometer	Direction measured
5	1	X, Y
12	2	Y, Z
29	5	X, Z
55	6	X, Y
75	7	X
79	8	Z
97	10	X, Y, Z

Table 5.2. Measured nodes and the TOPAZ based direction in which they were measured for lateral vibration.

direction on the Ya-21U. The response to the excitation was measured in the accelerometer's +X direction. (The coordinate axis for the TOPAZ finite element model was changed to coincide with the Ya-21U unit for ease in correlation.) This point and direction on the Ya-21U correlates to node 75 on the TOPAZ finite element model, and measured in the X (axial) direction. Peaks observed during the experiment are shown in Figure 5.1 and summarized in Table 5.3.

Inst #8-I08/C01: Reactor Leg Bracket/+Y (X,20); node 75+X

Peak	Natural Freq ~ Hz	Amplitude
1	39.3775	0.145985
2	101.257	3.135029E-02
3	118.133	5.436304E-02
4	140.634	1.197833E-02

Table 5.3. Experimental PSD response for instrument #8 measured in the Ya-21U X (axial) direction for an axial excitation.

The peaks observed for the theoretical model are shown in Figure 5.2 and summarized in Table 5.4.

Node 75 DOF - X

Peak	Natural Freq ~ Hz
1	40.83
2	107.4
3	123.3
4	144.9
5	174.2

Table 5.4. Theoretical PSD response for node 75 measured in the TOPAZ model X direction (correlating to the Ya-21U X (axial) direction) for an axial response.

When the two responses are compared, similar frequencies at the peaks are noted, and shown in Figure 5.3 and summarized in Table 5.5.

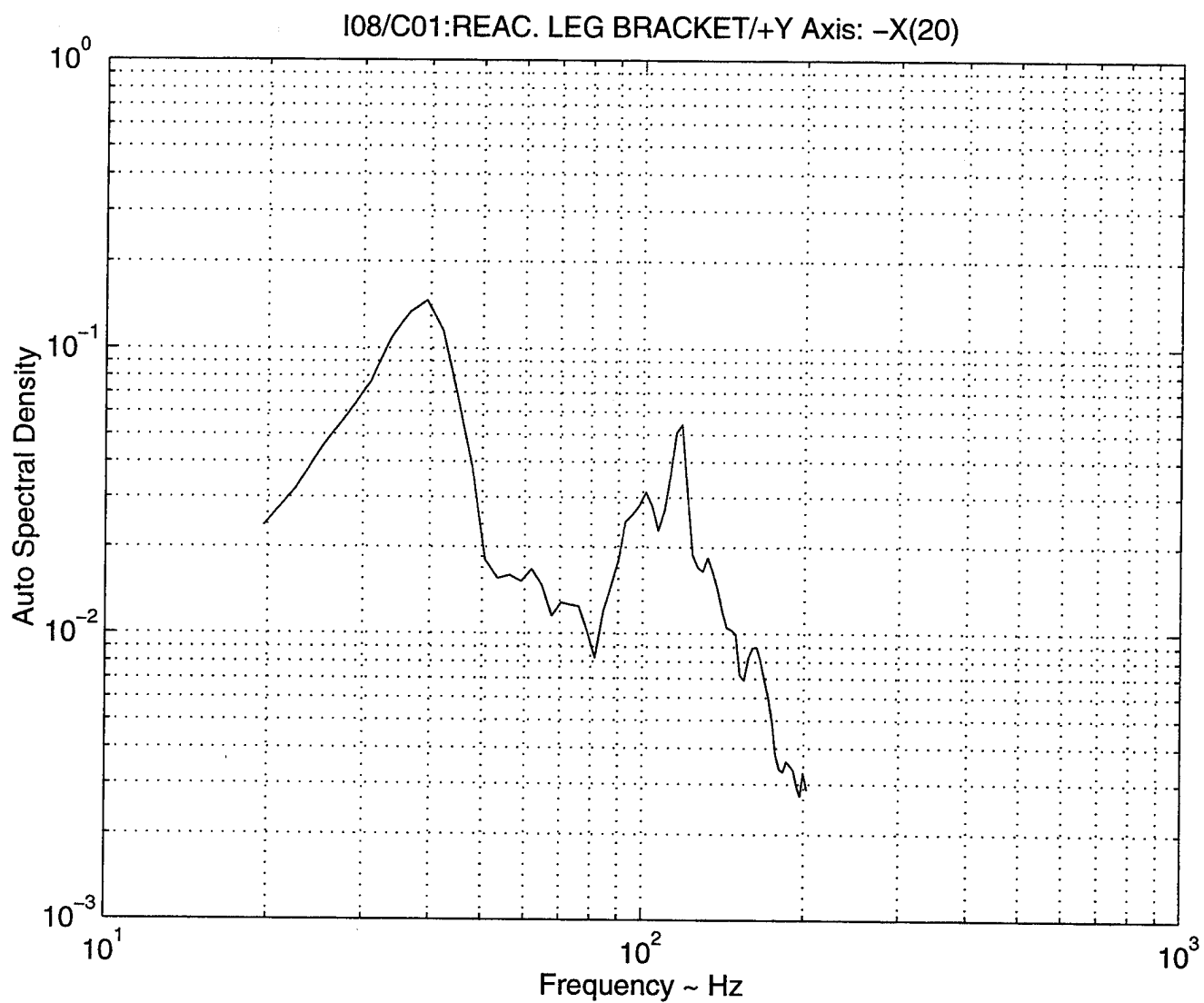


Figure 5.1. PSD response for the reactor leg bracket accelerometer instrument number 8 in the X (axial) direction. This point and direction on the Ya-21U correlates to node 75 in the X(axial) direction on the TOPAZ finite element model.

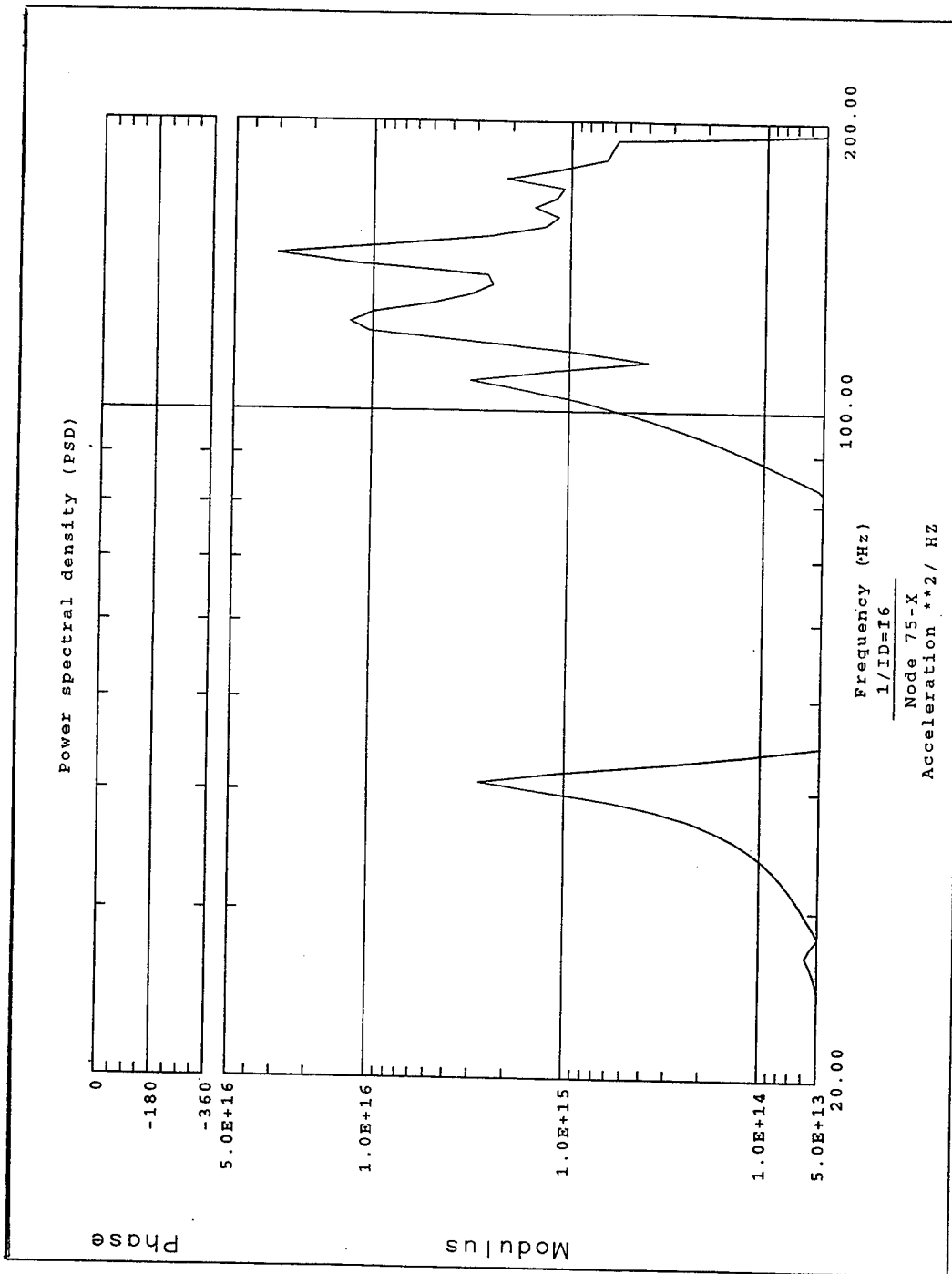


Figure 5.2. PSD response for node 75 in the X (axial) direction.

Comparison

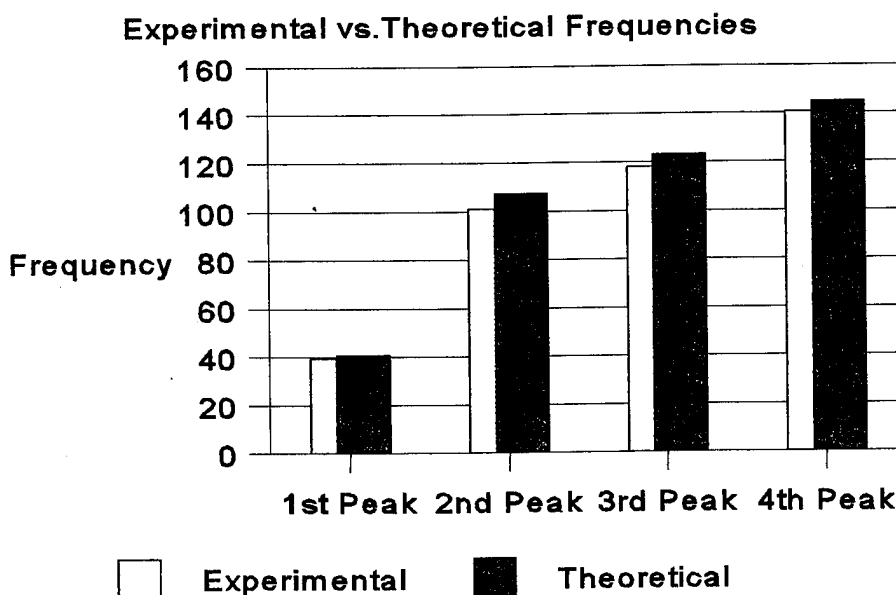


Figure 5.3. Graphic representation of comparison of experimental PSD axial response with theoretical axial response for node 75.

<i>Peak</i>	<i>Experimental Freq.</i>	<i>Theoretical Freq.</i>
1	39.3775	40.83
2	101.257	107.4
3	118.133	123.3
4	140.634	144.9

Table 5.5. Comparison of experimental PSD axial response with theoretical axial response for node 75.

Comparison of the theoretical natural frequencies with experimental natural frequencies for each mode are shown in Figure 5.4 and given in Table 5.6.

Comparison of theoretical results with experimental data indicate that the theoretical frequencies are slightly higher, but very close to experimental frequencies. Similar peaks and frequencies indicate that this model represents the Ya-21U

unit well and can be used to conduct further experimentation rather than test the actual unit to possible fatigue.

A summary of theoretical results as compared to the experimental data from NMERI for each tested node is detailed in Appendix E.

Mode	Theor Freq ~ Hz	Exper Freq ~ Hz	Error
1	9.294983		-
2	9.4301386		-
3	27.61518	25.3141	8.33%
4,5	40.57694	39.3775	2.96%
6	51.03082	53.4409	4.72%
7,8	58.43505	59.0663	1.08%
9	62.67895	61.879	1.28%
10,11	81.08845	81.5677	0.59%
12	98.03754	101.257	3.28%
13,14	108.2107	112.507	3.97%
16,17,18	121.0176	118.1	2.41%
19,20,21	124.4208	123.758	0.53%
22	142.177	140.634	1.09%
23,24	143.8577	143.447	0.29%
25	149.2695	151.885	1.75%
26	162.64	160.323	1.42%
27,28	165.166	168.761	2.18%
29,30	172.3828	171.574	0.47%
31,32,33	174.3021	174.386	0.05%
34	182.3664	182.824	0.25%
35,36	186.0211	185.637	0.21%
37,38	190.7578	188.133	1.38%
39	193.368	194.075	0.37%
40	201.081	199.7	0.69%

Table 5.6. Comparison of theoretical natural frequencies with experimental natural frequencies for each mode.

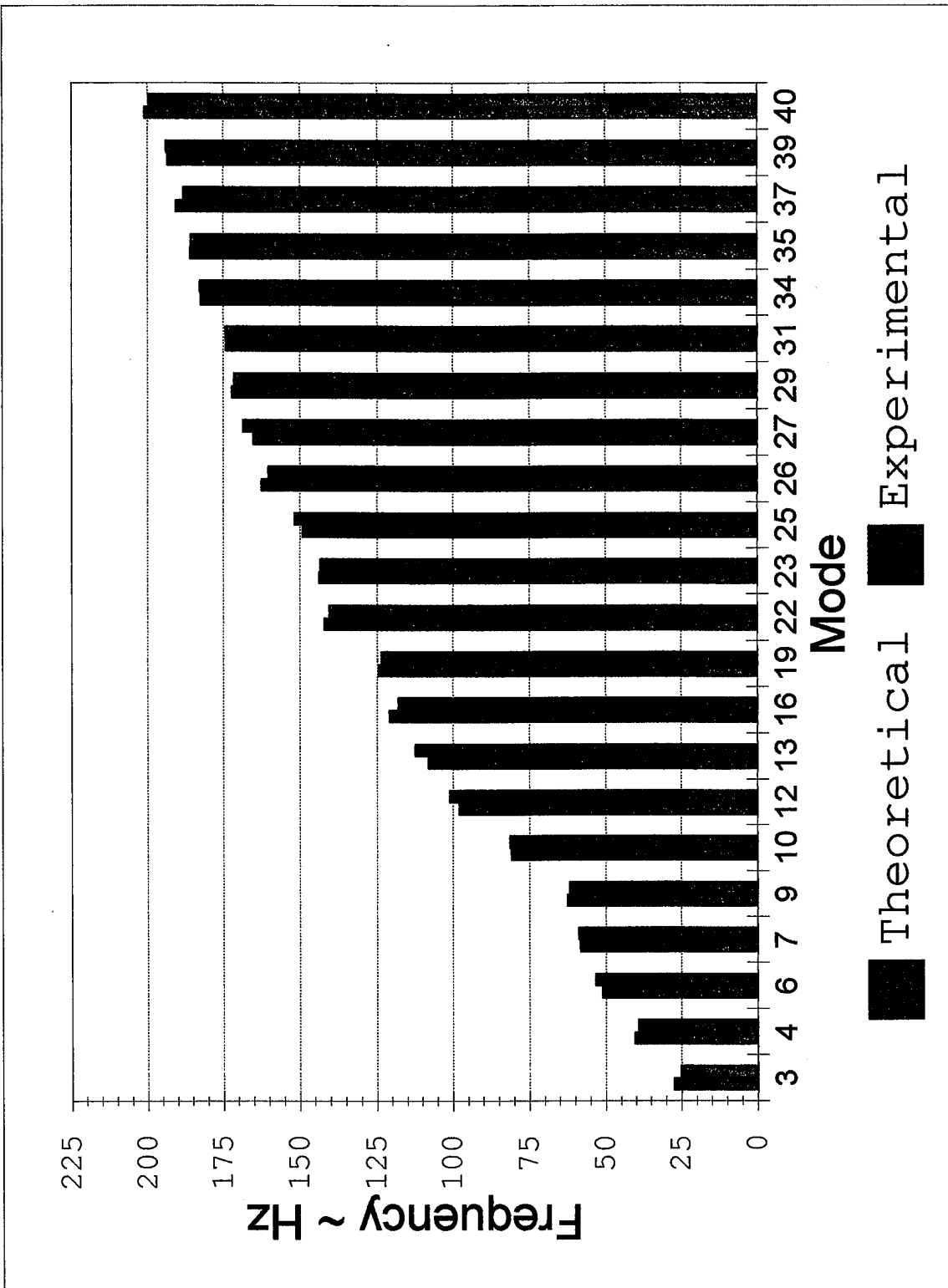


Figure 5.4. Graphical representation of comparison between theoretical natural frequencies and experimental natural frequencies for each mode.

VI. CONCLUSIONS AND RECOMMENDATIONS

A. CONCLUSIONS

The finite element model of TOPAZ-II is indeed an adequate analysis tool to simulate testing of the actual TOPAZ-II unit.

The normal dynamics analysis indicate that the highest stress level of the TOPAZ model is associated with mode five which shows the first axial compression. Other modes which are associated with high stresses are the first five modes.

The buckling analysis indicate that the TOPAZ can withstand a lateral acceleration of 12g's with a buckling factor of at least 14.2. This means that it would take an acceleration of 170.4g's to cause the unit to buckle. This buckling factor, however, is for the TOPAZ-II unit only. The mass of the satellite and the payload need to be considered; increasing the load on the TOPAZ-II will significantly decrease this buckling factor.

One other point which needs to be examined is that the Ya-21U unit is more flexible than the finite element model. Therefore, consideration should be given to the possibility of having to add stiffeners to the joints to ensure no buckling.

Analysis of the TOPAZ modal parameters of the finite element model have demonstrated to be within 8.33% of the experimental analysis of the Ya-21U unit. The I-DEAS software has proven to be an extremely valuable tool in the analysis of this system. Coordination and communication with NMERI is vital and has been good throughout this analysis.

B. RECOMMENDATIONS

The use of the present TOPAZ model is recommended for further analysis, rather than extensive testing on the actual TOPAZ units.

In addition, further improvements to the TOPAZ model are recommended. Although there were no errors while conducting analysis using this model, there were several warnings; most of which related to parabolic beam elements which were not well centered.

C. RESEARCH OPPORTUNITIES

There are many opportunities for further research in the area of structural analysis of the TOPAZ-II Nuclear Space Power System. NMERI is limited in their funding, yet there is a lot of work in this area. Some areas include the shock vibration analysis, and TOPAZ model modifications. The scientists at NMERI are looking to find additional Naval Postgraduate School students who are interested to work in this field to aid in validating this system.

APPENDIX A: THEORETICAL RANDOM VIBRATION PSD RESPONSE

A. Theoretical PSD response for axial excitation placed at the center of the test stand, node 339.

Node 5 DOF-X

Peak	Natural Freq ~ Hz	Modulus
1	40.83	2.98E+13
2	51.41	5.52E+13
3	107.4	4.60E+14
4	120.5	3.28E+15
5	144.9	8.34E+13
6	174.2	1.27E+15
7	195.4	2.36E+14

Node 5 DOF-Y

Peak	Natural Freq ~ Hz	Modulus
1	107.4	4.14E+14
2	123.3	1.90E+14
3	174.2	1.16E+15

Node 5 DOF-Z

Peak	Natural Freq ~ Hz	Modulus
1	40.83	4.14E+14
2	51.41	3.28E+14
3	107.4	2.10E+14
4	120.5	1.10E+16
5	144.9	2.83E+14
6	174.2	4.59E+15

Node 12 DOF-X

Peak	Natural Freq ~ Hz	Modulus
1	107.4	4.85E+16
2	120.5	6.89E+15
3	144.9	1.11E+16
4	174.2	2.91E+17

Node 12 DOF-Y

Peak	Natural Freq ~ Hz	Modulus
1	107.4	1.35E+16
2	120.5	3.85E+14
3	144.9	3.29E+15
4	174.2	2.91E+17

Node 12 DOF-Z

Peak	Natural Freq ~ Hz	Modulus
1	40.83	4.94E+13
2	51.41	4.53E+14
3	107.4	5.48E+14
4	123.3	2.65E+15
5	144.89	7.73E+13
6	174.19	1.18E+15

Node 24 DOF-X

Peak	Natural Freq ~ Hz	Modulus
1	107.4	4.95E+16
2	120.5	7.52E+15
3	144.9	1.17E+16
4	174.2	2.75E+17

Node 24 DOF-Y

Peak	Natural Freq ~ Hz	Modulus
1	107.4	1.30E+16
2	144.9	3.50E+15
3	174.2	7.74E+16

Node 24 DOF-Z

Peak	Natural Freq ~ Hz	Modulus
1	40.83	8.93E+13
2	51.41	4.61E+14
3	107.4	9.12E+14
4	120.5	6.35E+15
5	174.2	2.26E+15

Node 29 DOF-X

Peak	Natural Freq ~ Hz	Modulus
1	40.83	1.96E+16
2	107.4	3.42E+17
3	123.3	7.86E+17
4	174.2	6.62E+17

Node 29 DOF-Y

Peak	Natural Freq ~ Hz	Modulus
1	40.83	2.77E+14
2	79.62	8.34E+13
3	107.4	4.12E+15
4	120.5	2.79E+16
5	174.2	8.82E+15

Node 29 DOF-Z

Peak	Natural Freq ~ Hz	Modulus
1	51.41	5.40E+15
2	107.4	7.16E+15
3	123.3	1.03E+16
4	174.2	5.12E+16

Node 55 DOF-X

Peak	Natural Freq ~ Hz	Modulus
1	40.83	4.94E+16
2	107.4	5.62E+15
3	123.3	4.57E+16
4	174.2	2.17E+17
5	191	4.82E+16

Node 55 DOF-Y

Peak	Natural Freq ~ Hz	Modulus
1	40.83	2.15E+15
2	107.4	2.81E+16
3	123.3	3.21E+16
4	174.2	2.88E+16
5	191	4.76E+16

Node 55 DOF-Z

Peak	Natural Freq ~ Hz	Modulus
1	41.79	3.43E+14
2	51.41	1.10E+16
3	107.4	2.74E+15
4	123.3	3.52E+15
5	148.3	7.10E+14
6	170.2	1.86E+15
7	191	1.22E+16

Node 75 DOF-X

Peak	Natural Freq ~ Hz	Modulus
1	40.83	2.72E+15
2	107.4	3.17E+15
3	123.3	1.29E+16
4	144.9	3.03E+16
5	174.2	2.13E+15

Node 75 DOF-Y

Peak	Natural Freq ~ Hz	Modulus
1	40.83	4.08E+13
2	107.4	2.35E+13
3	120.5	1.81E+14
4	148.3	1.17E+15
5	182.4	5.37E+14

Node 75 DOF-Z

Peak	Natural Freq ~ Hz	Modulus
1	39.91	1.84E+14
2	51.41	1.54E+16
3	120.5	3.77E+14
4	148.3	7.90E+14
5	170.2	1.22E+15
6	182.4	2.46E+15

Node 79 DOF-X

Peak	Natural Freq ~ Hz	Modulus
1	40.83	2.99E+15
2	107.4	3.08E+15
3	123.3	1.34E+16
4	144.9	4.27E+16
5	174.2	7.18E+15

Node 79 DOF-Y

Peak	Natural Freq ~ Hz	Modulus
1	40.83	5.48E+13
2	107.4	2.30E+13
3	120.5	2.78E+14
4	148.3	6.19E+14
5	178.3	1.18E+15
6	195.4	4.99E+14

Node 79 DOF-Z

Peak	Natural Freq ~ Hz	Modulus
1	40.83	3.06E+15
2	51.41	1.57E+16
3	107.4	1.94E+15
4	120.5	3.13E+15
5	144.9	7.69E+15
6	170.2	1.25E+16
7	191	2.65E+16

Node 92 DOF-X

Peak	Natural Freq ~ Hz	Modulus
1	40.83	5.24E+16
2	79.62	3.99E+14
3	107.4	2.74E+16
4	123.3	7.57E+16
5	144.9	2.32E+16
6	170.2	1.62E+16
7	191	9.73E+16

Node 92 DOF-Y

Peak	Natural Freq ~ Hz	Modulus
1	40.83	7.52E+14
2	7.962	1.60E+13
3	107.4	1.09E+16
4	120.5	1.24E+15
5	151.7	8.87E+14
6	182.4	7.92E+15

Node 92 DOF-Z

Peak	Natural Freq ~ Hz	Modulus
1	39.91	1.62E+14
2	51.41	1.64E+16
3	120.5	6.11E+14
4	148.3	4.25E+14
5	191	1.64E+15

Node 97 DOF-X

Peak	Natural Freq ~ Hz	Modulus
1	40.83	5.24E+16
2	79.62	4.01E+14
3	107.4	2.73E+16
4	123.3	7.49E+16
5	144.9	2.27E+16
6	170.2	1.57E+16
7	191	8.72E+16

Node 97 DOF-Y

Peak	Natural Freq ~ Hz	Modulus
1	40.83	7.51E+14
2	79.62	1.65E+13
3	107.4	9.92E+13
4	120.5	1.12E+15
5	151.7	8.03E+14
6	182.4	7.63E+15

Node 97 DOF-Z

Peak	Natural Freq ~ Hz	Modulus
1	40.83	1.81E+15
2	51.41	1.67E+16
3	107.4	3.38E+15
4	120.5	7.95E+15
5	144.9	4.18E+15
6	162.6	2.97E+14

B. Theoretical PSD response for lateral excitation placed at the center of the test stand, node 339.

Node 5 DOF-X

Peak	Natural Freq ~ Hz	Modulus
1	41.79	3.50E+11
2	51.41	1.31E+13
3	107.4	4.67E+12
4	120.5	5.05E+13
5	174.2	6.45E+12

Node 5 DOF-Y

Peak	Natural Freq ~ Hz	Modulus
1	107.4	4.20E+13
2	123.3	5.81E+12
3	174.2	7.18E+13
4	195.4	4.97E+11

Node 5 DOF-Z

Peak	Natural Freq ~ Hz	Modulus
1	41.79	1.88E+12
2	51.41	7.81E+13
3	107.4	2.02E+13
4	120.5	1.60E+14
5	174.2	2.38E+13
6	191	1.06E+13

Node 12 DOF-X

Peak	Natural Freq ~ Hz	Modulus
1	51.41	3.93E+12
2	107.4	1.36E+14
3	120.5	3.14E+13
4	144.9	3.57E+13
5	174.2	1.52E+15

Node 12 DOF-Y

Peak	Natural Freq ~ Hz	Modulus
1	51.41	1.05E+13
2	107.4	3.78E+13
3	120.5	3.16E+12
4	144.9	1.19E+13
5	174.2	4.47E+14

Node 12 DOF-Z

Peak	Natural Freq ~ Hz	Modulus
1	40.83	1.31E+12
2	51.41	1.05E+15
3	95.73	8.94E+11
4	109.9	1.78E+12
5	123.3	1.95E+13
6	174.2	8.81E+12

Node 24 DOF-X

Peak	Natural Freq ~ Hz	Modulus
1	51.41	3.65E+12
2	107.4	4.14E+14
3	123.3	8.47E+13
4	144.9	3.80E+13
5	174.2	1.28E+15

Node 24 DOF-Y

Peak	Natural Freq ~ Hz	Modulus
1	51.41	1.12E+13
2	107.4	1.20E+14
3	123.3	9.02E+12
4	144.9	1.18E+13
5	174.2	3.31E+14

Node 24 DOF-Z

Peak	Natural Freq ~ Hz	Modulus
1	40.83	1.44E+12
2	51.41	1.06E+14
3	95.73	6.10E+11
4	107.4	2.76E+12
5	123.3	2.34E+13
6	174.2	2.37E+13

Node 29 DOF-X

Peak	Natural Freq ~ Hz	Modulus
1	40.83	1.83E+14
2	51.41	1.96E+13
3	79.62	1.98E+13
4	107.4	2.09E+15
5	123.3	7.41E+15
6	174.2	4.03E+15

Node 29 DOF-Y

Peak	Natural Freq ~ Hz	Modulus
1	107.4	2.73E+14
2	123.3	2.37E+14
3	174.2	3.55E+14

Node 29 DOF-Z

Peak	Natural Freq ~ Hz	Modulus
1	51.41	1.27E+15
2	109.9	3.42E+13
3	123.3	9.63E+13
4	174.2	3.73E+14

Node 55 DOF-X

Peak	Natural Freq ~ Hz	Modulus
1	40.83	4.57E+14
2	79.62	2.85E+12
3	107.4	3.99E+13
4	123.3	6.29E+14
5	174.2	1.45E+15
6	182.4	7.91E+14

Node 55 DOF-Y

Peak	Natural Freq ~ Hz	Modulus
1	40.83	9.06E+12
2	50.24	3.46E+12
3	79.62	2.30E+12
4	107.4	1.71E+14
5	123.3	6.06E+14
6	162.6	7.05E+13
7	191	4.26E+14

Node 55 DOF-Z

Peak	Natural Freq ~ Hz	Modulus
1	51.41	2.58E+15
2	107.4	6.21E+13
3	120.5	1.01E+14
4	141.6	1.22E+13
5	162.6	9.12E+12
6	182.4	3.64E+13
7	195.4	1.10E+13

Node 75 DOF-X

Peak	Natural Freq ~ Hz	Modulus
1	26.98	8.60E+11
2	40.83	2.54E+13
3	79.62	3.10E+11
4	107.4	1.33E+13
5	123.3	1.03E+14
6	144.9	1.44E+14
7	195.4	2.38E+13

Node 75 DOF-Y

Peak	Natural Freq ~ Hz	Modulus
1	107.4	2.99E+11
2	148.3	1.13E+14
3	182.4	2.89E+13

Node 75 DOF-Z

Peak	Natural Freq ~ Hz	Modulus
1	51.41	3.56E+15
2	148.3	9.22E+13
3	170.4	7.82E+13
4	182.4	1.28E+14

Node 79 DOF-X

Peak	Natural Freq ~ Hz	Modulus
1	26.98	6.21E+11
2	40.83	2.79E+13
3	107.4	1.61E+13
4	123.3	1.24E+14
5	144.9	1.98E+14
6	174.2	4.03E+13
7	195.4	1.02E+13

Node 79 DOF-Y

Peak	Natural Freq ~ Hz	Modulus
1	27.61	2.16E+11
2	107.4	1.12E+12
3	120.5	3.54E+12
4	148.3	7.11E+13
5	182.4	7.14E+13
6	195.4	5.40E+13

Node 79 DOF-Z

Peak	Natural Freq ~ Hz	Modulus
1	40.83	5.18E+13
2	51.41	3.52E+15
3	107.4	6.23E+13
4	120.5	6.68E+13
5	148.3	1.17E+14
6	170.2	1.82E+14
7	191	1.58E+14

Node 92 DOF-X

Peak	Natural Freq ~ Hz	Modulus
1	26.98	1.89E+12
2	40.83	4.92E+14
3	79.62	6.17E+12
4	107.4	1.78E+14
5	123.3	8.11E+14
6	170.2	1.24E+14
7	191	8.78E+14

Node 92 DOF-Y

Peak	Natural Freq ~ Hz	Modulus
1	40.83	7.11E+11
2	123.3	8.46E+11
3	151.7	5.21E+13
4	182.4	4.38E+14

Node 92 DOF-Z

Peak	Natural Freq ~ Hz	Modulus
1	51.41	3.79E+15
2	123.3	4.28E+13
3	148.3	5.33E+13
4	191	4.94E+13

Node 97 DOF-X

Peak	Natural Freq ~ Hz	Modulus
1	40.83	4.92E+14
2	79.62	6.12E+12
3	107.4	1.71E+14
4	123.3	7.75E+14
5	170.2	1.16E+14
6	191	6.96E+14

Node 97 DOF-Y

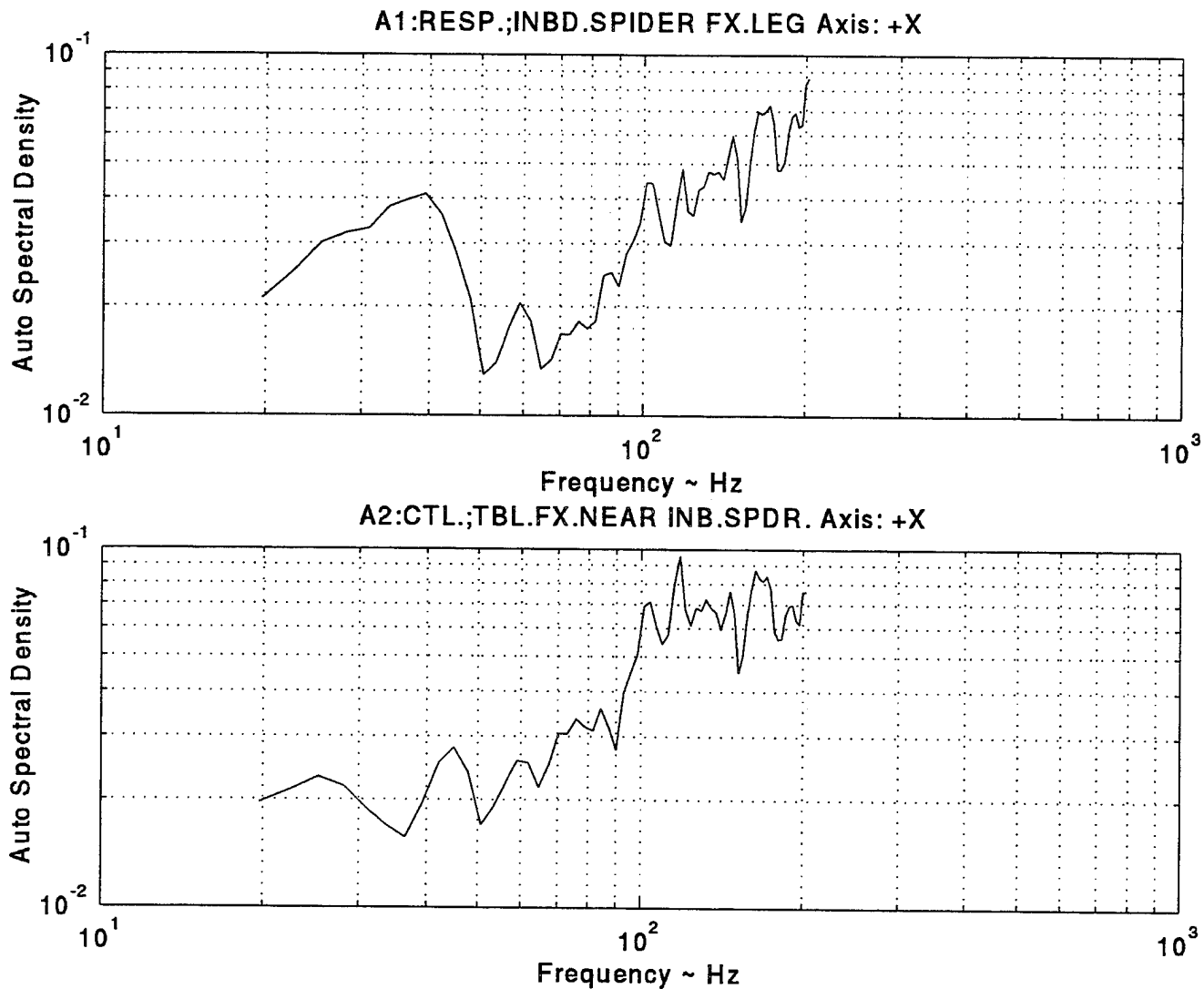
Peak	Natural Freq ~ Hz	Modulus
1	40.83	7.05E+11
2	151.7	4.60E+13
3	182.4	4.14E+14

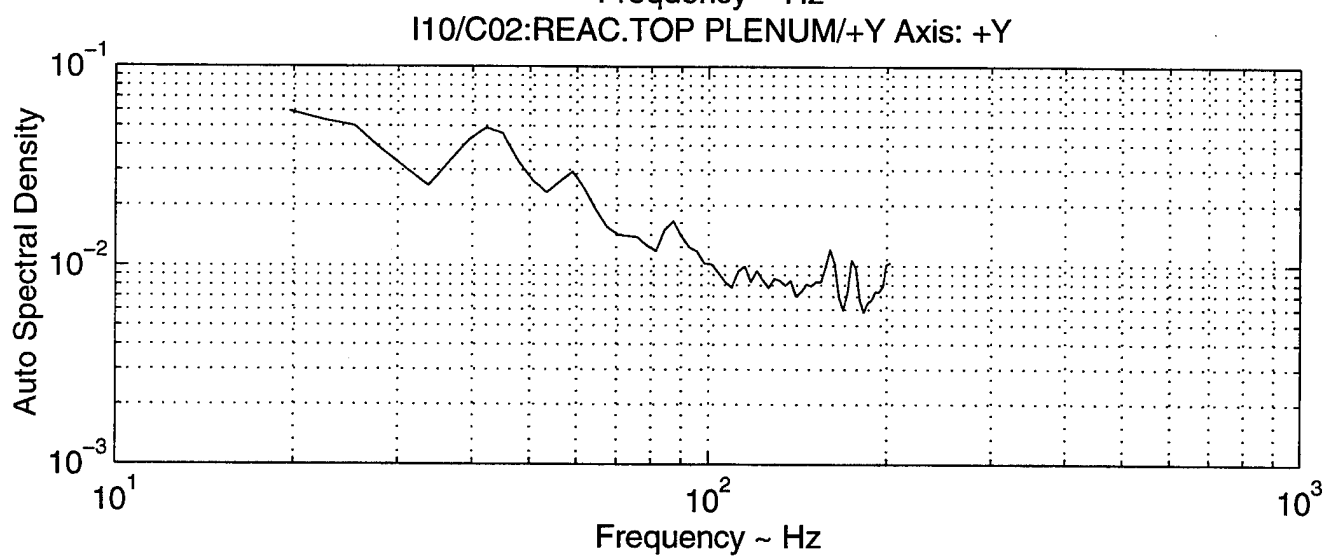
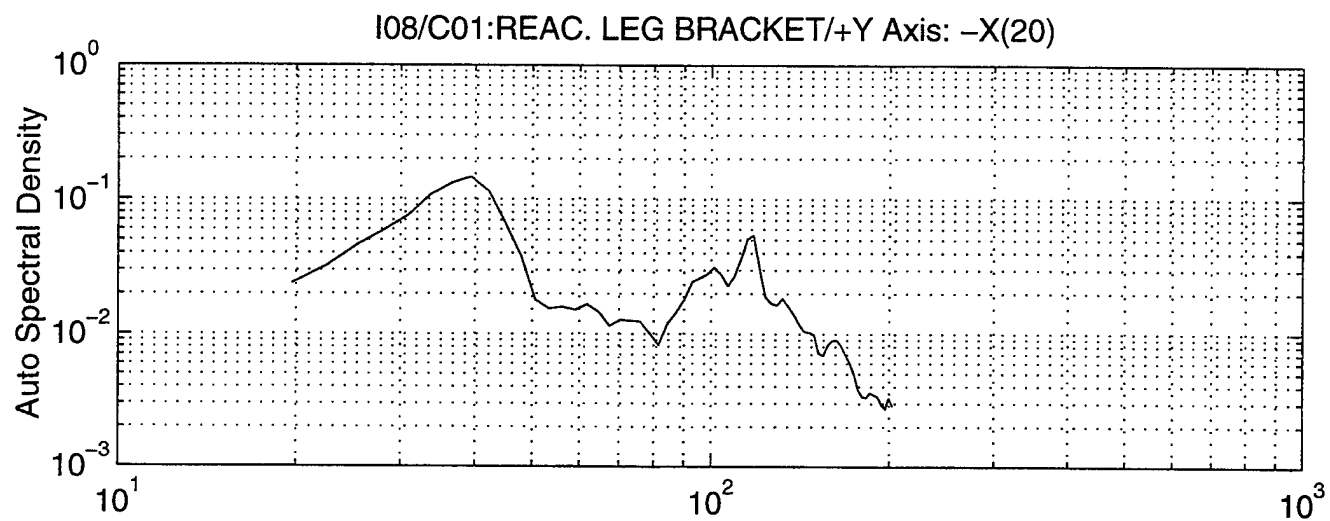
Node 97 DOF-Z

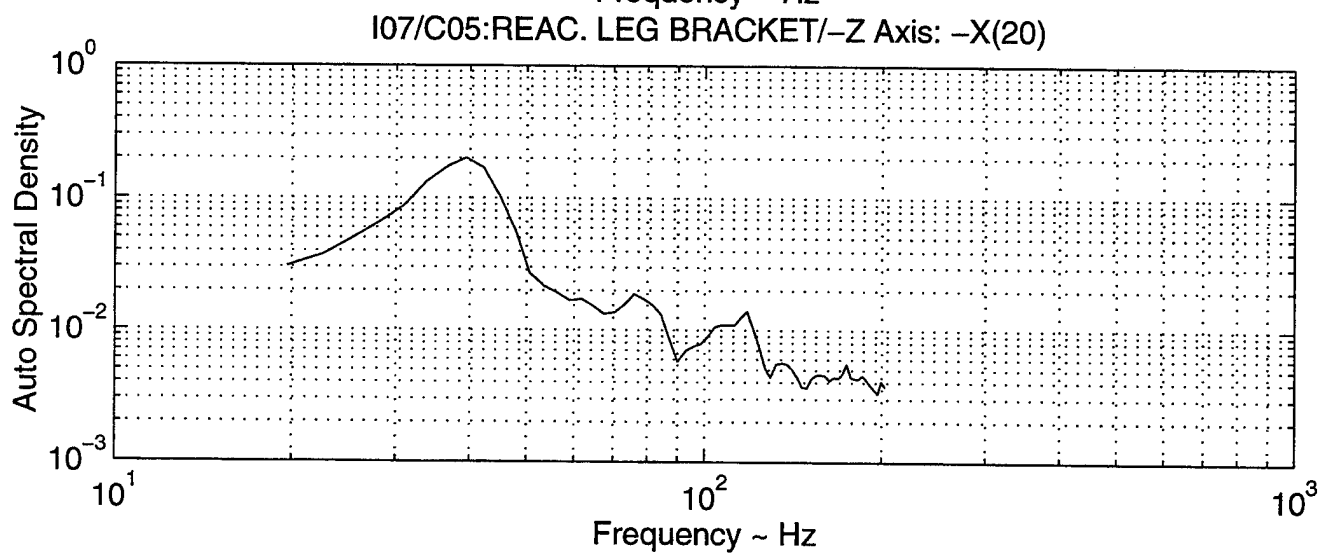
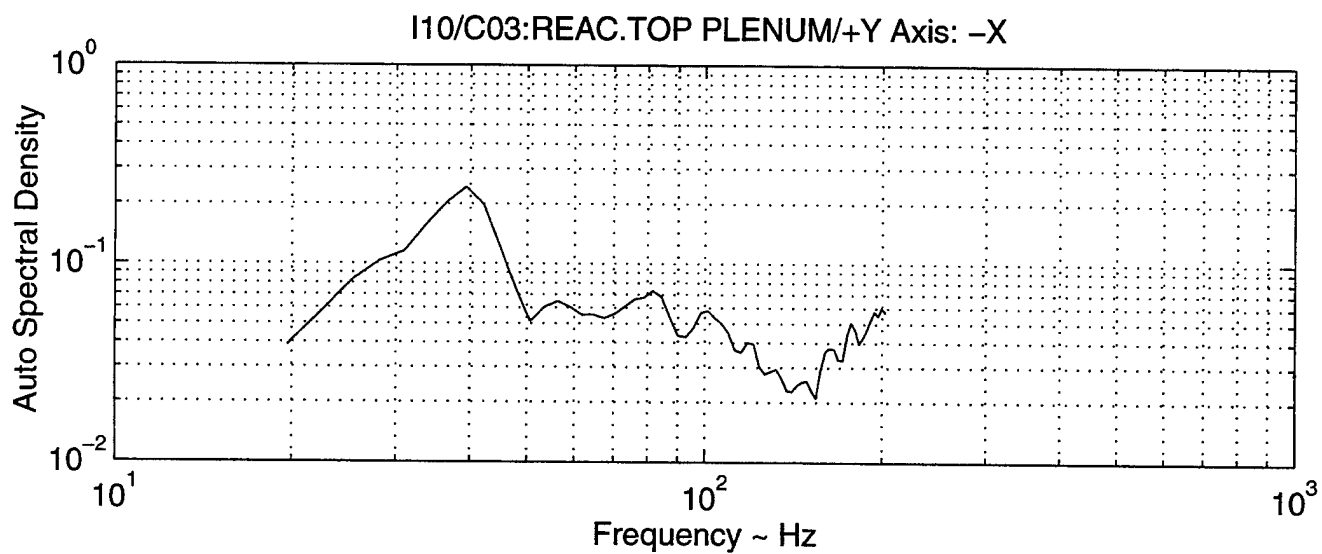
Peak	Natural Freq ~ Hz	Modulus
1	40.83	4.12E+13
2	51.41	3.77E+15
3	107.4	7.39E+13
4	120.5	9.80E+13
5	148.3	4.43E+13
6	195.4	

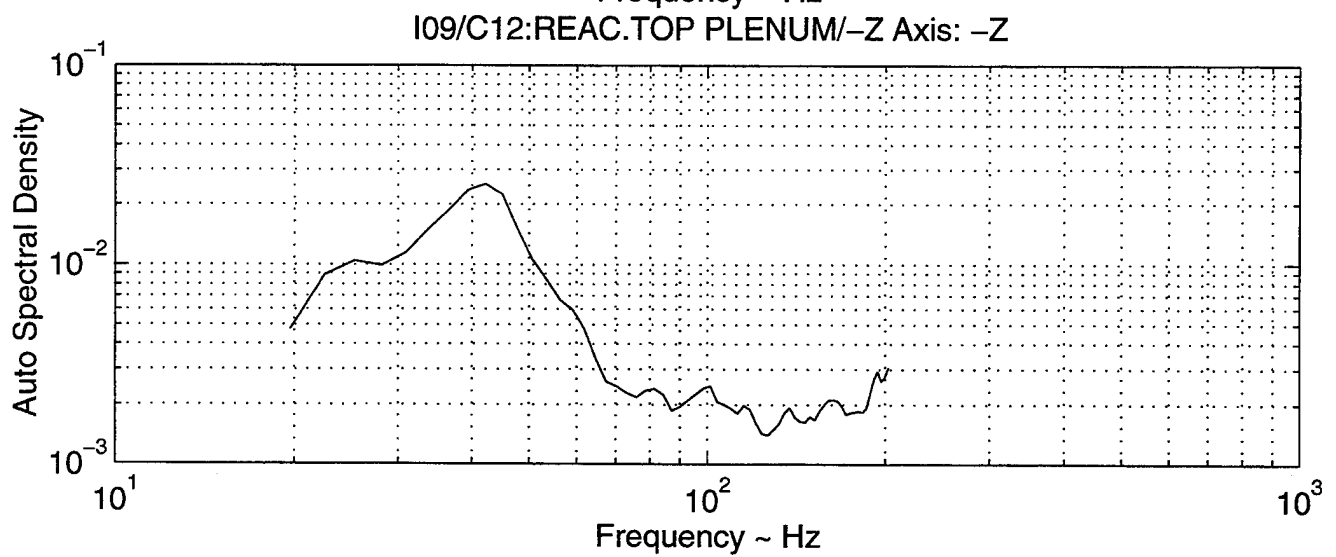
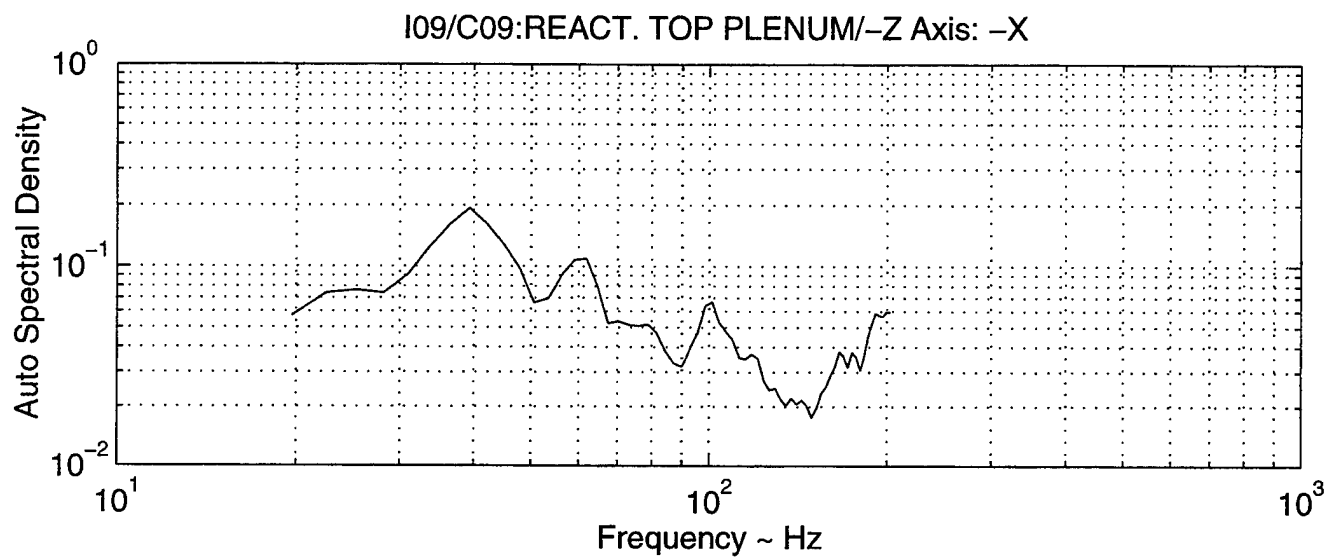
APPENDIX B: EXPERIMENTAL RANDOM VIBRATION PSD RESPONSE

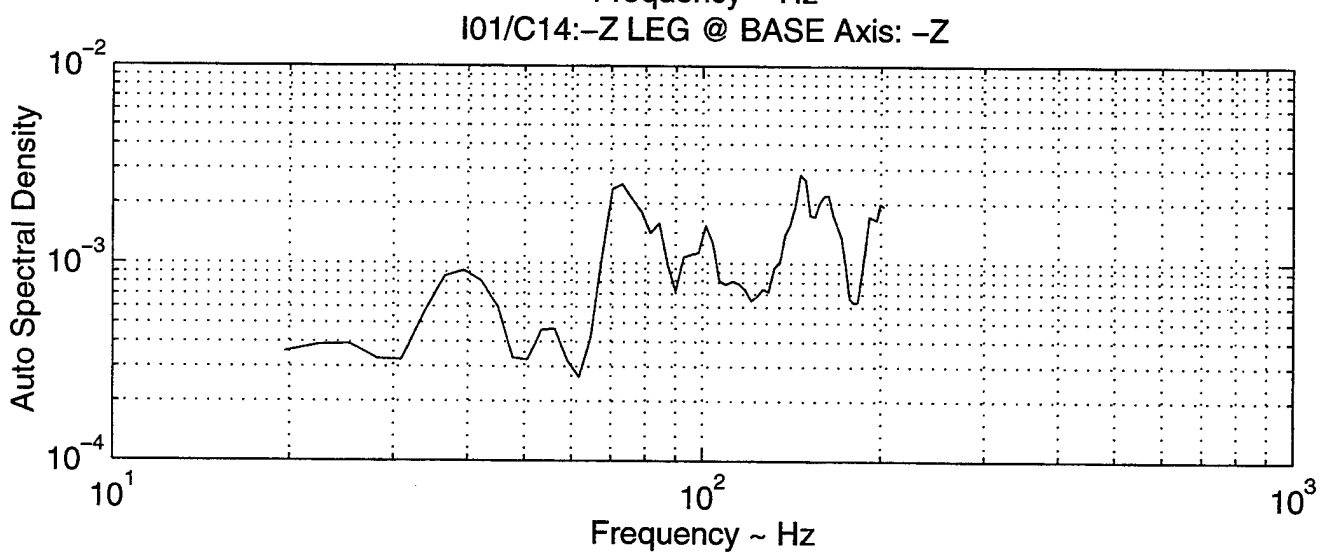
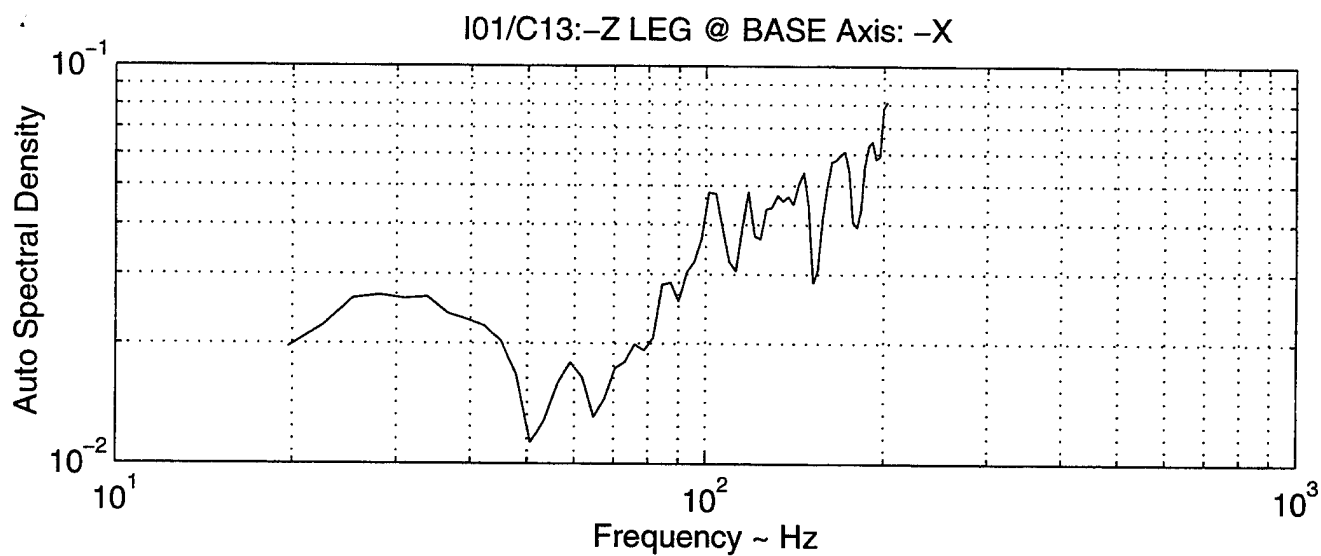
A. The following plots are the graphical representation of experimental PSD response (20 Hz - 200 Hz) for an axial excitation placed on the test stand.

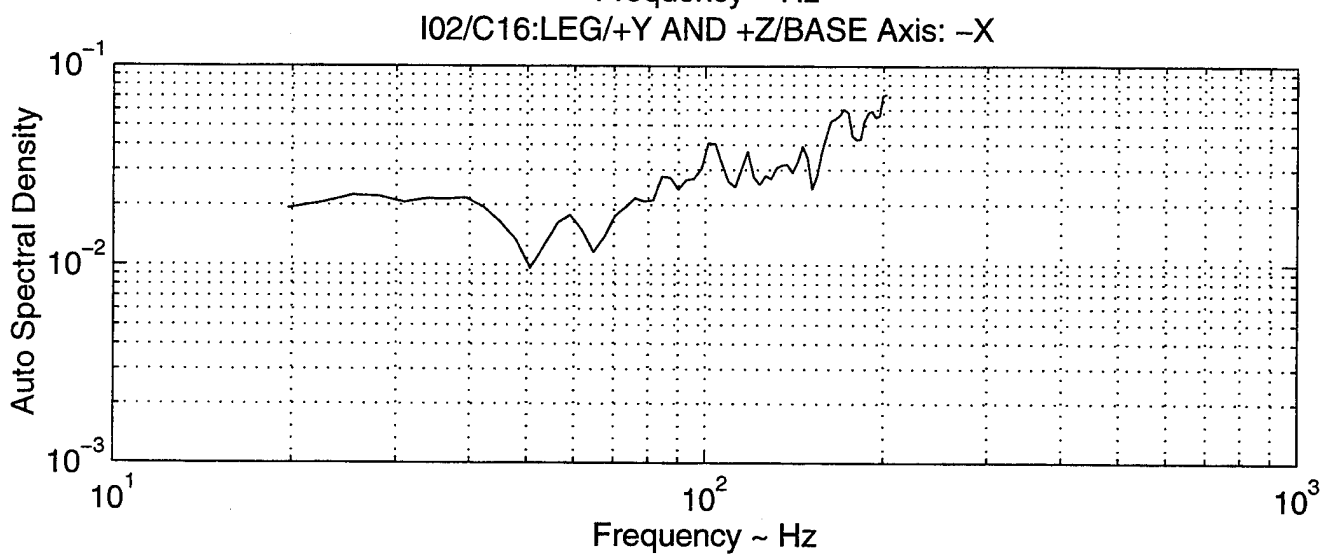
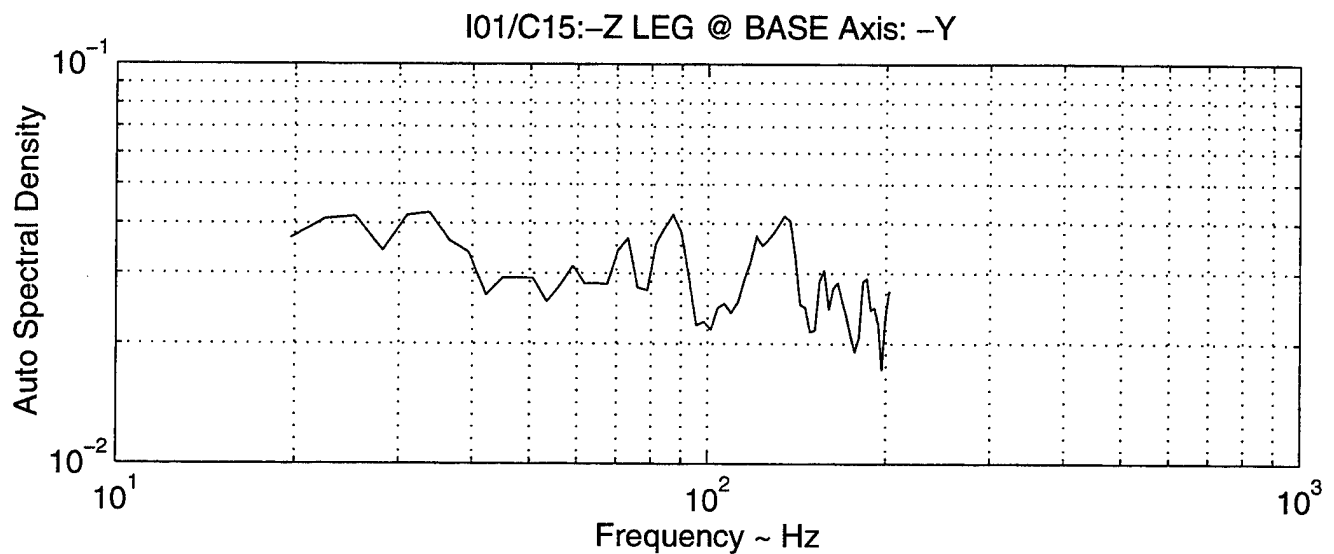


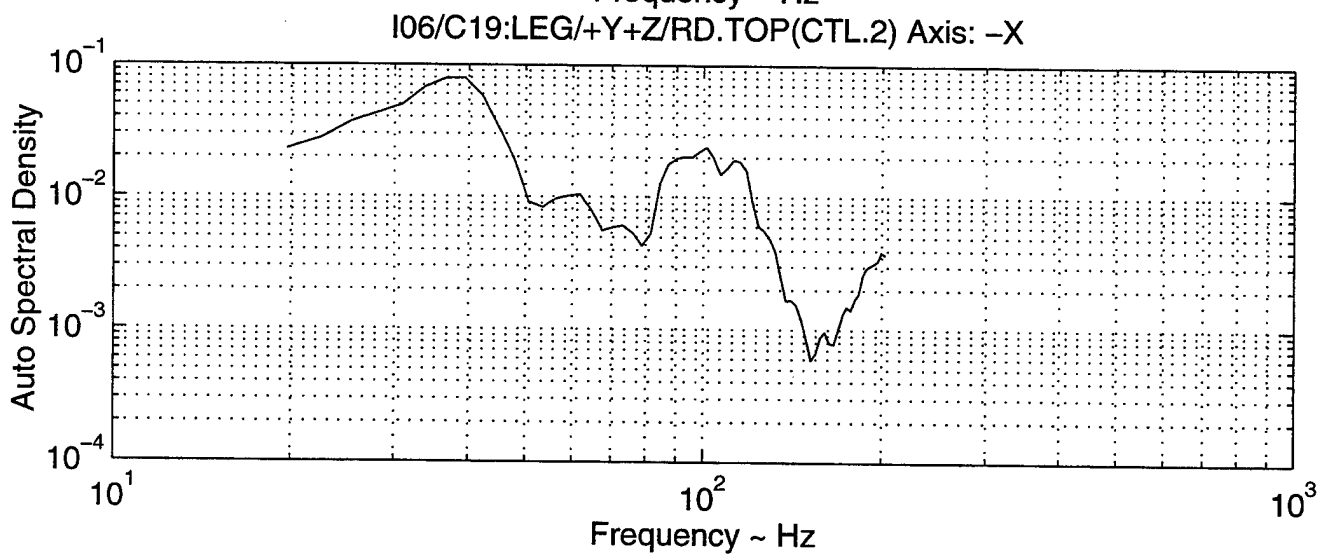
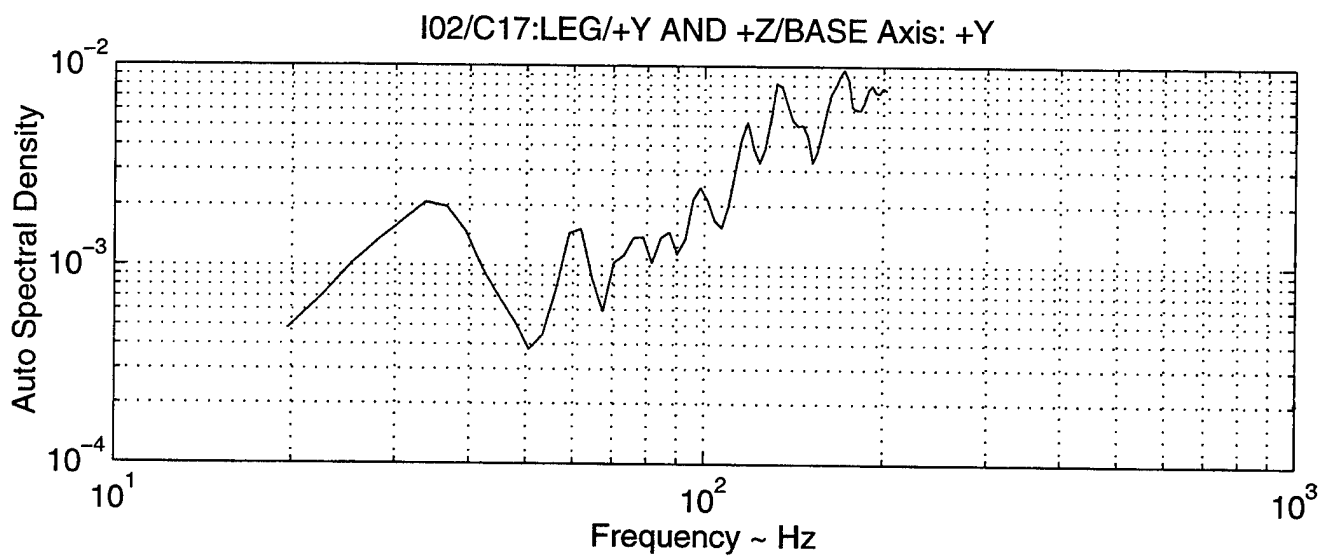


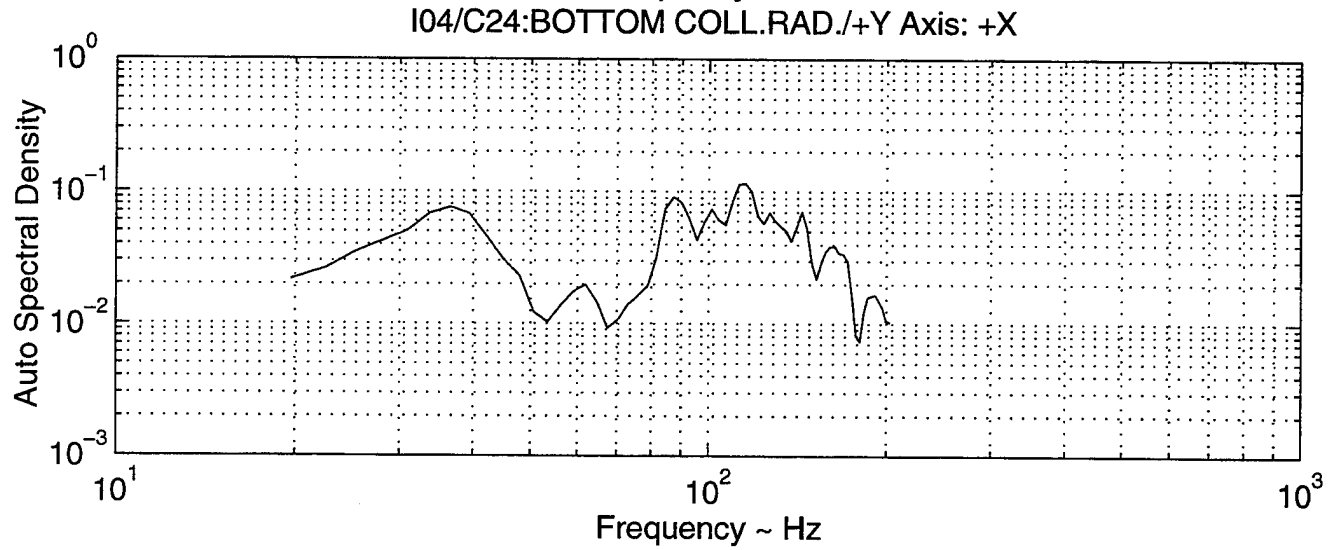
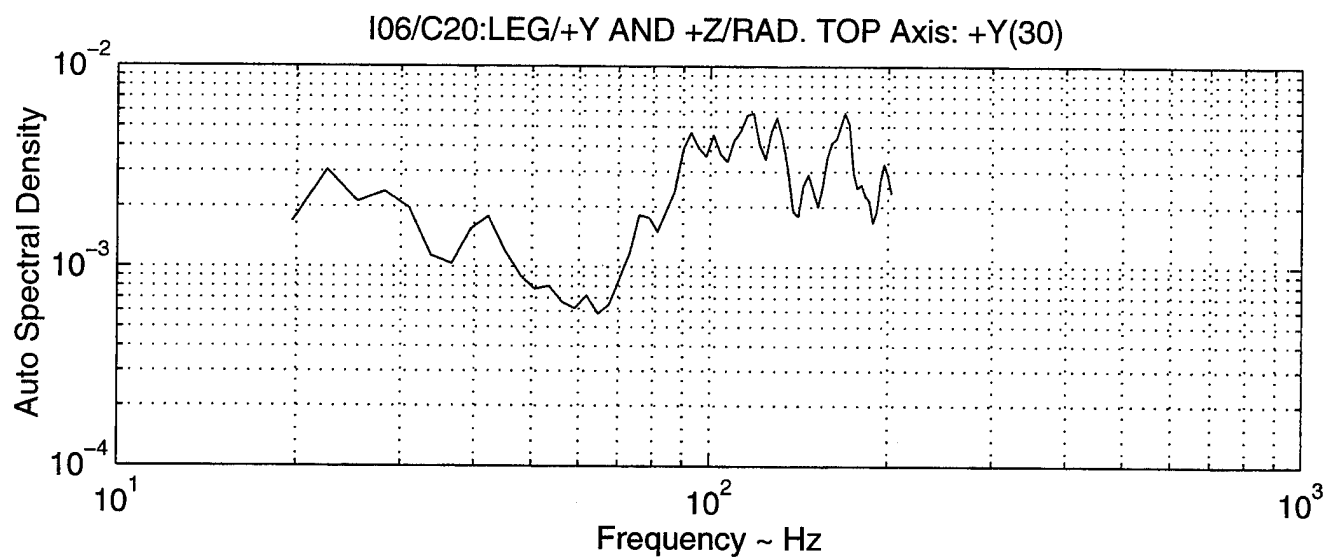


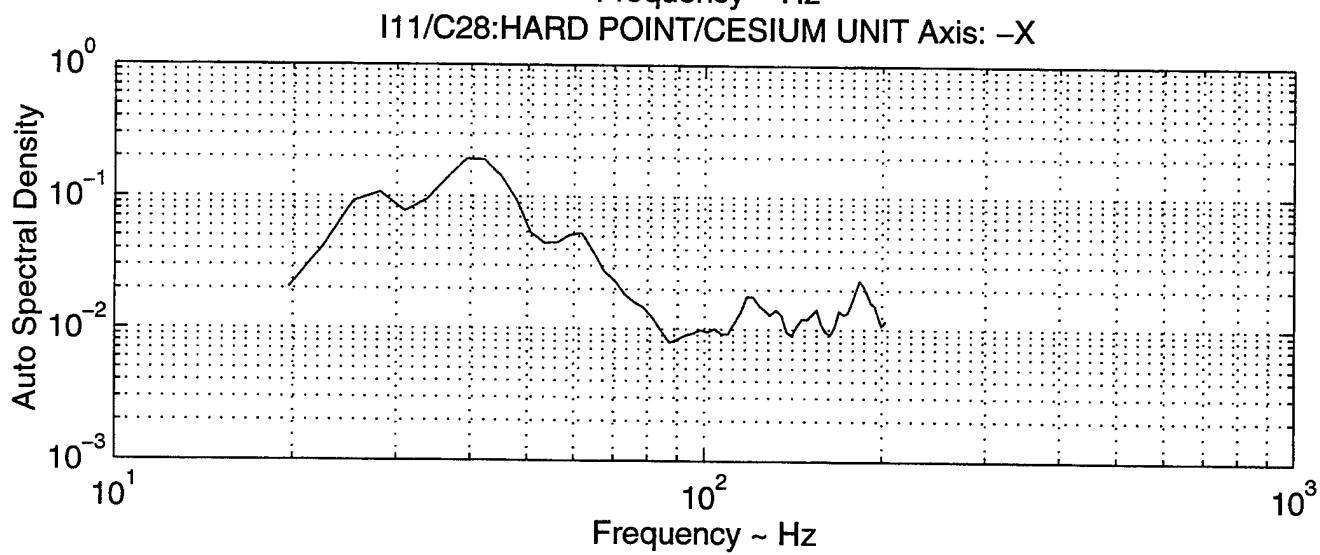
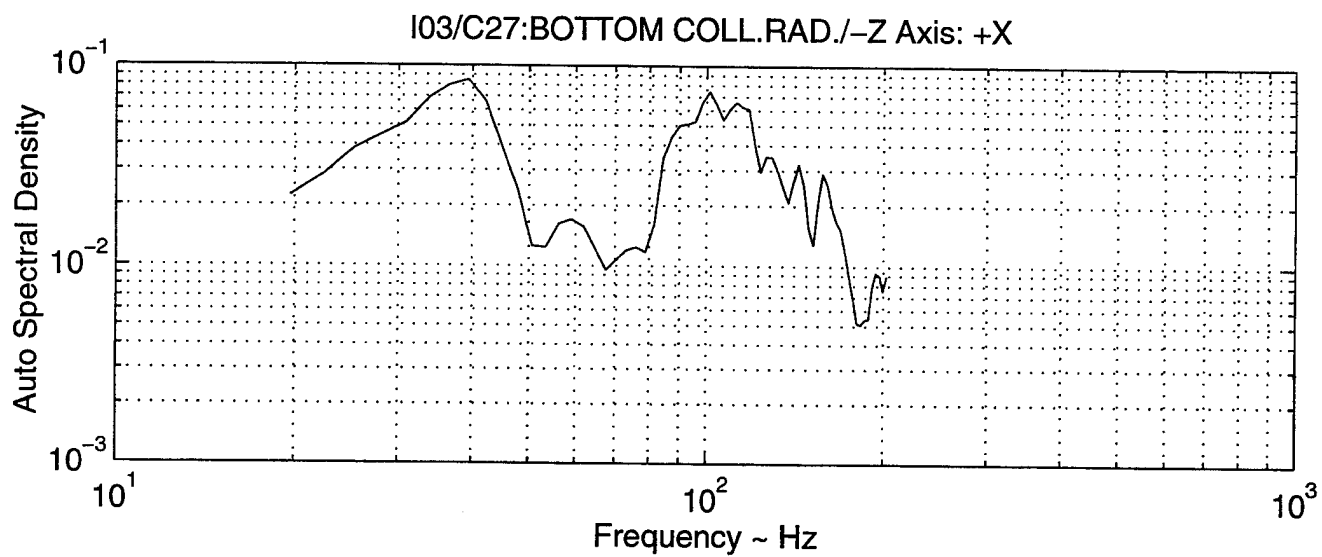


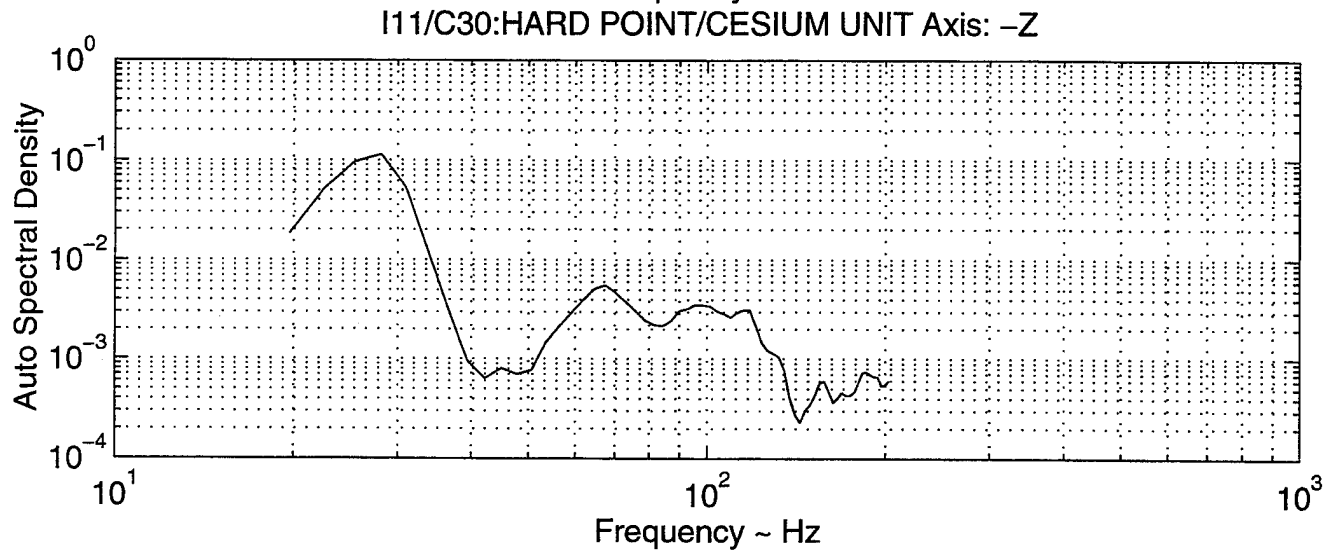
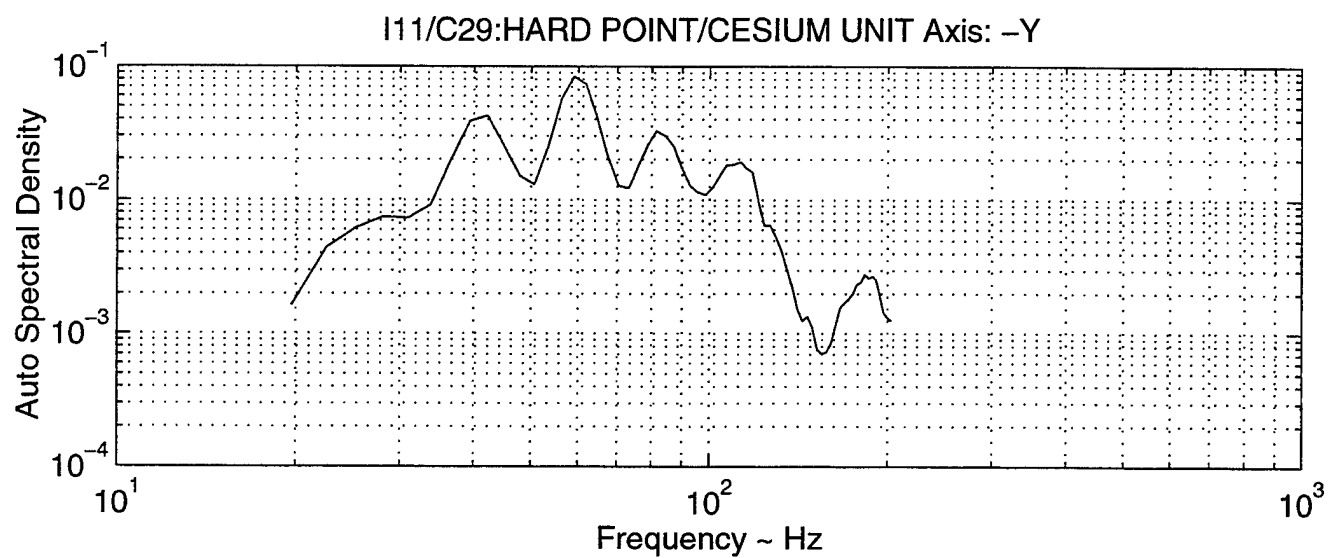




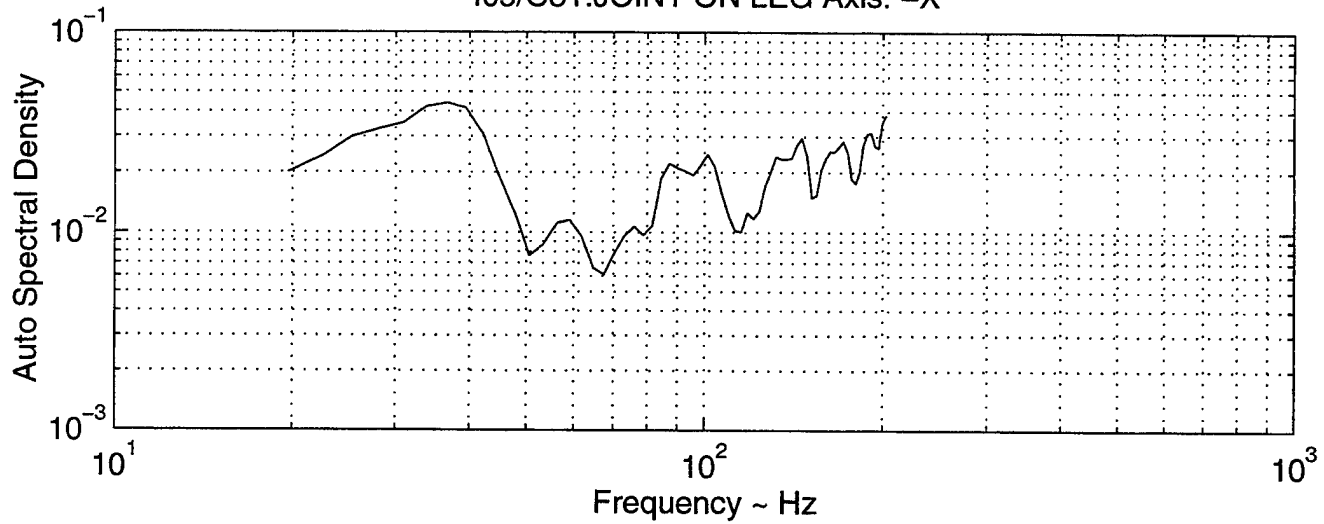




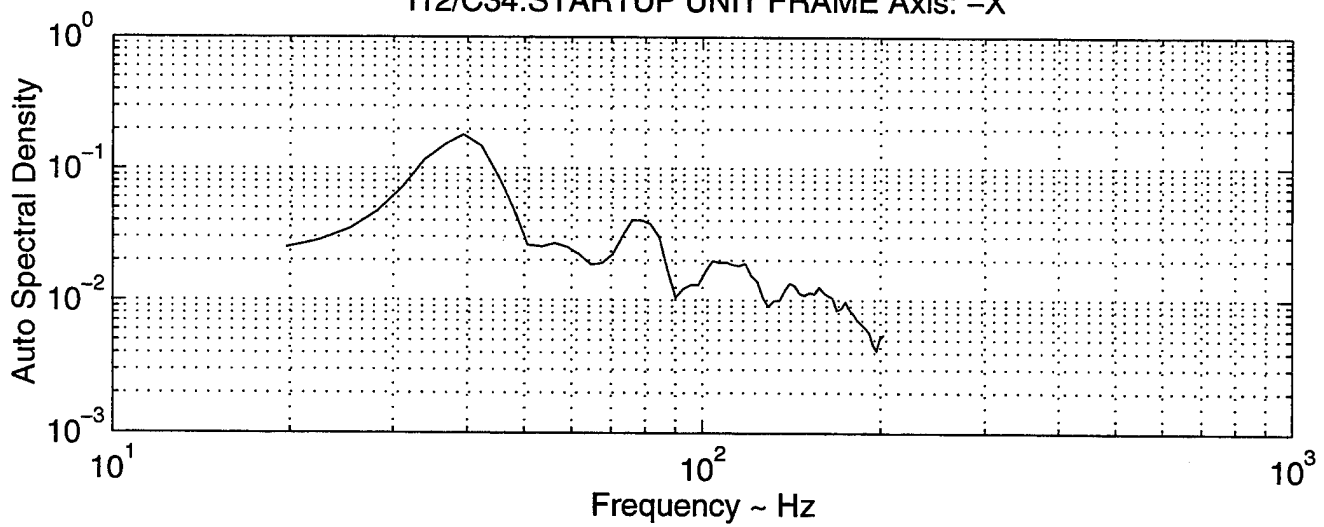


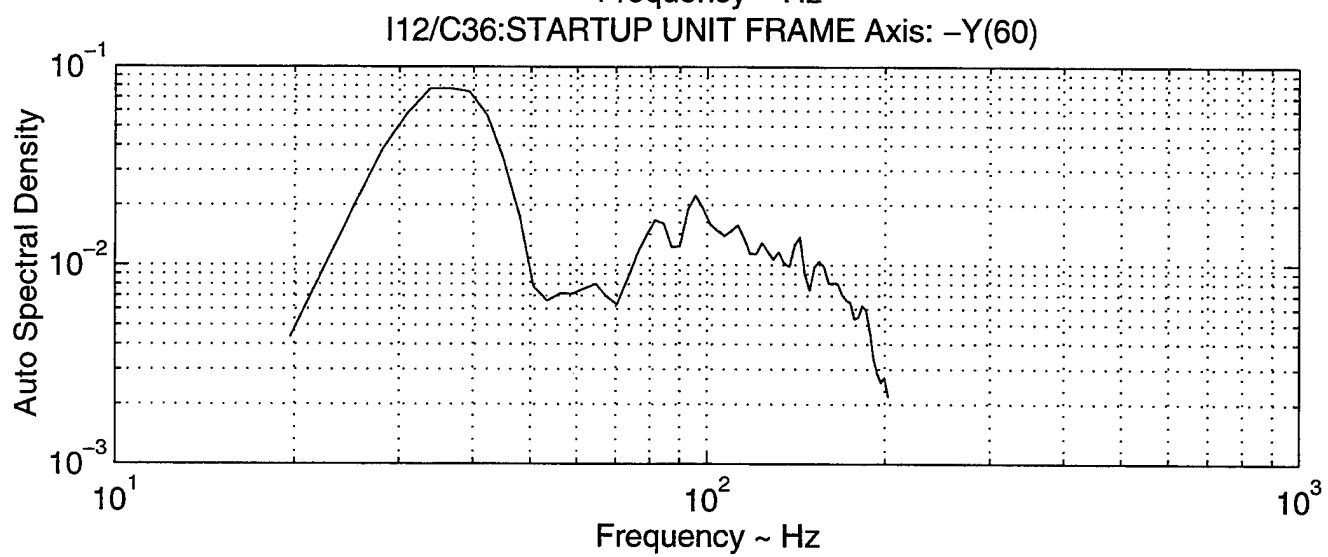
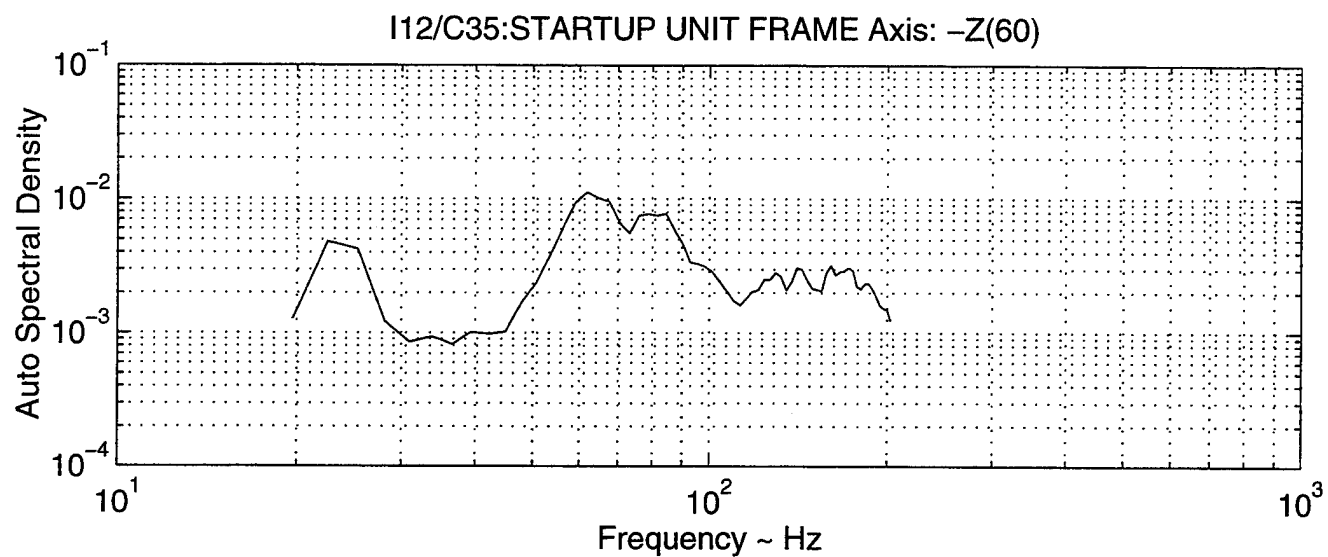


I05/C31:JOINT ON LEG Axis: -X

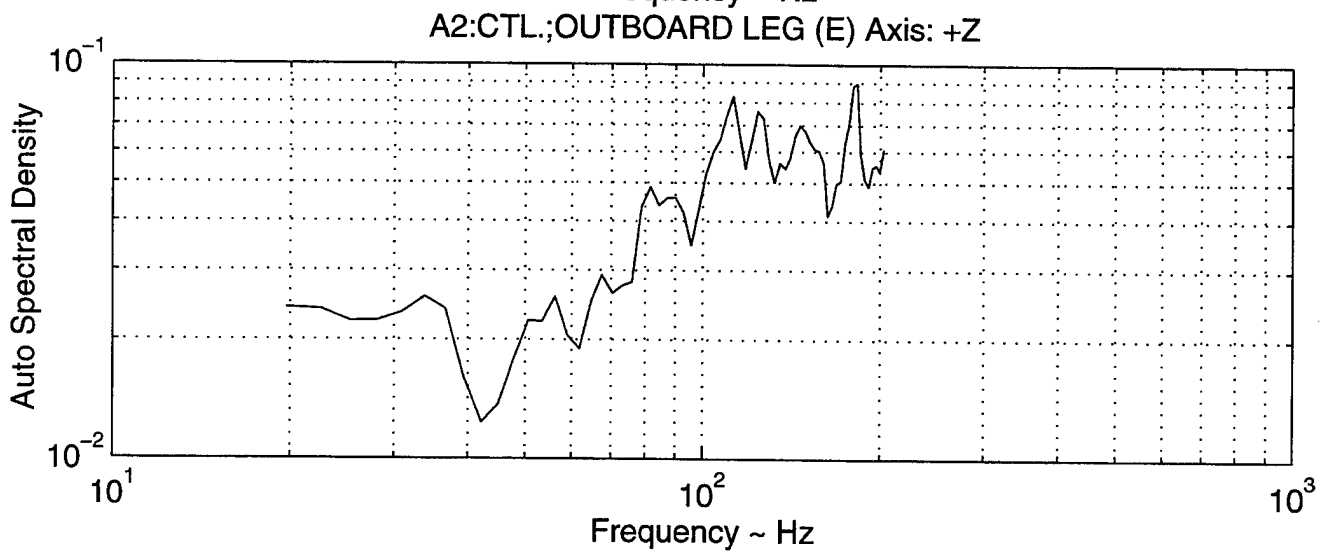
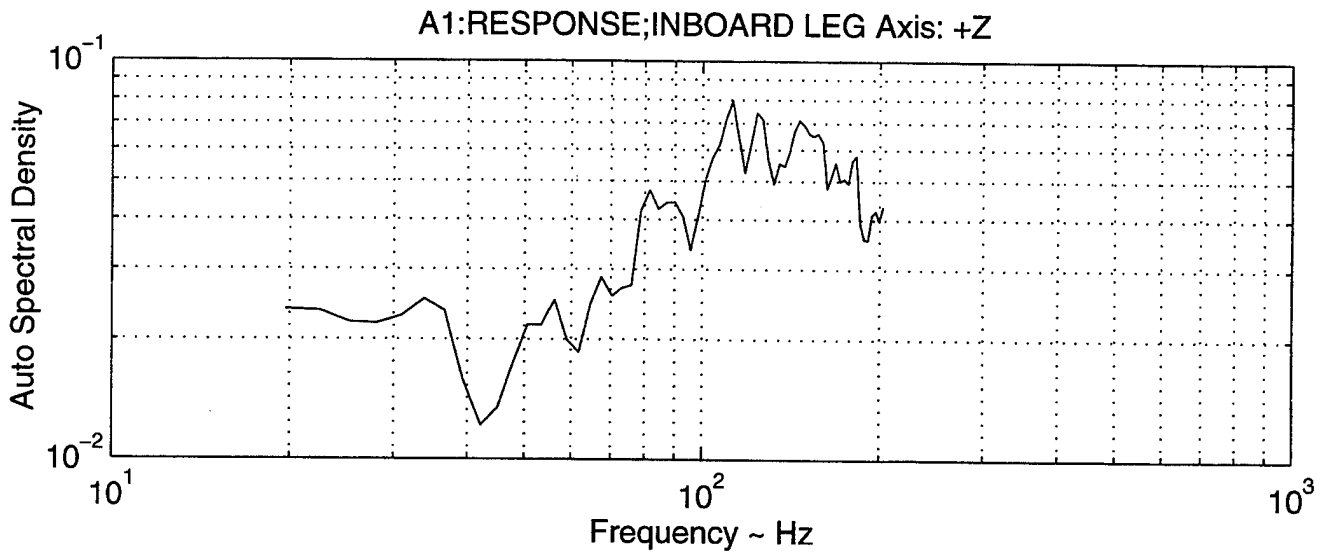


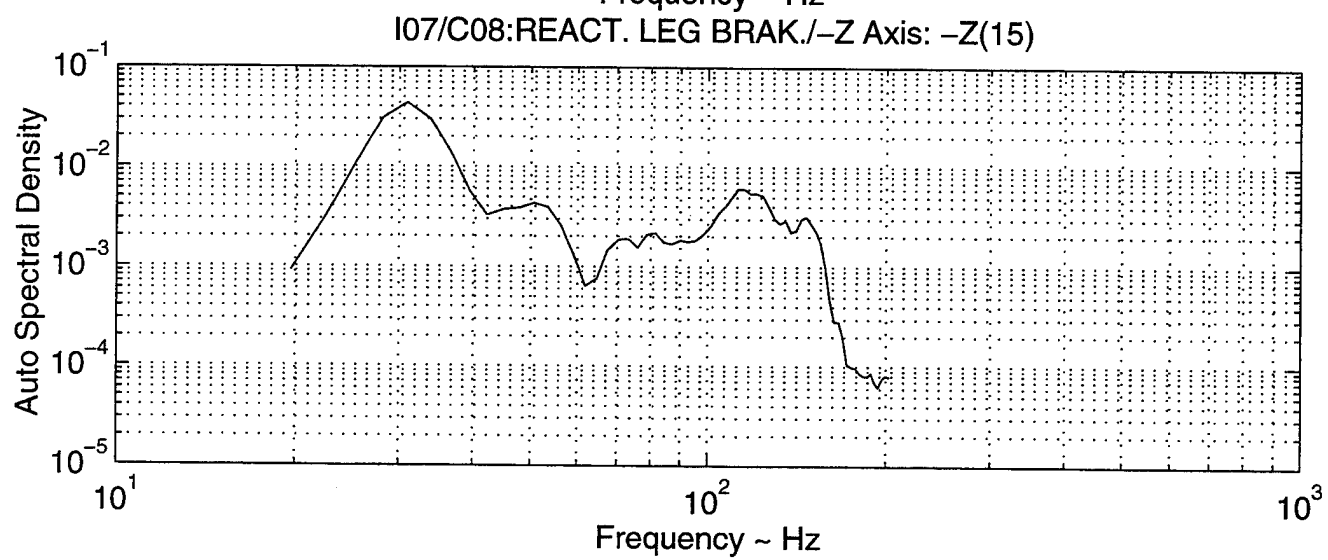
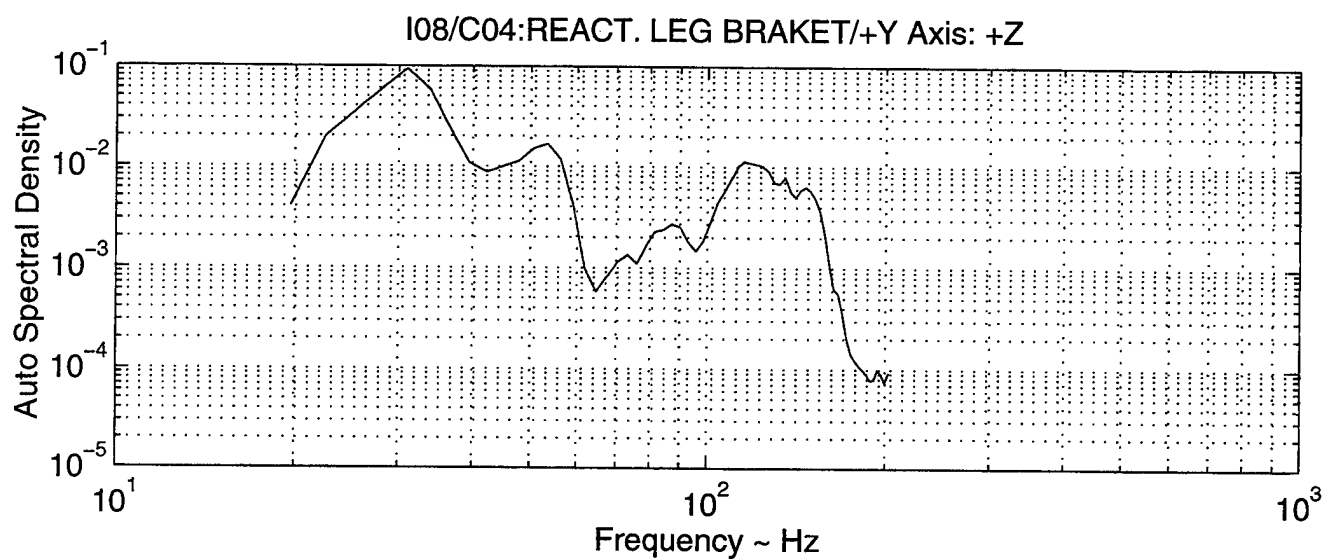
I12/C34:STARTUP UNIT FRAME Axis: -X

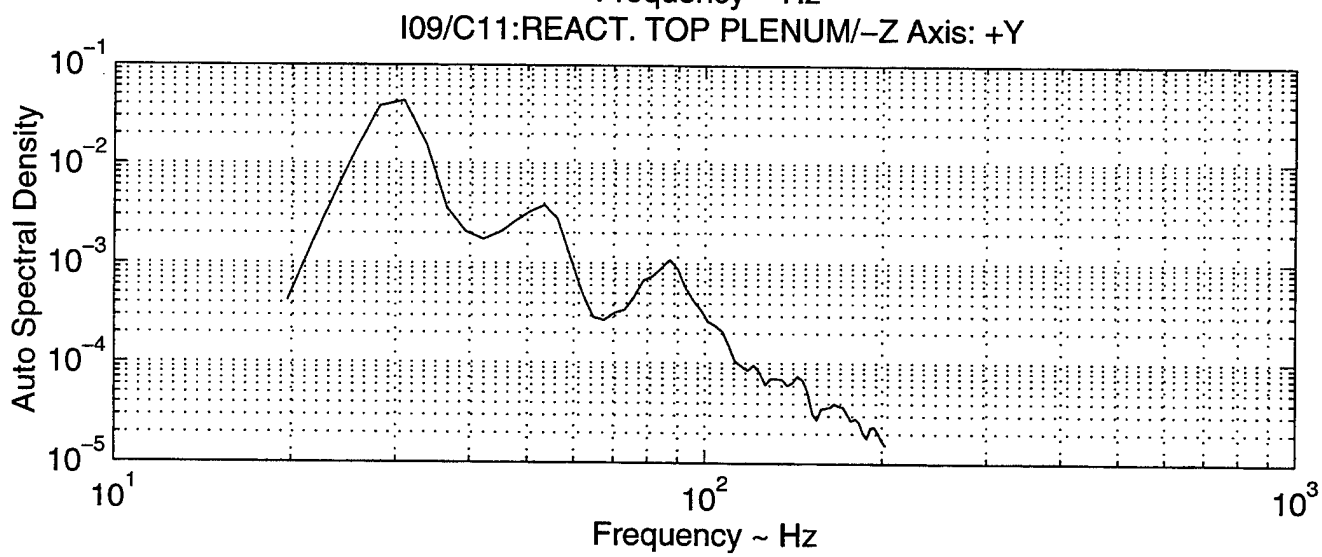
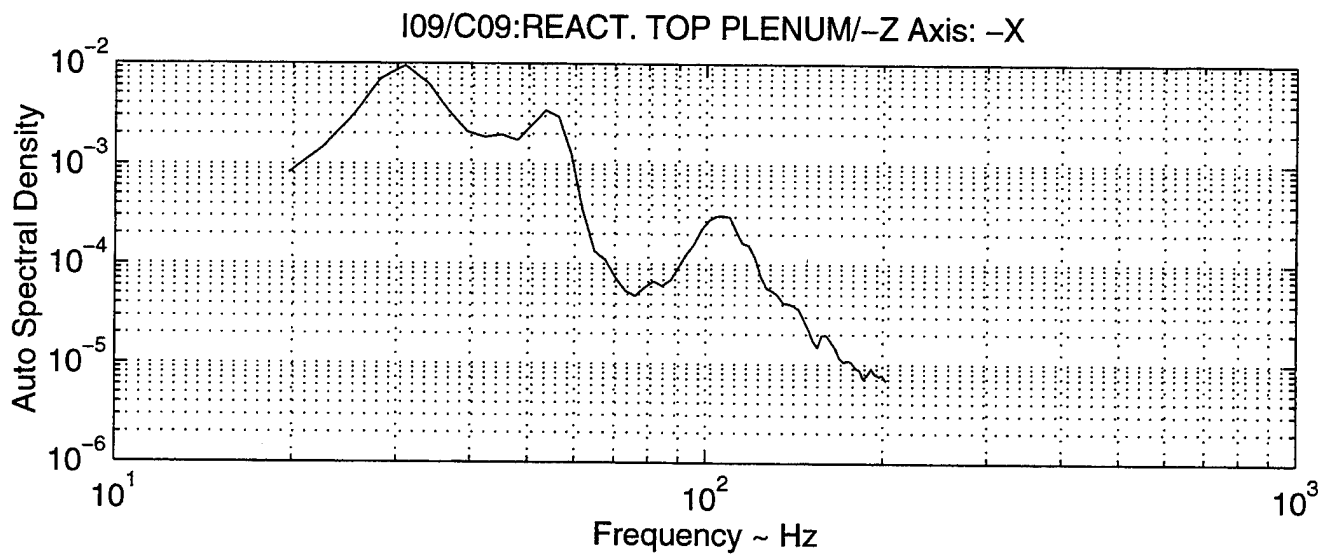


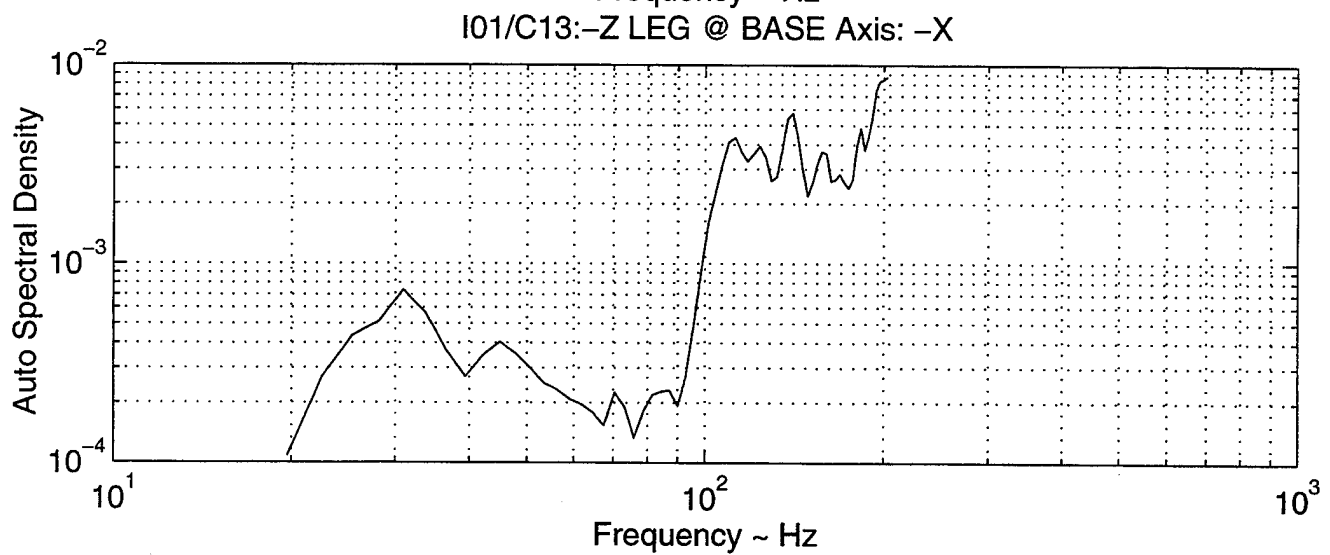
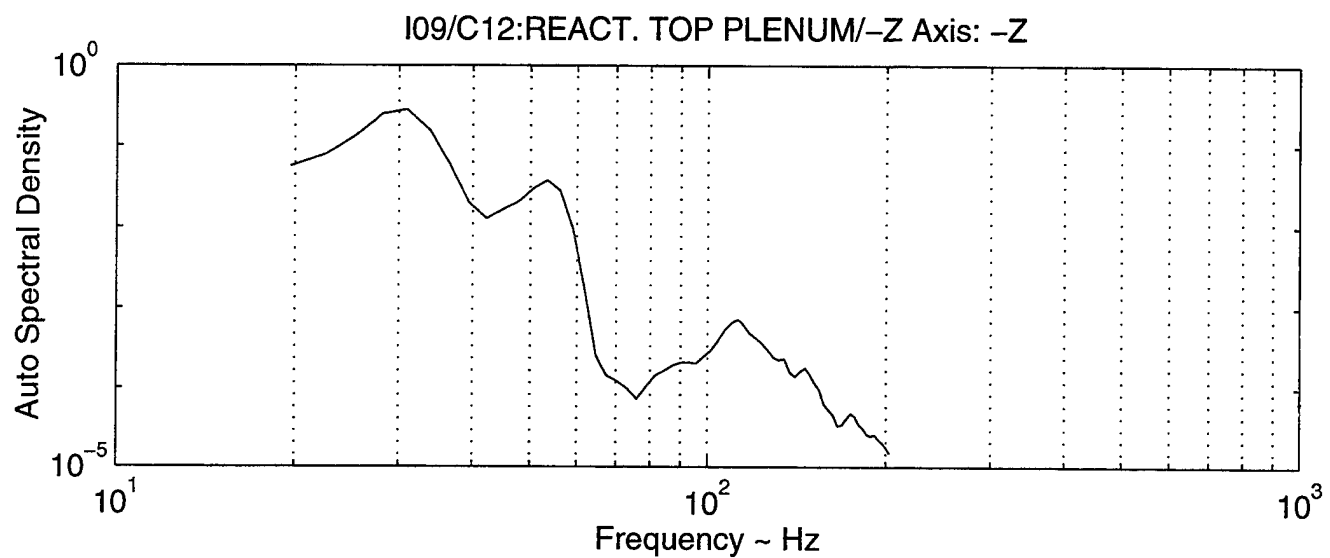


B. The following plots are the graphical representation of experimental PSD response (20 Hz - 200 Hz) for a lateral excitation placed on the test stand .

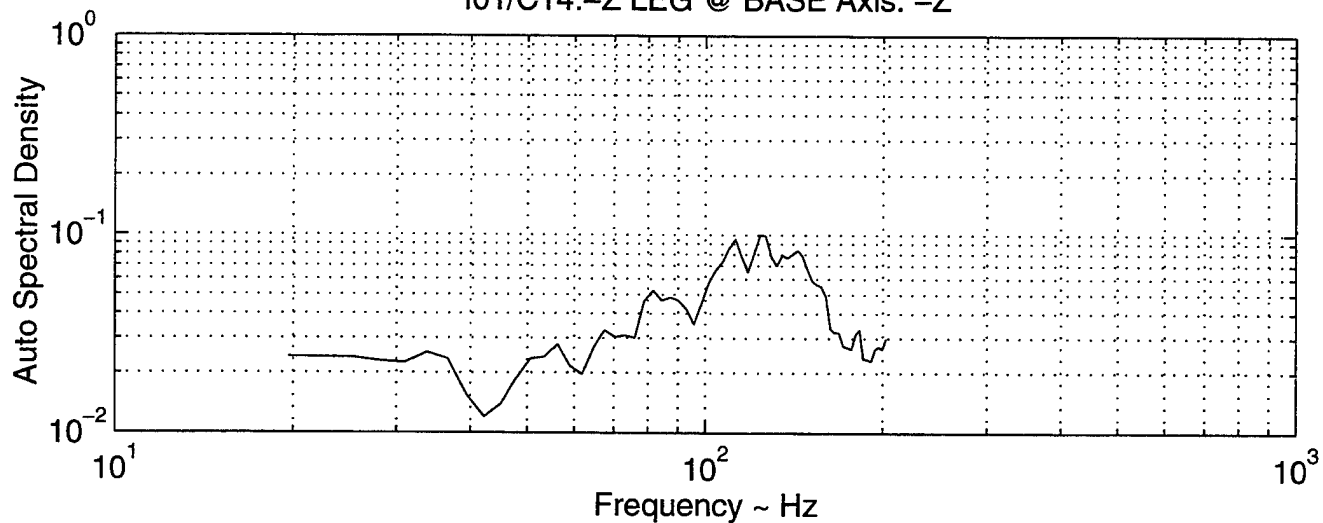




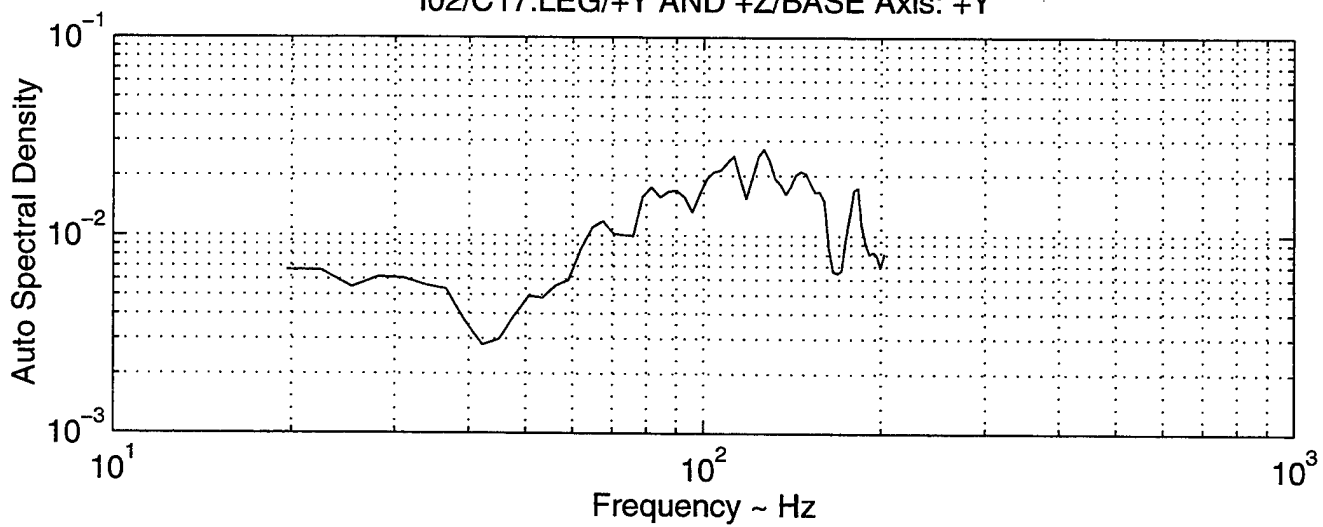


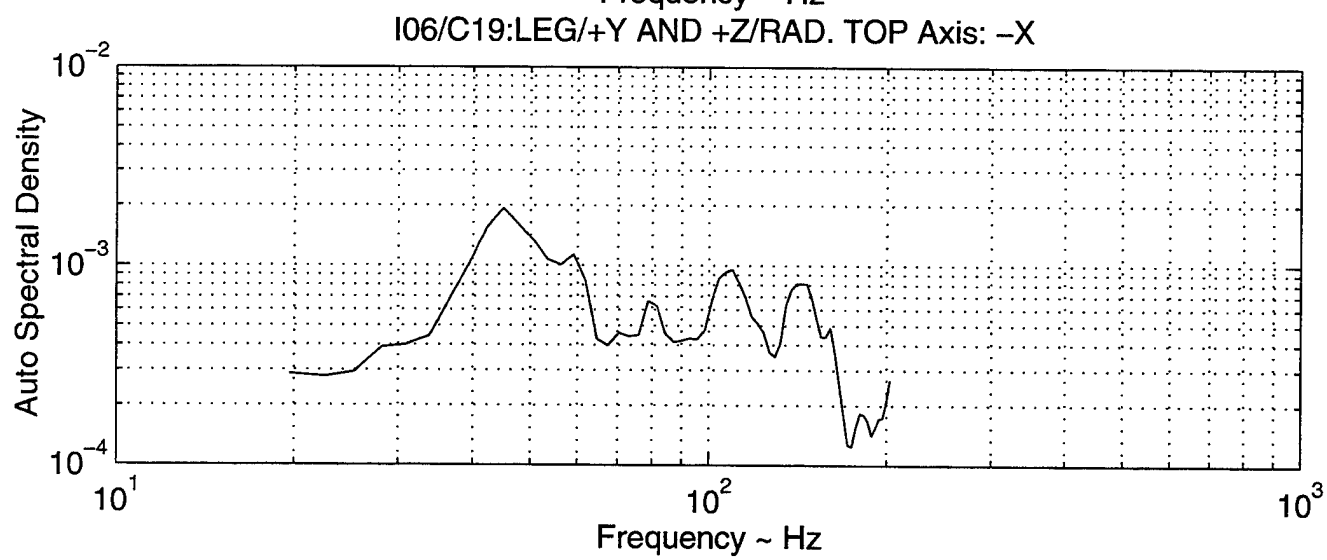
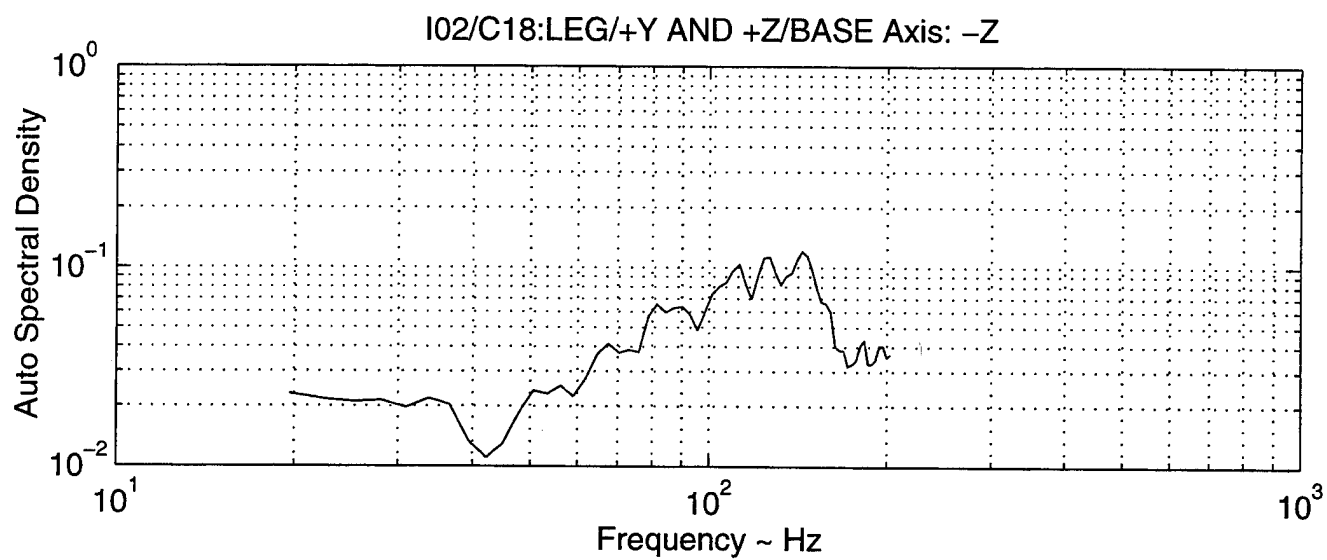


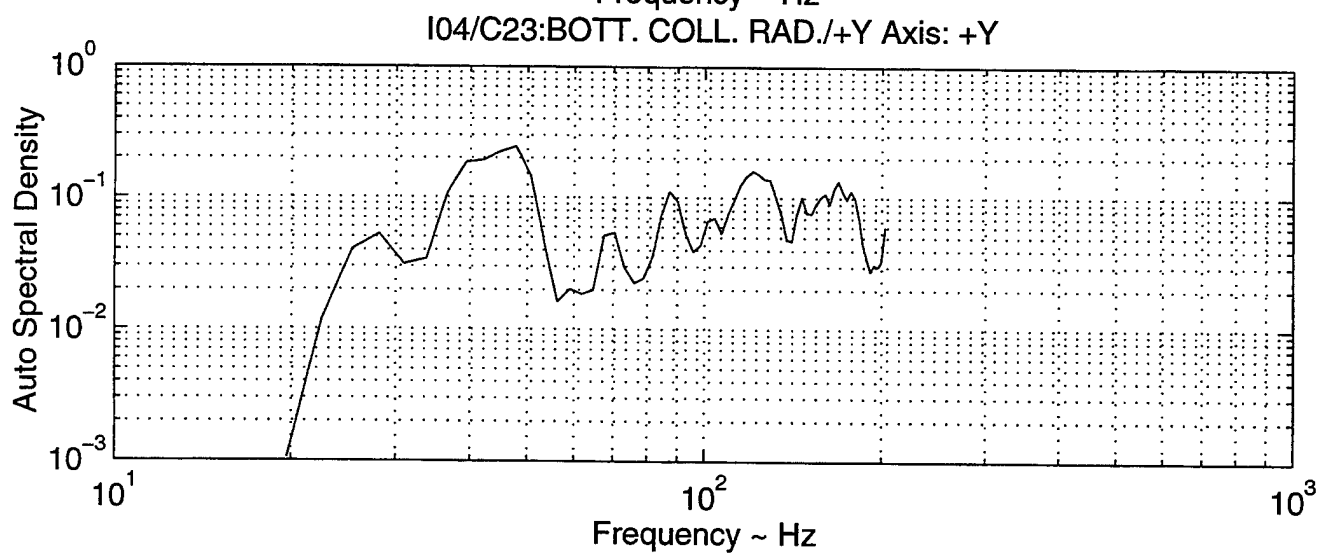
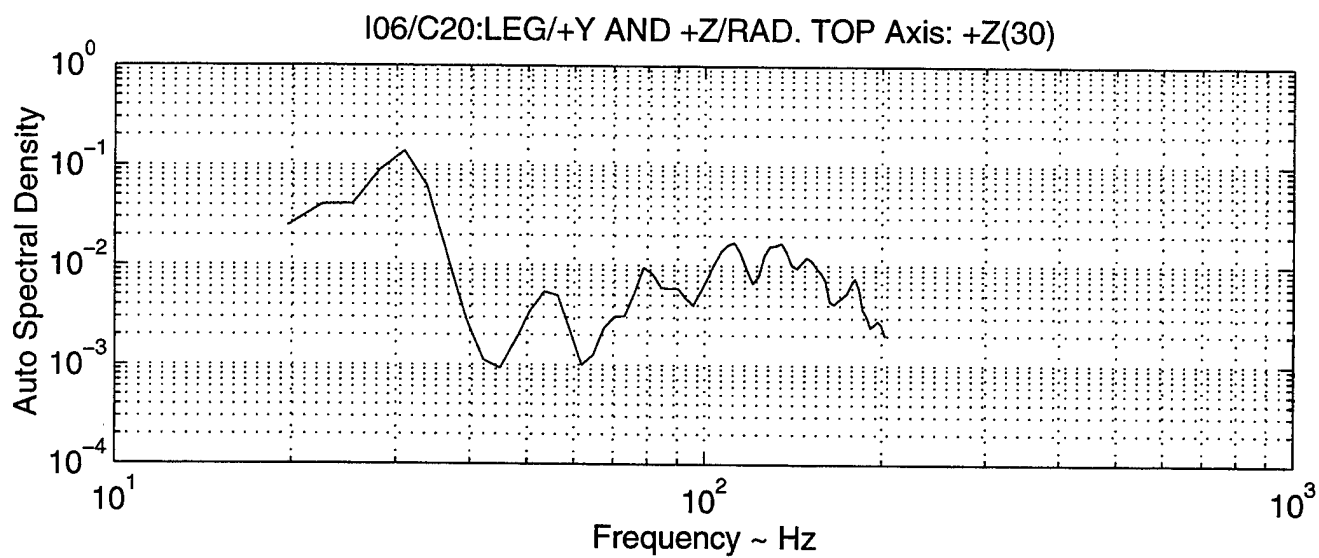
I01/C14:-Z LEG @ BASE Axis: -Z

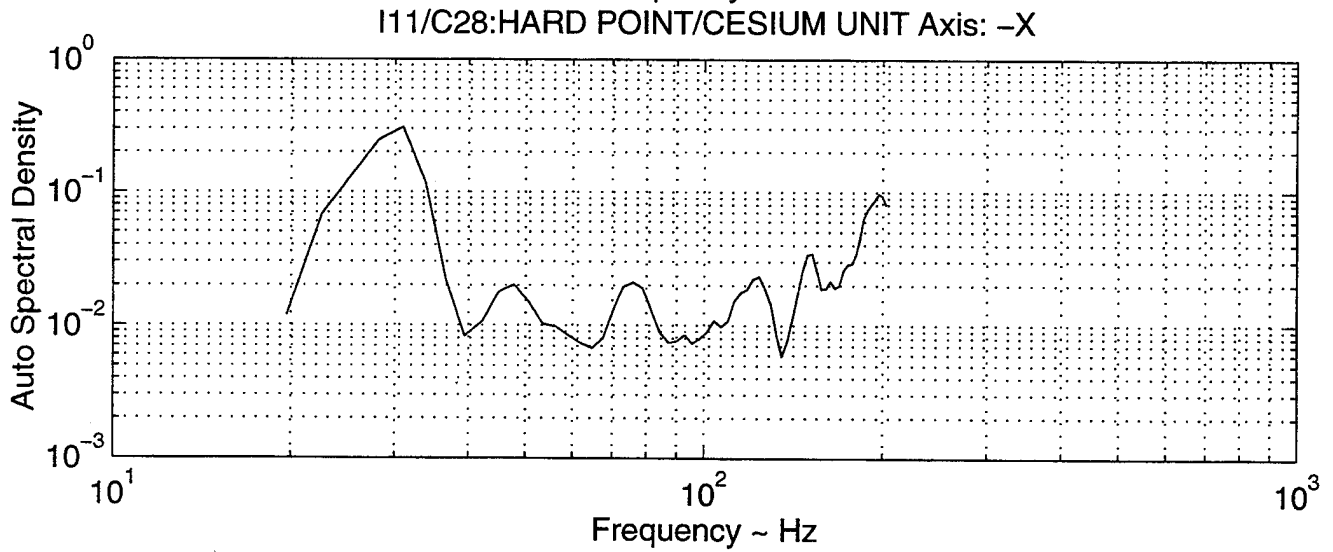
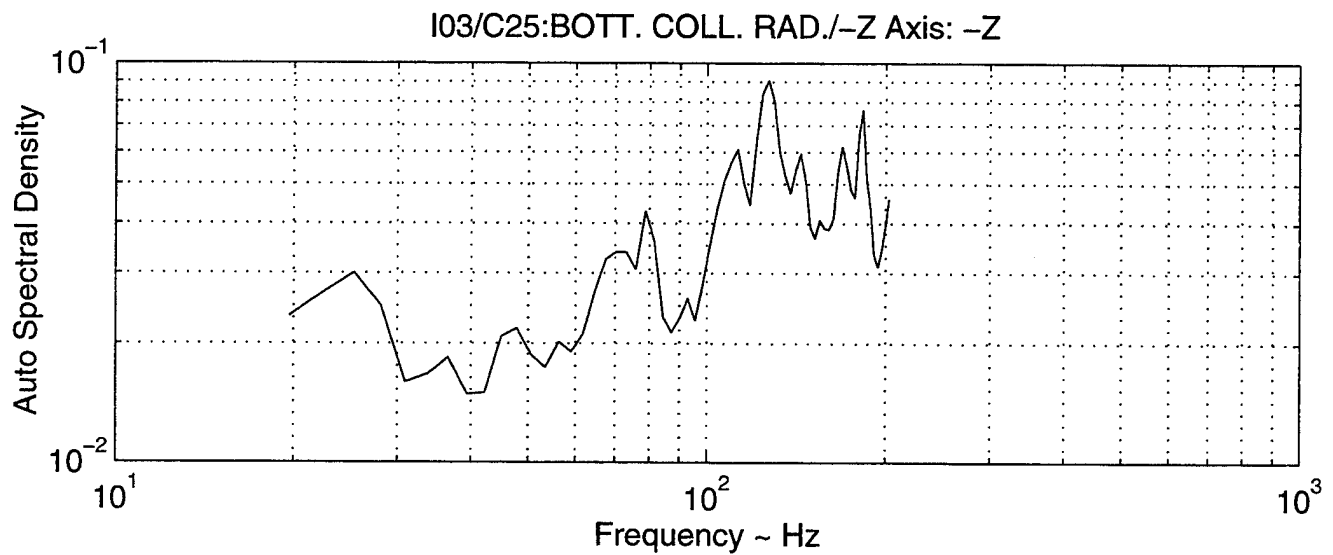


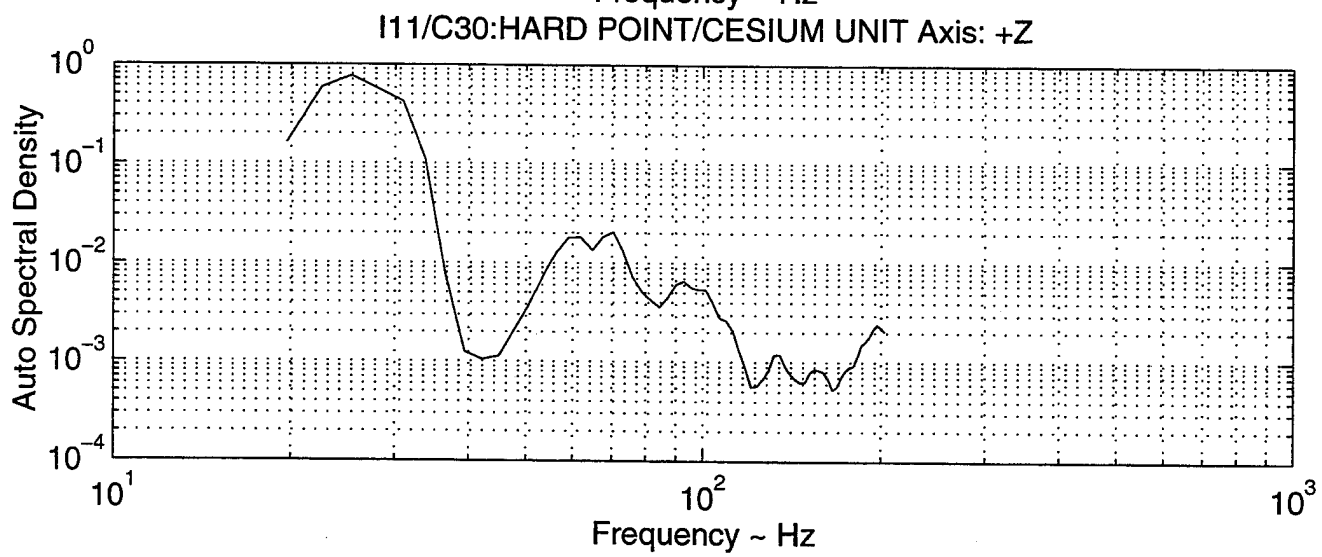
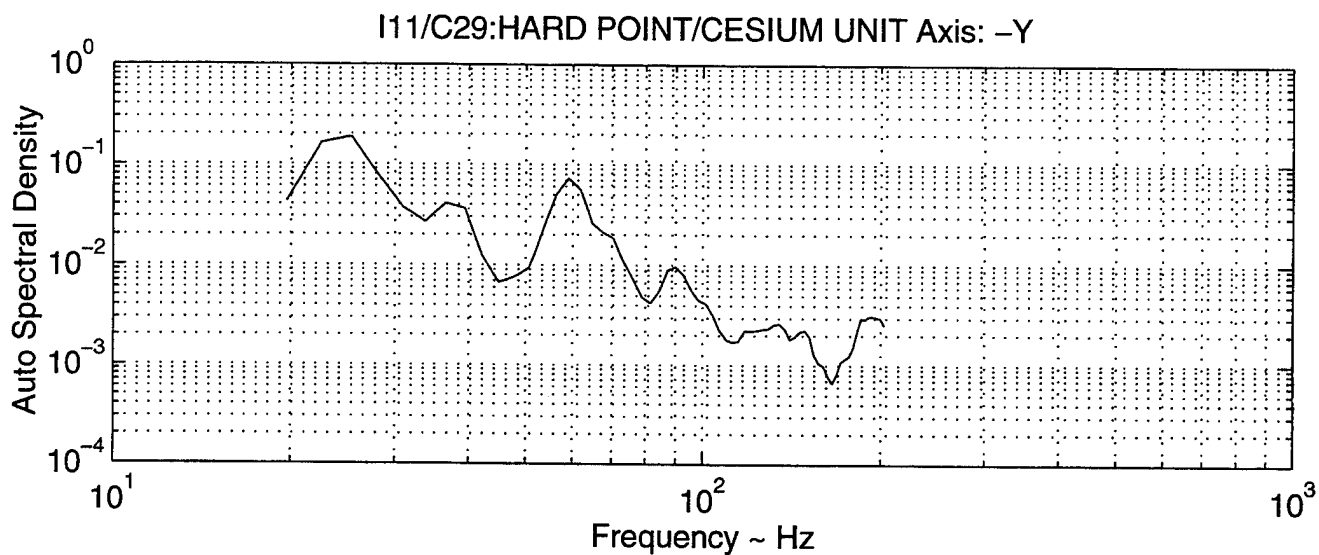
I02/C17:LEG/+Y AND +Z/BASE Axis: +Y

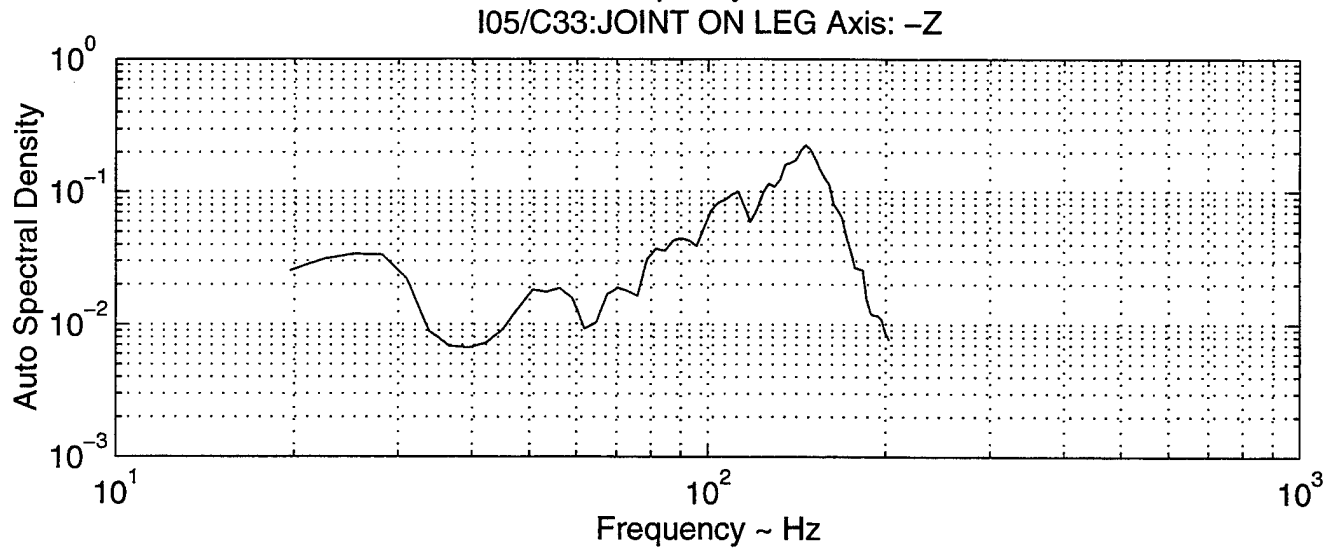
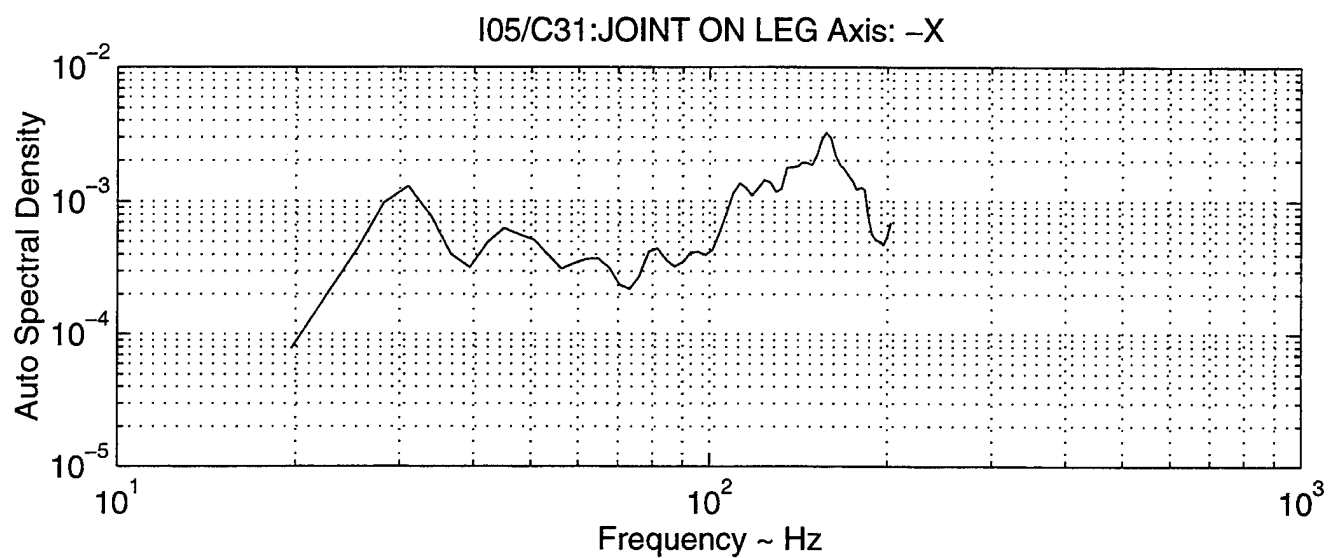




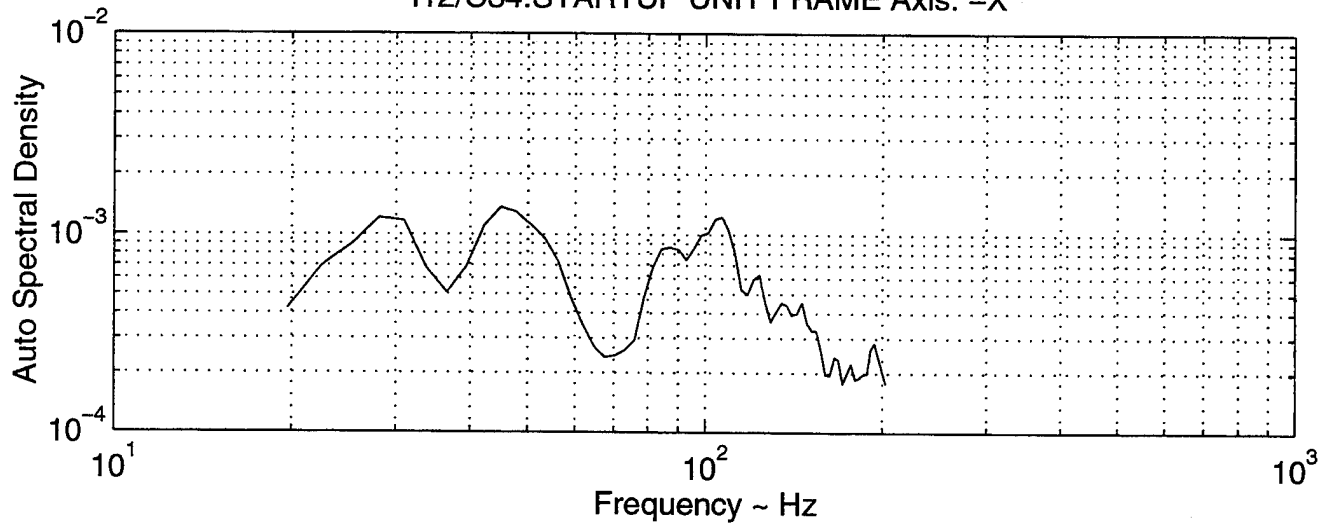




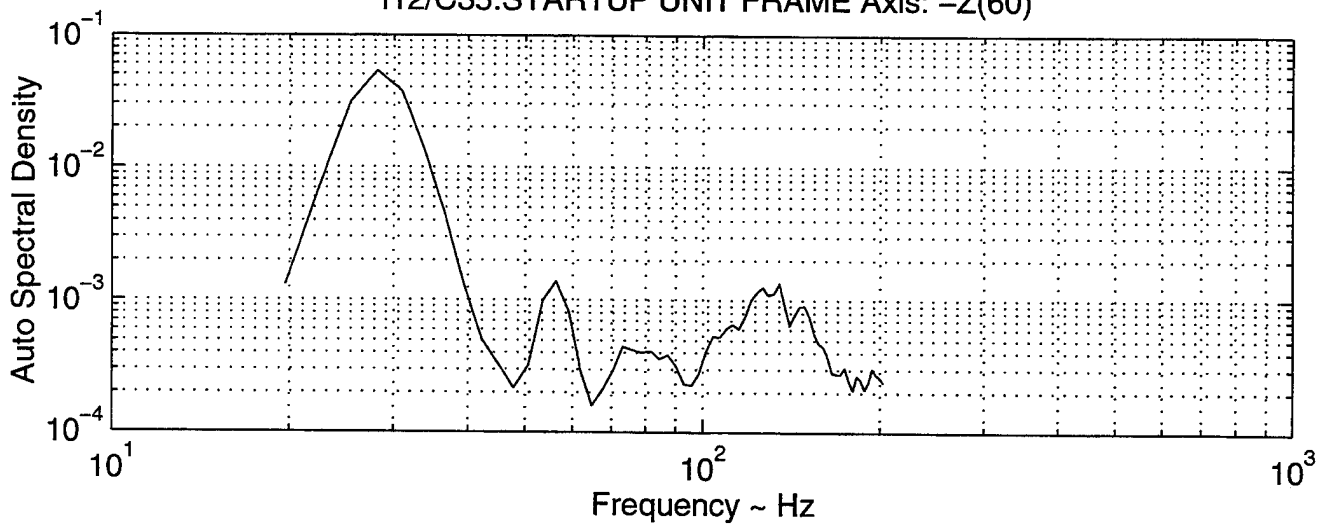


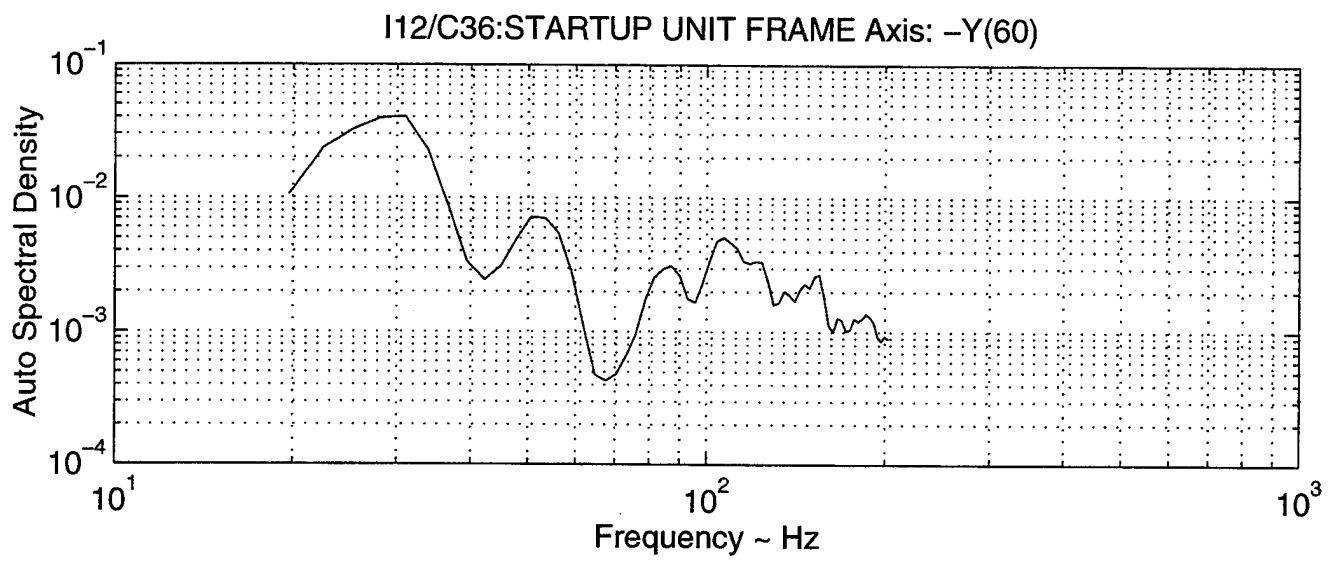


I12/C34:STARTUP UNIT FRAME Axis: -X



I12/C35:STARTUP UNIT FRAME Axis: -Z(60)





APPENDIX C: EXPERIMENTAL RANDOM VIBRATION PSD RESPONSE

A. Summary of experimental PSD response for axial excitation placed at the center of the test stand.

Instrument # 8 - I08/C01:React LegBracket/+Y (X,20)

Peak	Natural Freq~Hz	Amplitude
1	39.3775	0.145985
2	101.257	3.135029-02
3	118.133	5.436304-02
4	140.634	1.197833-02

Instrument # 10 - I10/C02:React Top Plenum/+Y (+Y)

Peak	Natural Freq~Hz	Amplitude
1	42.1902	4.893149-02
2	59.0663	2.940890-02
3	87.1931	1.671294-02
4	160.323	1.206401-02
5	174.386	1.067403-02

Instrument # 10 - I10/C03:React; Top Plenum/+Y (-X)

Peak	Natural Freq~Hz	Amplitude
1	39.3775	0.242672
2	81.5677	7.314822-02
3	101.257	5.819444-02
4	199.7	6.042137-02

Instrument # 7 - I07/C05:React Leg Bracket/-Z (-X,20)

Peak	Natural Freq~Hz	Amplitude
1	39.3775	0.200940
2	75.9424	1.888600-02
3	118.133	1.395260-02

Instrument # 9 - I09/C09:React Top Plenum/-Z (-X)

Peak	Natural Freq~Hz	Amplitude
1	39.3775	0.193046
2	61.879	0.109084
3	101.257	6.674236-02

Instrument # 9 - I09/C12: Reactor Top Plenum/-Z (-Z)

Peak	Natural Freq~Hz	Amplitude
1	42.1902	2.535465-02
2	101.257	2.466876-03

Instrument # 1 - I01/C13: -Z Leg @ Base (-X)

Peak	Natural Freq~Hz	Amplitude
1	45.0029	2.034021-02
2	59.0663	1.794421-02
3	101.257	4.820386-02
4	188.133	4.833439-02
5	146.259	5.398086-02
6	171.574	6.097842-02

Instrument # 1 - I01/C14: -Z Leg @Base (-Z)

Peak	Natural Freq~Hz	Amplitude
1	39.3775	9.159814-04
2	56.2536	4.646390-04
3	73.1297	2.496831-03
4	101.257	1.550436-03
5	146.259	2.813150-03
6	199.7	1.996545-03

Instrument # 1 - I01/C15: Z Leg @Base (-Y)

Peak	Natural Freq~Hz	Amplitude
1	25.3141	4.160663-02
2	33.7522	4.247391-02
3	73.1297	3.678656-02
4	87.1931	4.208175-02
5	135.009	4.178403-02

Instrument # 2 - I01/C16: Leg/+Y and +Z/Base (-X)

Peak	Natural Freq~Hz	Amplitude
1	25.3141	2.236830-02
2	59.0663	1.778245-02
3	101.257	4.079650-02
4	118.133	3.699999-02
5	146.259	3.931678-02
6	171.574	6.039139-02

Instrument # 2 - I02/C17: Leg/+Y and +Z/Base (+Y)

Peak	Natural Freq~Hz	Amplitude
1	33.7522	2.064734-03
2	61.879	1.524224-03
3	98.4438	2.457572-03
4	132.196	8.242004-03
5	171.574	9.640172-03

Instrument # 6 - I06/C19: Leg/+Y +Z/RD. Top (CTL.2) (-X)

Peak	Natural Freq~Hz	Amplitude
1	39.3775	7.916725-02
2	101.257	2.393894-02

Instrument # 6 - I06/C20: Leg/+Y and +Z/Rad. Top (+Y,30)

Peak	Natural Freq~Hz	Amplitude
1	22.5014	3.046443-03
2	42.1902	1.785206-03
3	75.9424	1.817525-03
4	118.133	5.856740-03
5	129.383	5.555836-03
6	168.761	5.877442-03

Instrument # 4 - I04/C24: Bottom Collector Radiator/+Y (+X)

Peak	Natural Freq~Hz	Amplitude
1	36.5648	7.586296-02
2	61.879	1.979974-02
3	115.32	0.115721
4	143.447	7.072005-02

Instrument # 3 - I03/C27: Bottom Collector Radiator/-Z (+X)

Peak	Natural Freq~Hz	Amplitude
1	39.3775	8.474086-02
2	59.0663	1.701377-02
3	101.257	7.474965-02

Instrument # 11 - I11/C28: Hard Point/Cesium Unit (X)

Peak	Natural Freq~Hz	Amplitude
1	28.1268	0.107933
2	39.3775	0.193079
3	61.879	5.303257-02
4	118.133	1.782029-02
5	182.824	2.349582-02

Instrument # 11 - I11/C29: Hard Point/Cesium Unit (-Y)

Peak	Natural Freq~Hz	Amplitude
1	42.1902	4.243232-02
2	59.0663	8.437806-02
3	84.3804	3.001004-02
4	112.507	1.917203-02
5	182.824	2.797795-03

Instrument # 11 - I11/C30: Hard Point Cesium Unit (-Z)

Peak	Natural Freq~Hz	Amplitude
1	28.1268	0.114188
2	67.5043	5.562947-03
3	95.6311	3.542342-03
4	157.51	5.971567-04
5	185.637	7.469532-04

Instrument # 5 - I05/C31: Joint on Leg (-X)

Peak	Natural Freq~Hz	Amplitude
1	36.5648	4.408289-02
2	59.0663	1.153627-02
3	101.257	2.446166-02
4	146.259	2.942323-02

Instrument # 12 - I12/C34: Startup Unit Frame (-X)

Peak	Natural Freq~Hz	Amplitude
1	39.3775	0.180869
2	75.9424	4.030387-02
3	104.069	1.993886-02
4	140.634	1.347441-02

Instrument # 12 - I12/C35: Startup Unit Frame (-Z,60)

Peak	Natural Freq~Hz	Amplitude
1	22.5014	4.823374-03
2	61.879	1.116814-02
3	84.3804	7.741034-03
4	160.323	3.212814-03

Instrument # 12 - I12/C36: Startup Unit Frame (-Y,60)

Peak	Natural Freq~Hz	Amplitude
1	36.5648	7.765563-02
2	81.5677	1.677481-02
3	95.6311	2.238195-02
4	143.447	1.380891-02

B. Summary of experimental PSD response for lateral excitation placed at the center of the test stand.

Instrument # 8 - I08/C04:React LegBraket/+Y (+Z)

Peak	Natural Freq ~ Hz	Amplitude
1	30.9395	9.4395910E-02
2	53.4409	1.6740400E-02
3	87.1931	2.6997180E-03
4	115.32	1.1328360E-02

Instrument # 7 - I07/C08:React Leg Brak/-Z (-Z,15)

Peak	Natural Freq ~ Hz	Amplitude
1	30.9395	4.3816620E-02
2	112.507	6.1013230E-03
3	146.259	3.1857690E-03

Instrument # 9 - I09/C09:React; Top Plenum/-Z (-X)

Peak	Natural Freq ~ Hz	Amplitude
1	30.9395	9.4693140E-03
2	53.4409	3.4278440E-03
3	106.882	3.1081620E-03

Instrument # 9 - I09/C11:React Top Plenum/-Z (+Y)

Peak	Natural Freq ~ Hz	Amplitude
1	30.9395	4.3547600E-02
2	53.4409	3.8660720E-03
3	87.1931	1.0879280E-03

Instrument # 9 - I09/C12:React Top Plenum/-Z (-Z)

Peak	Natural Freq ~ Hz	Amplitude
1	30.9395	2.8000100E-01
2	53.4409	3.745182E-02
3	112.507	7.269852E-04

Instrument # 1 - I01/C13: -Z Leg @ Base (-X)

Peak	Natural Freq ~ Hz	Amplitude
1	30.9395	7.3560660E-04
2	45.0029	4.042286E-04
3	70.317	2.257575E-04
4	112.507	4.326333E-03
5	123.758	3.924026E-03
6	140.634	5.743470E-03
7	157.51	3.693443E-03
8	182.824	4.835220E-03

Instrument # 1 - I01/C14: -Z Leg @ Base (-Z)

Peak	Natural Freq ~ Hz	Amplitude
1	33.7522	2.5343420E-02
2	56.2536	2.777200E-02
3	67.5043	3.291509E-02
4	81.5677	5.238445E-02
5	112.507	9.510401E-02
6	126.571	9.927261E-02
7	143.447	8.365023E-02
8	182.824	3.329352E-02

Instrument # 2 - I02/C17: Leg/+Y and +Z/Base (+Y)

Peak	Natural Freq ~ Hz	Amplitude
1	67.5043	1.179287E-02
2	81.5677	1.746374E-02
3	112.507	2.5088130E-02
4	126.571	2.721874E-02
5	146.259	2.103265E-02
6	182.824	1.733857E-02

Instrument # 2 - I02/C18: Leg/+Y and +Z/Base (-Z)

Peak	Natural Freq ~ Hz	Amplitude
1	67.5043	4.128630E-02
2	81.5677	6.562868E-02
3	112.507	0.103643
4	126.571	0.112783
5	143.447	0.120485

Instrument # 6 - I06/C19: Leg/+Y and +Z/Radiator Top (-X)

Peak	Natural Freq ~ Hz	Amplitude
1	45.0029	1.934899E-03
2	59.0663	1.136854E-03
3	78.7551	6.647710E-04
4	109.695	9.564564E-04
5	143.447	8.124720E-04

Instrument # 6 - I06/C20: Leg/+Y and +Z/Rad Top (+Z)

Peak	Natural Freq ~ Hz	Amplitude
1	33.7522	6.237024E-02
2	53.4409	5.409322E-03
3	78.7551	9.474857E-03
4	112.507	1.715656E-02
5	135.009	1.681939E-02
6	149.072	1.222427E-02
7	180.012	7.525838E-03

Instrument # 4 - I04/C23: Bottom Coll. Rad./+Y (+Y)

Peak	Natural Freq ~ Hz	Amplitude
1	28.1268	5.266047E-02
2	47.8156	0.245235
3	70.317	5.412591E-02
4	87.1931	0.112140
5	104.069	7.072186E-02
6	120.945	0.160821
7	146.259	0.101910
8	168.761	0.134381

Instrument # 3 - I03/C25: Bottom Collector Radiator/-Z (-Z)

Peak	Natural Freq ~ Hz	Amplitude
1	25.3141	3.003612E-02
2	36.5648	1.842493E-02
3	47.8156	2.181759E-02
4	78.7551	4.283077E-02
5	112.507	6.099534E-02
6	126.571	9.061356E-02
7	143.447	5.961075E-02
8	168.761	6.192042E-02
9	182.824	7.639891E-02

Instrument # 11 - I11/C28: Hard Point/Cesium Unit (-X)

Peak	Natural Freq ~ Hz	Amplitude
1	30.9395	0.306490
2	47.8156	2.010432E-02
3	75.9424	2.097343E-02
4	123.758	2.333932E-02
5	151.885	3.452326E-02
6	196.075	9.746875E-02

Instrument # 11 - I11/C29: Hard Point/Cesium Unit (-Y)

Peak	Natural Freq ~ Hz	Amplitude
1	25.3141	0.187757
2	36.5648	4.068818E-02
3	59.0663	7.271490E-02
4	90.0058	9.698337E-03

Instrument # 11 - I11/C30: Hard Point/Cesium Unit (+Z)

Peak	Natural Freq ~ Hz	Amplitude
1	25.3141	0.765666
2	61.879	1.828158E-02
3	70.317	2.063659E-02
4	92.8185	6.595816E-03
5	135.009	1.201656E-03
6	199.7	2.275005E-03

Instrument # 5 - I05/C31: Joint on Leg (-X)

Peak	Natural Freq ~ Hz	Amplitude
1	30.9395	1.292841E-03
2	45.0029	6.324854E-04
3	64.6917	3.732801E-04
4	81.5677	4.458326E-04
5	112.507	1.357943E-03
6	123.758	1.437721E-03
7	157.51	3.243534E-03

Instrument # 5 - I05/C33: Joint on Leg (-Z)

Peak	Natural Freq ~ Hz	Amplitude
1	24.3141	3.393982E-02
2	56.2536	1.874030E-02
3	70.317	1.887515E-02
4	112.507	0.100142
5	146.259	0.225938

Instrument # 12 - I12/C34: Startup Unit Frame (-X)

Peak	Natural Freq ~ Hz	Amplitude
1	28.1268	1.209400E-03
2	45.0029	1.366851E-03
3	106.882	1.227689E-03
4	123.758	6.259511E-04
5	146.259	4.539397E-04
6	194.075	2.841036E-04

Instrument # 12 - I12/C35: Startup Unit Frame (-Z,60)

Peak	Natural Freq ~ Hz	Amplitude
1	28.1268	5.328806E-02
2	56.2536	1.386571E-03
3	73.1297	4.448066E-04
4	126.571	1.253007E-03
5	135.009	1.343956E-03
6	149.072	9.038899E-04

Instrument # 12 - I12/C36: Startup Unit Frame (-Y,60)

Peak	Natural Freq ~ Hz	Amplitude
1	30.9395	4.040794E-02
2	50.6283	7.203744E-03
3	87.1931	3.120361E-03
4	106.882	5.093914E-03
5	154.697	2.704453E-03

APPENDIX D: COORELATION OF COORDINATE SYSTEMS

The coordinate system that was used to model the TOPAZ-II power system in I-DEAS, is not the same coordinate system used on the physical system (Ya-21U). The following conversion table can assist in any confusion.

NODE	Accel (Inst)	TOPAZ C/S	F.E.M. C/S	ACCEL C/S
N5	1	- Z	+ X	+Y
N5	1	+ Y	+ Y	+Z
N5	1	+ X	+ Z	-X
N12	2	- Z	+ X	+Z
N12	2	+ Y	+ Y	+Y (rot -30)
N12	2	+ X	+ Z	-X
Radiator	3	- Z	+ X	+X
Radiator	3	+ Y	+ Y	+Y
Radiator	3	+ X	+ Z	+Z
Radiator	4	- Z	+ X	+X
Radiator	4	+ Y	+ Y	+Y
Radiator	4	+ X	+ Z	+Z
N 29	5	- Z	+ X	+ Z
N 29	5	+ Y	+ Y	+ Y
N 29	5	+ X	+ Z	- X
N 55	6	- Z	+ X	- Y (rot -30)
N 55	6	+ Y	+ Y	- Z (rot -30)
N 55	6	+ X	+ Z	- X
N 79	7	- Z	+ X	+ Z (rot -20) *
N 79	7	+ Y	+ Y	+ Y
N 79	7	+ X	+ Z	- X (rot -20)
N 75	8	- Z	+ X	- Y
N 75	8	+ Y	+ Y	+ Z (rot -20) *
N 75	8	+ X	+ Z	- X (rot -20)
N 97	9	- Z	+ X	+ Z

NODE	Accel(Inst)	TOPAZ C/S	F.E.M. C/S	ACCEL C/S
N 97	9	+ Y	+ Y	+ Y
N 97	9	+ X	+ Z	- X
N 92	10	- Z	+ X	- Y
N 92	10	+ Y	+ Y	+ Z
N 92	10	+ X	+ Z	- X
Cesium Unit	11	- Z	+ X	-Z
Cesium Unit	11	+ Y	+ Y	-Y
Cesium Unit	11	+ X	+ Z	-X
Start-up unit	12	- Z	+ X	+Y **
Start-up unit	12	+ Y	+ Y	-Z **
Start-up unit	12	+ X	+ Z	-X

* offset by 15 degrees

** offset by 60 degrees

APPENDIX E: CORRELATION AND COMPARISON OF THEORETICAL AND EXPERIMENTAL RESULTS

The experimental and theoretical PSD responses were correlated and compared to find common peaks in frequency.

A. Comparison of experimental and theoretical PSD responses for an axial excitation.

Instrument # 8 - I08/C01:React LegBraket/+Y (X,20); node 75+X

Peak	Natural Freq~Hz	Natural Freq ~ Hz
1	39.3775	40.83
2	101.257	107.4
3	118.133	123.3
4	140.634	144.9
		174.2

Comparison

1	39.3775	40.83
2	101.257	107.4
3	118.133	123.3
4	140.634	144.9

Instrument # 10 - I10/C02:React Top Plenum/+Y (+Y); node 92+Z

Peak	Natural Freq~Hz	Natural Freq ~ Hz
1	42.1902	39.91
2	59.0663	51.41
3	87.1931	120.5
4	160.323	148.3
5	174.386	191

Comparison

1	42.1902	39.91
---	---------	-------

Instrument # 10 - I10/C03:React; Top Plenum/+Y (-X); node 92+X

Peak	Natural Freq~Hz	Natural Freq ~ Hz
1	39.3775	40.83
2	81.5677	79.62
3	101.257	107.4
4	199.7	123.3
		144.9
		170.2
		191

Comparison

1	39.3775	40.83
2	81.5677	79.62
3	101.257	107.4
4	199.7	191

Instrument # 7 - I07/C05:React Leg Bracket/-Z (-X,20); node 79+X

Peak	Natural Freq~Hz	Natural Freq ~ Hz
1	39.3775	40.83
2	75.9424	107.4
3	118.133	123.3
		144.9
		174.2

Comparison

1	39.3775	40.83
2	118.133	123.3

Instrument # 9 - I09/C09:React Top Plenum/-Z (-X); node 97+X

Peak	Natural Freq~Hz	Natural Freq ~ Hz
1	39.3775	40.83
2	61.879	79.62
3	101.257	107.4
		123.3
		144.9
		170.2
		191

Comparison

1	39.3775	40.83
2	101.257	107.4

Instrument # 9 - I09/C12: Reactor Top Plenum/-Z (-Z); node 97+Z

Peak	Natural Freq~Hz	Natural Freq ~ Hz
1	42.1902	40.83
2	101.257	51.41
		107.4
		120.5
		144.9
		162.6

Comparison

1	42.1902	40.83
2	101.257	107.4

Instrument # 1 - I01/C13: -Z Leg @ Base (-X); node 5+X

Peak	Natural Freq~Hz	Natural Freq ~ Hz
1	45.0029	40.83
2	59.0663	51.41
3	101.257	107.4
4	118.133	120.5
5	146.259	144.9
6	171.574	174.2
		195.4

Comparison

1	45.0029	40.83
2	101.257	107.4
3	118.133	120.5
4	146.259	144.9
5	171.574	174.2

Instrument # 1 - I01/C14: -Z Leg @Base (-Z); node 5-Y

Peak	Natural Freq~Hz	Natural Freq ~ Hz
1	39.3775	107.4
2	56.2536	123.3
3	73.1297	174.2
4	101.257	
5	146.259	
6	199.7	

Comparison

1	101.257	107.4
---	---------	-------

Instrument # 1 - I01/C15: Z Leg @Base (-Y); node 5+Z

Peak	Natural Freq~Hz	Natural Freq ~ Hz
1	25.3141	40.83
2	33.7522	51.41
3	73.1297	107.4
4	87.1931	120.5
5	135.009	144.9
		174.2

Instrument # 2 - I01/C16: Leg/+Y and +Z/Base (-X); node 12-X

Peak	Natural Freq~Hz	Natural Freq ~ Hz
1	25.3141	107.4
2	59.0663	120.5
3	101.257	144.9
4	118.133	174.2
5	146.259	
6	171.574	

Comparison

1	101.257	107.4
2	118.133	120.5
3	146.259	144.9
4	171.574	174.2

Instrument # 2 - I02/C17: Leg/+Y and +Z/Base (+Y); node 12+Y

Peak	Natural Freq~Hz	Natural Freq ~ Hz
1	33.7522	107.4
2	61.879	120.5
3	98.4438	144.9
4	132.196	174.2
5	171.574	

Comparison

1	171.574	174.2
---	---------	-------

Instrument # 6 - I06/C19: Leg/+Y +Z/RD. Top (CTL.2) (-X); node 55+X

Peak	Natural Freq~Hz	Natural Freq ~ Hz
1	39.3775	40.83
2	101.257	107.4
		123.3
		174.2
		191

Comparison

1	39.3775	40.83
2	101.257	107.4

Instrument # 6 - I06/C20: Leg/+Y and +Z/Rad. Top (+Y,30); node 55+Z

Peak	Natural Freq~Hz	Natural Freq ~ Hz
1	22.5014	41.79
2	42.1902	51.41
3	75.9424	107.4
4	118.133	123.3
5	129.383	148.3
6	168.761	170.2
		191

Comparison

1	42.1902	41.79
2	118.133	123.3
3	168.761	170.2

Instrument # 5 - I05/C31: Joint on Leg (-X); node 29+X

Peak	Natural Freq~Hz	Natural Freq ~ Hz
1	36.5648	40.83
2	59.0663	107.4
3	101.257	123.3
4	146.259	174.2

Comparison

1	36.5648	40.83
2	101.257	107.4

B. Comparison of experimental and theoretical PSD responses for a lateral excitation.

Instrument # 8 - I08/C04:React LegBraket/+Y (+Z); node 75+Y

Peak	Exper. Freq ~ Hz	Theor. Freq ~ Hz
1	30.9395	107.4
2	53.4409	148.3
3	87.1931	182.4
4	115.32	

Instrument # 7 - I07/C08:React Leg Brak/-Z (-Z,15); node 79+Z

Peak	Exper Freq ~ Hz	Theor Freq ~ Hz
1	30.9395	40.83
2	112.507	51.41
3	146.259	107.4
		120.5
		148.3
		170.2
		191

Comparison

1	112.507	107.4
2	146.259	148.3

Instrument # 9 - I09/C09:React; Top Plenum/-Z (-X); node 97+X

Peak	Exper Freq ~ Hz	Theor Freq ~ Hz
1	30.9395	40.83
2	53.4409	79.62
3	106.882	107.4
		123.3
		170.2
		191

Comparison

1	106.882	107.4
---	---------	-------

Instrument # 9 - I09/C11:React Top Plenum/-Z (+Y); node 97+Y

Peak	Exper Freq ~ Hz	Theor Freq ~ Hz
1	30.9395	40.83
2	53.4409	151.7
3	87.1931	182.4

Instrument # 9 - I09/C12:React Top Plenum/-Z (-Z); node 97+Z

Peak	Exper Freq ~ Hz	Theor Freq ~ Hz
1	30.9395	40.83
2	53.4409	51.41
3	112.507	107.4
		120.5
		148.3
		195.4

Comparison

1	53.4409	51.41
2	112.507	107.4

Instrument # 1 - I01/C13: -Z Leg @ Base (-X); node 5+X

Peak	Exper Freq ~ Hz	Theor Freq ~ Hz
1	30.9395	41.79
2	45.0029	51.41
3	70.317	107.4
4	112.507	120.5
5	123.758	174.2
6	140.634	
7	157.51	
8	182.824	

Comparison

2	45.0029	41.79
3	112.507	107.4
4	123.758	120.5

Instrument # 1 - I01/C14: -Z Leg @ Base (-Z); node 5-Y

Peak	Exper Freq ~ Hz	Theor Freq ~ Hz
1	33.7522	107.4
2	56.2536	123.3
3	67.5043	174.2
4	81.5677	195.4
5	112.507	
6	126.571	
7	143.447	
8	182.824	

Comparison

1	112.507	107.4
2	126.571	123.3

Instrument # 2 - I02/C17: Leg/+Y and +Z/Base (+Y); node 12+Y

Peak	Exper Freq ~ Hz	Theor Freq ~ Hz
1	67.5043	51.41
2	81.5677	107.4
3	112.507	120.5
4	126.571	144.9
5	146.259	174.2
6	182.824	

Comparison

1	112.507	107.4
2	126.571	120.5
3	146.259	144.9
4	182.824	174.2

Instrument # 2 - I02/C18: Leg/+Y and +Z/Base (-Z); node 12+Z

Peak	Exper Freq ~ Hz	Theor Freq ~ Hz
1	67.5043	40.83
2	81.5677	51.41
3	112.507	95.73
4	126.571	109.9
5	143.447	123.3
		174.2

Comparison

1	112.507	109.9
2	126.571	123.3

Instrument # 6 - I06/C19: Leg/+Y and +Z/Radiator Top (-X); node 55+X

Peak	Exper Freq ~ Hz	Theor Freq ~ Hz
1	45.0029	40.83
2	59.0663	79.62
3	78.7551	107.4
4	109.695	123.3
5	143.447	174.2
		182.4

Comparison

1	45.0029	40.83
2	78.7551	79.62
3	109.695	107.4

Instrument # 6 - I06/C20: Leg/+Y and +Z/Rad Top (+Z); node 55-Y

Peak	Exper Freq ~ Hz	Theor Freq ~ Hz
1	33.7522	40.83
2	53.4409	50.24
3	78.7551	79.62
4	112.507	107.4
5	135.009	123.3
6	149.072	162.6
7	180.012	191

Comparison

1	53.4409	50.24
2	78.7551	79.62
3	112.507	107.4

Instrument # 5 - I05/C31: Joint on Leg (-X); node 29+X

Peak	Exper Freq ~ Hz	Theor Freq ~ Hz
1	30.9395	40.83
2	45.0029	51.41
3	64.6917	79.62
4	81.5677	107.4
5	112.507	123.3
6	123.758	174.2
7	157.51	

Comparison

1	45.0029	40.83
2	81.5677	79.62
3	112.507	107.4
4	123.758	123.3

Instrument # 5 - I05/C33: Joint on Leg (-Z); node 29+Z

Peak	Exper Freq ~ Hz	Theor Freq ~ Hz
1	24.3141	51.41
2	56.2536	109.9
3	70.317	123.3
4	112.507	174.2
5	146.259	

Comparison

2	56.2536	51.41
3	112.507	109.9

LIST OF REFERENCES

- Agrawal, Brig N. (1986), *Design of Geosynchronous Spacecraft*, Prentice Hall Inc., Englewood Cliffs, N.J.
- Benke, S.M. and Venable, R.J. (1995), "Operational Testing and Thermal Modeling of a TOPAZ-II Single-Cell Thermionic Fuel Element Test Stand", American Institute of Physics, Twelfth Symposium on Space Nuclear Power and Propulsion, Albuquerque, N.M., (8-12 January 1995). AIP Conf. Proc. 324.
- Devore, Jay L. (1995), *Probability and Statistics for Engineering and the Sciences*, Wadsworth Publishing Company, Belmont, CA.
- Donaldson, Bruce (1993), *McGraw Hill Series in Aeronautical and Aerospace Engineering*, McGraw Hill, Inc., Highstown, NJ.
- Lacy, J.M. (September 1993), *TOPAZ-II Structural Analysis FY 1993 Activity Report*, Idaho National Laboratories.
- Larson, Wiley J. and Wertz, James R. (1993), *Space Mission Analysis and Design*, Microcosm, Inc., Torrance, CA.
- Lawry, Mark H. (1993), *I-DEAS Master Series*, Structural Dynamics Research Corporation, Milford, OH.
- Mayes, R.L. (May 1993), "TOPAZ Ya-21 Modal Test Series Results," Sandia National Laboratories, Albuquerque, NM.

Meirovitch, Leonard (1986), *Elements of Vibration Analysis*,
Second Edition, McGraw Hill, Inc., New York, NY.

Schaefer, E.D. (September 1994), *Preliminary Test Report
Ya-21U*, John Hopkins University / Applied Physics
Laboratory.

U.S. TOPAZ-II Flight Safety Team (November 1992), *NEP Space
Test Program Preliminary Nuclear Safety Assessment*.

Wyant, Frank J. and Schmidt, G. (August 1994), *Shock and
Vibration Testing of Ya-21U*, TSET Experiment #93-16,
TOPAZ International Program, Albuquerque, N.M.

INITIAL DISTRIBUTION LIST

Defense Technical Information Center Cameron Station Alexandria, VA 22304-6145	2
Library, Code 52 Naval Postgraduate School Monterey, CA 93943-5101	2
Chairman Department of Aeronautics and Astronautics, Code AA Naval Postgraduate School Monterey, CA 93943-5106	1
Chairman Space Systems Academic Group, Code SP Naval Postgraduate School Monterey, CA 93943-5101	1
Professor Sandra Scrivener Department of Aeronautics and Astronautics, Code AA/SS Naval Postgraduate School Monterey, CA 93943-5106	2
Professor Oscar Biblarz Department of Aeronautics and Astronautics, Code AA/BI Naval Postgraduate School Monterey, CA 93943-5106	1

TOPAZ International Program 2

Attn: Frank Thome

Frank Wyant

901 University Blvd, S.E.

Albuquerque, NM 87106

LT Sheryl Elaine Campbell 2

665 Copper Kettle Drive

Virginia Beach, VA 23464